



Sudan University of Science and Technology

College of Graduate Studies

**Synthesis and Characterization of Cellulosic Ether
Derivatives from Mesquite**

تخليق و توصيف مشتقات الإيثر السليلوزية من المسكيت

A Thesis Submitted in Fulfillment of the Requirements of the PhD degree in
Chemistry

By: Sanad Khalifa Abdulfattah Etri

(B.sc. Honours, M.Sc. Chem.)

Supervisor: Prof. Mohammed Elmubark Osman

Co- Supervisors: Dr. Adil Elhag Ahmed

Dr. Ahmed Salma Mohammed (N. R. C. , Cairo, Egypt)

Dr. Salah Abdelmohsin (N. R. C. , Cairo, Egypt)

October 2017

الإستهلال

قال الله تعالى:

وَأَخْفِلْ جُرْأَيْخِمًا نَحِيًّا مُدْجَلًا صَدِيقًا وَاجْعَلْ لِي مِّنْ لَّدُنكَ سُدًّا لِّطَانًا
نَصِيرًا). الآية (80) سورة الإسراء .

Dedication

To my little and grand family

To my colleagues and friends

Acknowledgements

I thank Almighty Allah for completing this work.

I would like to thank my supervisor Prof. Mohammed Elmubark Osman for help, useful advice and scientific support throughout the course of this work.

I wish to express my gratitude to my co-supervisors, Prof. Mohammed Elsakhawi (NRC), Dr. Adil Elhaj Ahmed, Dr. Ahmed Salama, and Dr. Salah Abdelmohsin for providing me with the numerous possibilities to pursue this scientific research.

I would like to thank the staff of the Faculty of forestry and Ranges (SUST) and National Research Center (Egypt) for technical support.

I wish to express my gratitude to the Ministry of Higher Education and Scientific Research, the republic of the Sudan for financial support.

Abstract

Cellulose pulp with yield of 35% and 92% alpha cellulose was extracted from mesquite tree wood, by anthraquinone Kraft pulping method and bleached by hypochlorite. The extracted cellulose was characterized by FT-IR, XRD spectroscopy, and thermal analysis (TGA/DTG/ DTA) and confirmed the cellulose structure.

The extracted cellulose was used for preparing carboxymethylcellulose (CMC), hydroxypropylcellulose (HPC), and methylcellulose (MC) cellulosic ether derivatives with yield of, 190%, and 160.61% and, 115.5% weight respectively.

The prepared cellulose ether derivatives products were characterized by FT-IR, XRD, NMR spectroscopy and thermal analysis (TGA/DTG/ DTA) and confirmed the ether derivatives structure.

The optimum conditions for preparing ether derivatives products were investigated. For CMC, the results were, 40 % NaOH, 7g monochloroacetic acid (MCA), at 55 C for 3.5 hours reaction time, and the degree of substitution (DS) was 1.3. For HPC, the results were, 2.8 ml propylene oxide (PO) /g cellulose, for 6 hours at 70 C, and the degree of substitution (DS) was 1.72. For MC, the results were, 300 % (v/w cellulose) dimethyl sulfate (DMS) concentration, for 5 hours at 50 C and the degree of substitution (DS) was 1.68.

Solubility of prepared ether derivatives products were investigated and found to be 6% , 7% , and 3% for CMC, HPC and MC respectively..

Viscosity of prepared ether derivatives products were investigated and found to be 2500 cPs, 2000 cPs, and 1500cPs for CMC, HPC and MC respectively.

Thermal stability of the prepared products was investigated and found that the products have acquired high thermal stability compared to cellulose.

The prepared ether derivatives, in optimum conditions, were used as stabilizers for preparing, carboxymethylcellulose/Fe₃O₄, hydroxypropylcellulose/Fe₃O₄, methylcellulose/Fe₃O₄, magnetite nanocomposite by co-precipitation, and characterized by FT-IR, XRD spectroscopy, and thermal analysis (TGA/DTG/DTA) and confirmed the magnetite composite structure.

The prepared magnetite nanocomposite, of carboxymethyl cellulose/Fe₃O₄ nanocomposite, was tested for removal of dyes in aqueous solutions using methylene blue solution. The optimum conditions for methylene blue (MB) dye adsorption capacity by 0.05 g of prepared carboxymethylcellulose/Fe₃O₄ nanocomposite were investigated which were, PH 7, rapid at ~40 min slowed at ~40 to ~60 min and reached plateau at 60 min, increased with increasing of dye concentration up to 1500 ppm.

The adsorption kinetics of carboxymethylcellulose/Fe₃O₄ nanocomposite for (MB) were studied and found to be compatible with the second-order kinetics model.

المستخلص

تم استخلاص لب السليلوز بناتج 35% و نسبة ألفا سليلوز بلغ 92% من نبات المسكيت, بواسطة طريقة انثراكينون كرافت و التبييض بواسطة الهايبوكلورايت.

تم التأكد من التركيب البنائي للسليلوز المستخلص بواسطة مطيافية FT-IR, XRD, و التحليل الحراري (TGA/DTG/DTA).

السليلوز المستخلص, أُستخدم لتحضير مشتقات السليلوز الإيثيرية, كاربوكسي ميثيل السليلوز (CMC), هيدروكسي بروبيل السليلوز (HPC), ميثيل السليلوز (MC) بناتج بلغ 190%, 160.61% و 115.15% زيادة في الوزن على التوالي.

تم التأكد من التركيب البنائي لمشتقات السليلوز الايثيرية المحضرة بواسطة مطيافية FT-IR, XRD, NMR و التحليل الحراري (TGA/DTG/DTA).

تمت دراسة الظروف المثلى لتحضير مشتقات السليلوز الايثيرية و وجدت أنها, لـ CMC, 40% تركيز NaOH, 7 جرامات احادي كلورو حمض الخليك, عند درجة حرارة 55 درجة مئوية, لمدة 3.5 ساعة, لكل 5 جرامات سليلوز, و درجة الاستبدال (DS) كانت 1.3.

لـ HPC, 2.8 مل من اكسيد البروبلين/ جرام سليلوز, عند درجة حرارة 70 C, لمدة 6 ساعات, و درجة الاستبدال (DS) كانت 1.72.

لـ MC, 300% تركيز كبريتات ثنائي الميثيل بالنسبة لكمية سليلوز, في درجة حرارة 50 C, لمدة 5 ساعات, و درجة الاستبدال (DS) كانت 1.68.

تم التحقق من ذوبانية مشتقات السليلوز الايثيرية المحضرة و وجدت أنها , 6%, 7% و 3% لـ CMC, HPC, و MC على الترتيب. كما تم التحقق من لزوجة مشتقات السليلوز الايثيرية المحضرة و وجدت أنها,

2000 cP, 2500 cP, و 1500 cP لـ CMC, HPC, و MC على الترتيب.

تمت دراسة الاستقرار الحراري لمشتقات السليلوز الإيثيرية و وجدت أنها اكتسبت استقراراً حرارياً عالياً مقارنة بالسليلوز.

استخدمت مشتقات السليلوز, المنتجة عند الظروف المثلى, كعامل إستقرار لتحضير هجين اكسيد الحديد المغنطيسي النانوية. و تم التحقق من التركيب البنائي للهجين بواسطة مطيافية FT-IR, XRD, و التحليل الحراري (TGA/DTG/DTA).

تم اختبار هجينكاربوكسي ميثيل السليلوز/ اكسيد الحديد المغنطيسي النانوية , في إزالة الالوان من المحاليل المائية بإستخدام صبغة الميثيلين الزرقاء.

تمت دراسة الظروف المثلى لإدمصاص صبغة الميثيلين الزرقاء بواسطة هجين كاربوكسي ميثيل السليلوز/ اكسيد الحديد المغنطيسي النانوية و اظهرت سعة ادمصاص جيدة عند PH 7 , و سرعة ادمصاص جيدة عند 40~ دقيقة و وصلت التشبع عند 60 دقيقة, و يزداد بزيادة تركيز الميثيل الازرق حتى 1500 ppm, لكل 0.05 جرام من الهجين.

تمت دراسة حركية إدمصاص الهجين للصبغة, و وجدت أنها متوافقة مع نموذج الرتبة الثانية .

Table of Contents

الإستهلال.....	I
Dedication	II
Acknowledgements.....	III
Abstract	IV
المستخلص.....	VI
Table of contents.....	VIII
List of tables	X
List of figures	XI
List of schemes	XIII
List of abbreviations	XV
1 Introduction and literature review	1
1.1 Prosopis spp. (Mesquite).....	1
1.1.1 Taxonomy of mesquite tree	2
1.2 Wood structure and chemical composition	3
1.2.1 Hemicelluloses	6
1.2.2 Lignin.....	11
1.2.3 Cellulose.....	14
1.2.4 Extractives.....	20
1.2.5 Inorganic compositions.....	20
1.3 Wood pulping	22
1.3.1 Mechanical pulping	23
1.3.2 Chemical pulping	24
1.3.3 Bleaching	40
1.3.4 Dissolving pulp	54

1.4	Cellulose derivatives.....	54
1.4.1	Carboxymethylcellulose (CMC)	57
1.4.2	Hydroxypropylcellulose (HPC)	61
1.4.3	Methylcellulose (MC).....	62
1.5	Magnetite nanoparticles	64
1.6	Cellulose derivatization	66
1.7	Problem statement	73
1.8	Objectives of the study	74
2	Material and Methods	73
2.1	Raw materials	73
2.1.1	Determination of moisture content.....	73
2.1.2	Determination of ash content.....	73
2.1.3	Lignin content determination.....	74
2.2	Preparation of dissolving pulp	75
2.3	Determination of alpha cellulose in bleached pulp.....	75
2.4	Preparation of carboxymethyl cellulose.	75
2.5	Preparation of methylcellulose (MC)	77
2.6	Preparation of hydroxypropylcellulose(HPC)	77
2.7	Synthesis of magnetite nanocomposite	78
2.8	Application of the carboxymethyl cellulose/Fe ₃ O ₄ nanocomposite for methylene blue (MB) adsorption from aqueous solution.....	78
2.9	Characterizations	79
3	Results and discussion	80
3.1	Conclusions	105
3.2	Recommendations:	106
	References	

List of tables

Table. 1.1: wood components of different wood species.	5
Table. 1. 2: Unit cell dimensions of cellulose polymorphs I, II, III and IV.	19
Table. 1. 3: wood extractives	21
Table. 1. 4: wood inorganic composition of several wood species.	22
Table. 1.5: Applications of CMC	61
Table 3.1 Mesquite woods analysis.....	80
Table 3.2 Effect of NaOH concentration on unbleached pulp properties.	81
Table 3.3 Extracted mesquite bleached pulp properties.....	81
Table 3.4 Kinetic parameters for MB adsorption by carboxymethyl cellulose/Fe ₃ O ₄ nanocomposite.	104

List of figures

Figure 1.1 Mesquite trees in the Sudan dryland (Dafalla et al., 2016)	2
Figure 1.2 Wood Structure: i) Cell wall, Part ii) and iii) composition of the interaction between cellulose, hemicelluloses and lignin.....	5
Figure 1.3: Structure of softwood xylan.....	8
Figure 1.4 Structure of hardwood xylan.....	8
Figure 1.5: The structure of softwood glucomannan	8
Figure 1.6: Structure of hardwood glucomannan.....	10
Figure 1.7: The minor hemicellulose components in wood.	10
Figure 1.8: Inter and intra-molecular bonds in lignin	12
Figure 1.9: Covalent bonds between lignin and polysaccharides.....	13
Figure 1.10: The conjugated chromophore structures present in wood lignin.	13
Figure 1.11 Molecular structure of cellulose representing the cellobiose units.	17
Figure 1.12: Cellulose structures with the intramolecular hydrogen bonding.	17
Figure 1.13: Fringed fibril model of the supramolecular structure of cellulose...	19
Figure 1.14: Composition of chlorine –water system at different PH.	50
Figure 1.15 : Structure of carboxymethylcellulose.	58
Figure 1.16: Structure of Hydroxypropylcellulose	61
Figure 1.17: Structure of methylcellulose.....	63
Figure 3.1 : (A) Effect of DMS on DS of MC, (B) Effect of reaction time on DS of MC.	82
Figure 3.2: (A) Effect of NaOH concentration of DS CMC, (B) Effect of amount of MCA on DS of CMC.	83
Figure 3.3 : (A) Effect of PO concentration on DS of HPC, (B) Effect of reaction time on DS of HPC.....	84
Figure 3.4 FT-IR spectrums of cellulose and cellulose and cellulosic ether derivatives.....	85
Figure 3.5 XRD patterns of cellulose and cellulosic ether derivatives.	87
Figure 3.6 Thermal analysis curves (A) TGA, (B) DTG, (C) DTA of cellulose and cellulosic derivatives.	90
Figure 3.7: (A) ^{13}C NMR (B) ^1H NMR spectrum of methylcellulose in DMSO.....	92
Figure 3.8: ^{13}C NMR of carboxymethylcellulose in DMSO.....	93
Figure 3.9: ^{13}C NMR of hydroxypropylcellulose in DMSO.....	94

Figure 3.10: FT-IR spectrum of stabilized magnetite nanocomposite and their stabilizer. (A) HPC/Fe ₃ O ₄ (B) MC/Fe ₃ O ₄ (C) CMC/Fe ₃ O ₄	96
Figure 3.11: XRD spectrum patterns of magnetite and their stabilizer.	98
Figure 3.12: TGA curves of stabilized magnetite nanoparticles and their stabilizer. (A) HPC/Fe ₃ O ₄ (B) CMC /Fe ₃ O ₄ (C) MC /Fe ₃ O ₄	100
Figure 3.13: Effect of PH on adsorption capacity of nanocomposite.....	102
Figure 3.14 Effect of time on adsorption capacity of nanocomposite	102
Figure 3.15: Effect of MB concentration on adsorption capacity nanocomposite	103

List of schemes

Scheme 1.1 Phenylpropanoid polymer lignin and its precursor structures.....	11
Scheme1. 2 : Reactions of a coniferaldehyde structure with sodium sulfite.....	25
Scheme1. 3: Sulfonation of a quinone structure by sodium sulfite.	25
Scheme1.4: Cleavage of phenolic β -O-4 structures in lignin during Kraft pulping conditions and competing reactions in the L denotes a lignin residue.	27
Scheme1. 5: Cleavage of non-phenolic β -O-4 structures in Kraft pulping.....	28
Scheme1.6: Formation of stilbenes from β -5 and β -1 lignin sub-structures in Kraft pulping.....	29
Scheme1. 7: Mechanism for the peeling reaction in Kraft pulping.	29
Scheme1.8: β -elimination in polysaccharide end groups resulting in a stopping reaction and formation of a metasaccharinic acid.	31
Scheme1.9: Alkaline hydrolysis of a glucosidic linkage	31
Scheme1.10: The elimination of methanol from 4-O-methylglucuronic acid.	33
Scheme1.11: Sulphonation of lignin in acidic sulphite pulping.	34
Scheme1.12: Sulphonation of lignin in neutral sulphite pulping	35
Scheme1.13: Mechanism for the acid catalysed condensation in lignin.....	35
Scheme1. 14: Mechanism for the alkaline cleavage of phenolic β -O-4 structures in lignin by anthrahydroquinone	36
Scheme1. 15: Formation of malodorous compounds in Kraft pulping.....	38
Scheme1. 16: Solvolytic cleavage of a phenolic α -aryl ether linkage via a quinone methide.....	39
Scheme1. 17: Quinone methide formation with α -ether cleavage on free phenolic.	40
Scheme1. 18: Oxidation of a phenol with oxygen in alkaline media.	43
Scheme1. 19: Major carbohydrate reactions the oxygenbleaches.....	44
Scheme1.20: Chain cleavage of a phenolic β -O-4 structure in lignin on oxidation with alkaline hydrogen peroxide	45
Scheme1.21: Decomposition reactions of hydrogen peroxide in alkaline solution. Influence of transition metal ions.	46

Scheme1.22: Possible modes of formation of carbonyl groups in carbohydrates on oxidation with oxygen in alkaline media.	46
Scheme1. 23: Reactions between a phenolic and a non-phenolic lignin structure with chlorine dioxide under acidic conditions.	48
Scheme1. 24: Reactions between a conjugated aromatic structure and chlorine dioxide under mild acidic conditions.	48
Scheme1. 25: Acidic hydrolysis of hexenuronic acid resulting in the formation of 5-formylfuroic(FFA) acid and furoic acid(FA).	48
Scheme1. 26: Reaction modes of lignin, in pulp bleaching with chlorine.	50
Scheme1. 27: Oxidation of aromatic structures.	52
Scheme1.28: Reaction sequence for the oxidation of aromatic lignin structures with peracetic acid.	52
Scheme1. 30: Lignin reactions in an alkaline extraction stage.	53
Scheme1. 31: Cellulose derivatives.	55
Scheme1. 32 : synthesis of cellulosic ether derivatives.	57
Scheme1.33: Reaction mechanism of synthesizing carboxymethylcellulose.	59
Scheme1.34: Reaction mechanism of iron oxide formation in the presence of a strong base.	65

List of abbreviations

AGU	Anhydroglucopyranose unit
AHQ	Anthrahydroquinone
AQ	Anthraquinone
ASAM	Alkali-sulphite-antraquinone-methanol
AS-AQ	Alkaline -Sulfite -Anthraquinone pulping
CTMP	Chemo-Thermo- Mechanical Pulping
CMC	Carboxymethylcellulose
DMS	Dimethyl sulfite
DP	Degree of polymerization
DS	Degree of substitution
ECF	Elemental chlorine free bleaching
HPC	Hydroxypropylcellulose
MC	Methylcellulose
MCA	Monochloroacetic acid
PO	Propylene oxide
TMP	Thermo- mechanical Pulping
TCF	Totally chlorine free bleaching

Chapter one

Introduction and literature review

1 Introduction and literature review

1.1 *Prosopis* spp. (Mesquite)

Prosopis spp. (Mesquite), includes 44 species worldwide (Figure 1.1). It's a xerophytic evergreen tree which grows in a wide array of environments. And not restricted by soil type, pH or salinity. It grows in semi-arid and arid tracts of tropical and sub-tropical regions of the world and they are fast spreading because the leaves are unpalatable and animals do not digest its seeds (Prabha et al. 2014). Some of the many adaptive abilities that allow mesquite to thrive under such conditions include ability of roots to adapt to a wide variety of soil conditions. Roots can grow upwards towards the soil surface to capitalize on little rainfall, but can also grow to depths of 80 m and extend laterally more than 30 m. This is the most extensive root system of any plant. Therefore, most of the native plants growing around a mesquite tree become withered and died (Oshino et al. 2012). *Prosopis* spp. (Mesquite) tree is native to South and North America was cultivated in Sudan in 1917, it was planted in Khartoum and eastern Sudan to check desert encroachment (Suliman et al. 2015; Talaat Dafalla et al., 2016). The common mesquite species in the Sudan are *Prosopis chilensis* and *Prosopis juliflora*. However, the introduction of mesquite into Sudan invaded both natural and managed habitats, including watercourses, floodplains, highways, degraded abandoned land and irrigated areas (Oshino et al., 2012). As a consequence, the livelihood of many rural communities in Sudan has been adversely affected. Accordingly, the Government of Sudan, in 1995, considered mesquite as a noxious weed and a Presidential Decree for its eradication was issued (Suliman et al., 2015). No efficient and cost effective methods have been found in Sudan, or elsewhere for complete eradication of mesquite. Several authors have suggested

that; the term eradication should be replaced by control, as it became clear that total eradication of mesquite from a site, once invaded, could not prevent further desert encroachment (Talaat Dafalla et al., 2016). Due to the high cost of its eradication, many attempts have been conducted to explore socio-economics of mesquite and focus in controlling mesquite through utilization, processing and marketing. For example, mesquite pod has been used for ethanol production (Silva et al., 2011), paper making (Goel and Behl., 2001) and activated carbon production for waste water treatment (Hamza 2013).



Figure 1.1 Mesquite trees in the Sudan dryland (Dafalla et al., 2016)

1.1.1 Taxonomy of mesquite tree

Kingdom: *Plantae*
Domain: *Eukaryota*
Phylum: *Spermatophyta*
Subphylum: *Angiospermae*
Class: *Dicotyledonae*
Family: *Mimosaceae*
Subfamily: *Mimosoideae*
Genus: *Prosopis*

1.2 Wood structure and chemical composition

Softwoods are woods that come from gymnosperms (mostly conifers), and hardwoods are woods that come from angiosperms (flowering plants). Softwoods are generally needle-leaved evergreen trees such as pine (*Pinus*) and spruce (*Picea*), whereas hardwoods are typically broadleaf, deciduous trees such as maple (*Acer*) and birch (Gellerstedt et al. 2009). An important cellular similarity between softwoods and hardwoods is that in both kinds of wood, most of the cells are dead at maturity even in the sapwood. The cells that are alive at maturity are known as parenchyma cells, and can be found in both softwoods and hardwoods. Additionally, despite what one might conclude based on the names, not all softwoods have soft, lightweight wood, nor do all hardwoods have hard, heavy wood (Sixta 2006).

A single plant cell consists of two primary domains: the protoplast and the cell wall. The protoplast is the sum of the living contents that are bound by the cell membrane. The cell wall is a non-living, largely carbohydrate matrix extruded by the protoplast to the exterior of the cell membrane (Sjostrom 1993). The plant cell wall protects the protoplast from osmotic lysis and can provide significant mechanical support to the plant. For cells in wood, the situation is somewhat more complicated than this highly generalized case. In many cases in wood, the ultimate function of the cell is borne solely by the cell wall. Thus many mature wood cells not only do not require their protoplasts, but indeed must completely remove their protoplasts prior to achieving functional maturity. For this reason, it is a common convention in wood literature to refer to a cell wall without a protoplast as a cell. In the case of a mature cell in wood, the open portion of the cell where the protoplast would have existed is known as the lumen. Thus, in most cells in wood there are two domains, the cell wall and the cell lumen (Gellerstedt et al. 2009).

Cell walls in wood are important structures. Unlike the lumen, which is a void space, of a highly regular structure, from one cell type to another, between species, and even when comparing softwoods and hardwoods. The cell wall consists of three main regions: the middle lamella, the primary wall, and the secondary wall. Table 1.1 shows the percentage of wood components of different wood species. In each region, the cell wall has three major components: cellulose microfibrils with characteristic distributions and organization (Figure 1.2), hemicelluloses, and a matrix or encrusting material, typically pectin in primary walls and lignin in secondary walls (Panshin and deZeeuw 1980). To understand these wall layers and their interrelationships, it is necessary to know that plant cells, generally, do not exist singly in nature; instead they are adjacent to many other cells, and this association of thousands of cells, taken together, form an organ such as a leaf. Each individual cells must adhere to others in a coherent way to ensure that they act as a unified whole. This means that they must be interconnected with one another to permit the movement of biochemicals and water. This adhesion is provided by the middle lamella, the layer of cell wall material between two or more cells, part of which is contributed by each of the individual cells. This layer is the outermost layer of the cell wall continuum, and in a non-woody organ is pectin rich. In the case of wood, the middle lamella is lignified. The next layer, formed by the protoplast just interior to the middle lamella, is the primary wall. The primary wall is characterized by a largely random orientation of cellulose microfibrils, like thin threads wound round and round a balloon in random order, where any microfibril angle from 0 to 90 degrees relative to the long axis of the cell may be present (Barnett and Bonham 2004). In wood cells, the primary wall is very thin, and is, generally, indistinguishable from the middle lamella. For this reason, the term compound middle lamella is used to denote the primary cell wall, the middle lamella, and the primary cell wall of the adjacent cell.

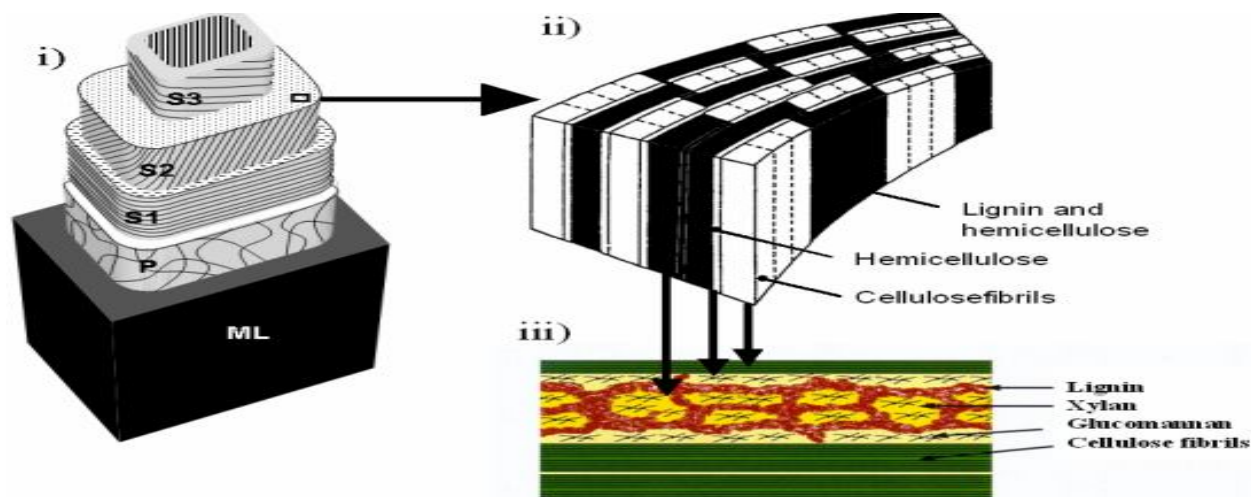


Figure 1.2 Wood Structure: i) Cell wall, Part ii) and iii) composition of the interaction between cellulose, hemicelluloses and lignin.

Species	Common name	Extractives*	Lignin	Cellulose	Glucoman- nan	Glucuro- noxylan	Other polysac- charides
Softwoods							
<i>Abies balsamea</i>	Balsam fir	2.7	29.1	38.8	17.4	8.4	2.7
<i>Pseudotsuga menziesii</i>	Douglas fir	5.3	29.3	38.8	17.5	5.4	3.4
<i>Tsuga canadensis</i>	Eastern hemlock	3.4	30.5	37.7	18.5	6.5	2.9
<i>Juniperus communis</i>	Common juniper	3.2	32.1	33.0	16.4	10.7	3.2
<i>Pinus radiata</i>	Monterey pine	1.8	27.2	37.4	20.4	8.5	4.3
<i>Pinus sylvestris</i>	Scots pine	3.5	27.7	40.0	16.0	8.9	3.6
<i>Picea abies</i>	Norway spruce	1.7	27.4	41.7	16.3	8.6	3.4
<i>Picea glauca</i>	White spruce	2.1	27.5	39.5	17.2	10.4	3.0
<i>Larix sibirica</i>	Siberian larch	1.8	26.8	41.4	14.1	6.8	8.7
Hardwoods							
<i>Acer rubrum</i>	Red maple	3.2	25.4	42.0	3.1	22.1	3.7
<i>Acer saccharum</i>	Sugar maple	2.5	25.2	40.7	3.7	23.6	3.5
<i>Fagus sylvatica</i>	Common beech	1.2	24.8	39.4	1.3	27.8	4.2
<i>Betula verrucosa</i>	Silver birch	3.2	22.0	41.0	2.3	27.5	2.6
<i>Betula papyrifera</i>	Paper birch	2.6	21.4	39.4	1.4	29.7	3.4
<i>Alnus incana</i>	Gray alder	4.6	24.8	38.3	2.8	25.8	2.3
<i>Eucalyptus globulus</i>	Blue gum	1.3	21.9	51.3	1.4	19.9	3.9
<i>Acacia mollissima</i>	Black wattle	1.8	20.8	42.9	2.6	28.2	2.8

Table 1.1: wood components of different wood species.

The compound middle lamella in wood is almost invariably lignified. The remaining cell wall domain, found in, virtually all cells in wood, is the secondary cell wall. The secondary cell wall is composed of three layers. The first-formed secondary cell wall layer is the S1 layer which is adjacent to compound middle lamella (or technically the primary wall). This layer is a thin layer and is characterized by a large microfibril angle. That is to say, the cellulose microfibrils are laid down in a helical fashion, and the angle between the mean microfibril direction and the long axis of the cell is large. The next wall layer is the S2 layer. This is the thickest secondary cell wall layer and it makes the greatest contribution to the overall properties of the cell wall. It is characterized by a lower lignin percentage and a low microfibril angle. Interior to the S2 layer is the S3 layer, a relatively thin wall layer. The microfibril angle of this layer is relatively high and similar to that of S1. This layer has the lowest percentage of lignin of any of the secondary wall layers (Sixta 2006).

1.2.1 Hemicelluloses

Hemicelluloses are the second most abundant polysaccharides in nature after cellulose. They occur in close association with cellulose and lignin and contribute to the rigidity of plant cell walls in lignified tissues. Hemicelluloses constitute about 20–30% of the total mass of annual and perennial plants and have a heterogeneous composition of various sugar units, depending on the type of plant and extraction process, being classified as xylans (β -1,4-linked D-xylose units), mannans (β -1,4-linked D-mannose units), arabinans (α -1,5-linked L-arabinose units), and galactans (β -1,3-linked D-galactose units) (Eduardo et al. 2012).

Almost all plants contain xylan(Figure 1.3).D-Xylosyls are linked to form homopolymer linear molecules as the main chain. Xylan hemicellulose is the glucan with a backbone of 1, 4- β -D-xylopyranose and branch chains of 4-oxymethylglucuronic acid(Teleman et al. 2002).

Hemicellulose of hardwoods and gramineous forbs is mainly composed of this kind of polysaccharide(Figure 1.4). The hemicellulose of Gramineae also contains L-arabinofuranose linking to the main chain as branch chains. The number of branch chains depends on different kinds of plants. The typical molecular structure of hemicellulose of Gramineae is chiefly composed of β -D-xylopyranosyl, which is linked by β -1, 4-glucosidic bonds. Branch chains consist of L-arabinofuranosyl and D -glucuronopyranosyl, respectively, on C3 and C2 of the main chain; there are also branch chains composed of xylosyl and acetyl (xylosyl acetate). Xylan hemicellulose in softwoods is 4-O methyl-glucuronic acid arabinose-xylan with almost no acetyl(Davis, 1985; Eduardo et al., 2012).

For the mannan hemicellulose of softwoods, glucose and mannose arrange randomly to form the main chain(Figure 1.5);galactosyl is linked to the glucose or mannose of the main chain by α -(1, 6) bonds, and acetyl seems to be evenly distributed on the C2 and C3 of mannose(Polle 2009).

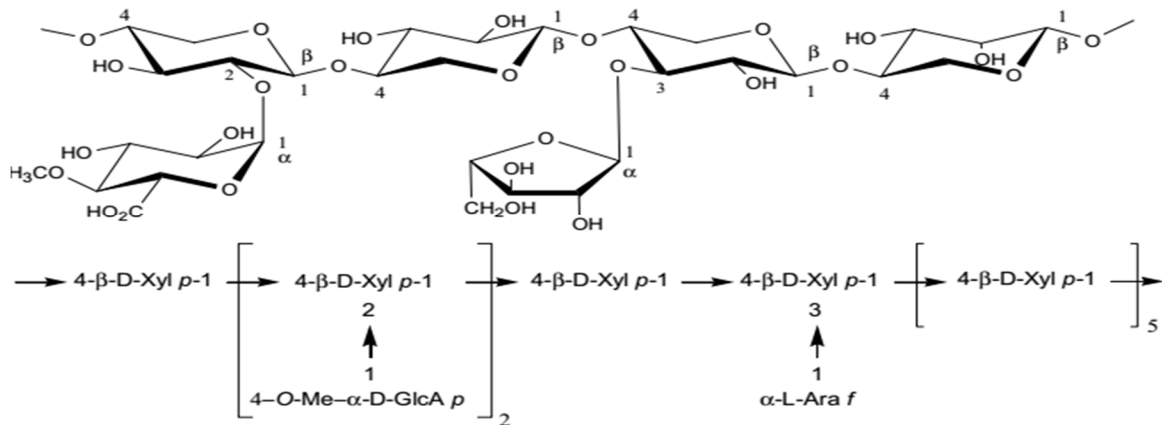


Figure 1.3: structure of softwood xylan.

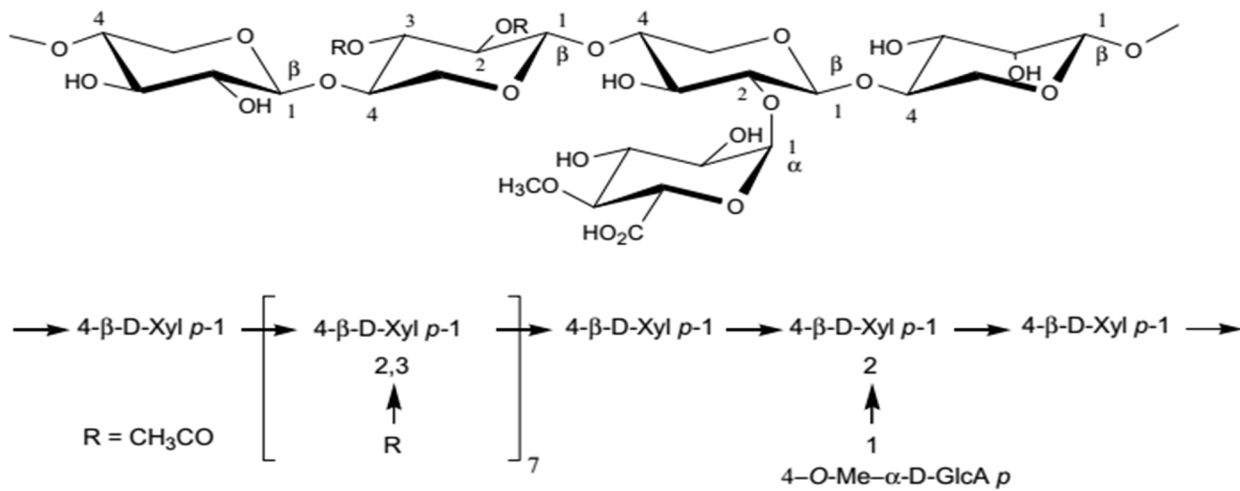


Figure 1.4 Structure of hardwood xylan

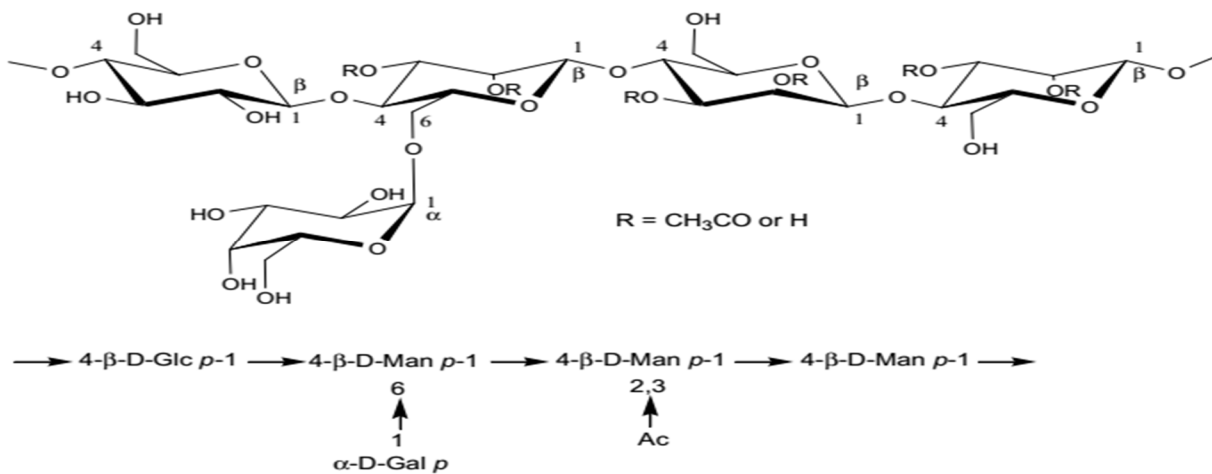


Figure 1.5: The structure of softwood glucomannan

In hard wood glucomannan, mannose and glucose are linked by β (1, 4) bonds to form inhomogeneous polymer as the main chain, (Figure 1.6). The main chain of mannan hemicellulose in hardwoods is composed of glucose and mannose, whether it is acetylated remains unclear(Polle 2009).

The minor hemicellulose units in wood include arabinogalactan (Figure 1.7). It has a backbone of β -(1, 3)-linked D-galactopyranose units and is highly branched at C6. The side chains are composed of β -(1, 6)-linked D-galactose units, D-galactose and L-arabinose units or single L-arabinose units and single D-glucuronic acid units(Willför et al. 2002).

Rhamnogalacturonan has a backbone of α -(1, 4)-linked D-galacturonic acid units and α - (1, 2) or α -(1, 4)-linked L-rhamnose(Davis, 1985; Morris et al., 2010). A galactan sometimes termed pectic galactan has a backbone of β -(1,4)-linked D-galactose units, partly substituted at the hydroxyl group of C6 with galacturonic acid units(Pierre et al. 2014).

Arabinan has backbone consists of α -(1, 5)-linked arabinose units with side chains of arabinose units joined by α -(1, 3) linkages(Dourado et al. 2006). Xyloglucan has the same backbone as cellulose with β -(1, 4)-linked D-glucose units, unlike in cellulose, there are side chains attached at the hydroxyl group of C6 in xyloglucans. The side chains consist either of single xylose units or of galactose, arabinose or fucose units (1, 2)-linked to xylose(Roger et al., 1989 ; Y. Kato and S. Ito 2008).

Xylem and laricinan consist of a backbone of β -(1, 3)-linked glucose units. Laricinan also has a small number of β -(1, 4)-linked glucose units and a few side chains of several glucuronic acid units and some galacturonic acid units(Hoffmann and Timell 1970).

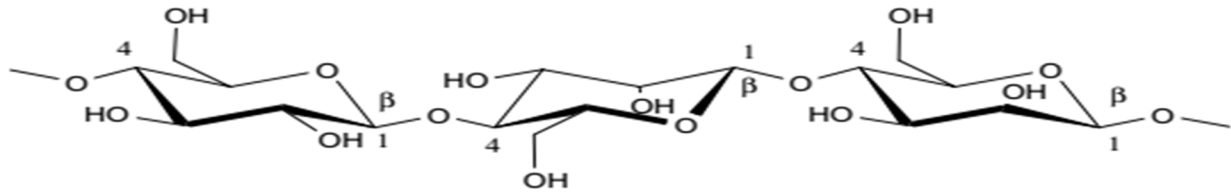
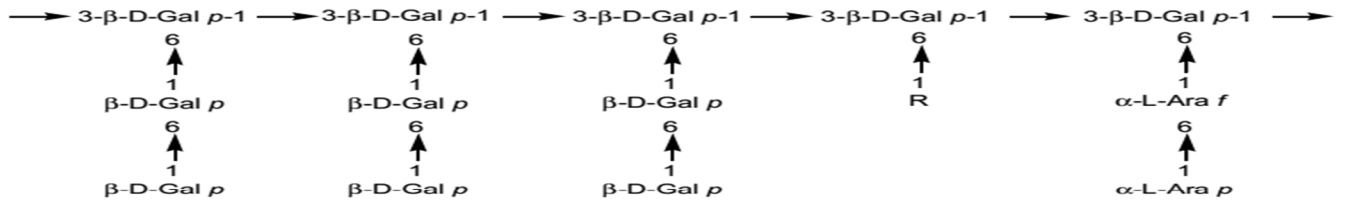


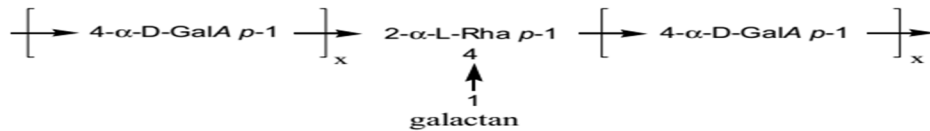
Figure1.6: Structure of hardwood glucomannan

Arabinogalactan

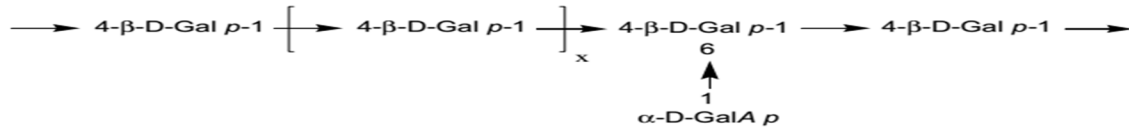


R = β-D-Gal *p*, α-L-Ara *f* or β-D-GlcA *p*

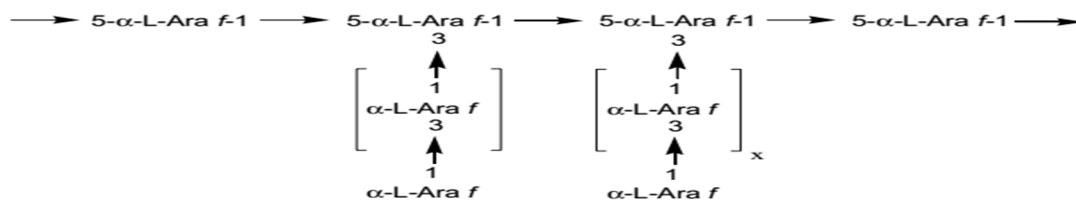
Rhamnogalacturonan



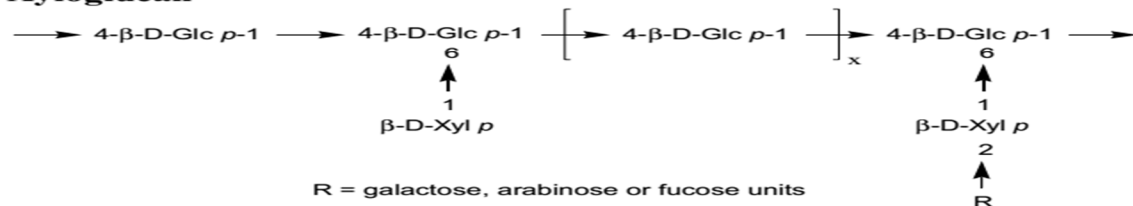
"Pectic" galactan



Arabinan



Xyloglucan



Laricinan (1->3-β-D-glucan)

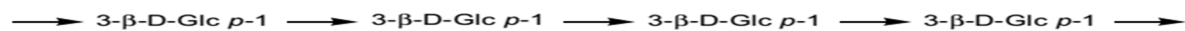
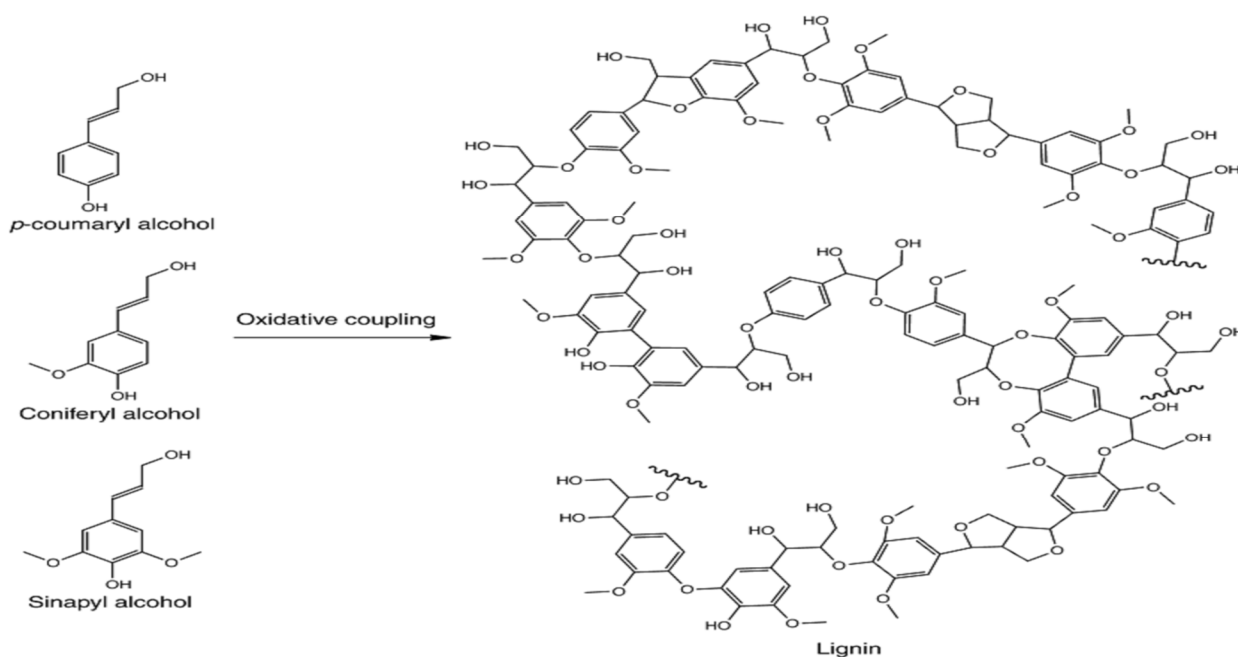


Figure1.7: The minor hemicellulose components in wood.

1.2.2 Lignin

Lignin is the third abundant and important organic substance in the plant kingdom. Its name derived from the Latin (lignum)for wood. Lignin can be described as a three-dimensional macromolecule with high molecular weight. It originates from phenylpropanoid precursors such as coumaryl, coniferyl, and sinapyl alcohol C_6C_3 , (Scheme 1.1) and is present in vascular plants. In the woody tissue of angiosperms, it is found in tracheids, fiber, vessels, and parenchyma cells (Whetten and Sederoff 1995).



Scheme 1.1 Phenylpropanoid polymer lignin and its precursor structures.

The proposed inter- and intra-molecular bonds involving lignin monomers and other polymers in the cell wall are C-O-C (ether) and C-C linkages, C-O-C linkages is the dominant. Phenylpropane units are joined together through (β -O-4, α -O-4, 5-5, 4-O-5, β -1, and β - β) bonds (Figure 1.8) (Abreu et al. 2009).

The possible existence of covalent bonds between lignin and polysaccharides has been a subject of much debate and intensive studies (Abreu et al. 2009). It is

obviously and now generally accepted that such chemical bonds must exist, and the term “lignin-carbohydrate complex (LCC)” is used for the covalently bonded aggregates of this type(Figure 1.9). Chemical bonds have been reported between lignin and practically all the hemicellulose constituents (even between lignin and cellulose). These linkages can be either of ester or ether type and even glycosidic bonds are possible(Abreu et al. 2009).

The major chromophore present in wood lignin is coniferaldehyde which has an abundance of around 5 units per 100 phenylpropane units. Its UV-maximum in solution is around 350 nm but in the solid state a strong red-shift to around 400 nm can be observed. Thus, this structure is yellow and can be assumed to be the predominant contributor to the wood color. Other types of conjugated carbonyl structures present in smaller or trace amounts include D-keto structures, ortho- and para-quinones and dienone structures (Figure 1.10). The natural abundance of iron in wood is present as iron-catechol the red complex, thus, contributing to the wood color.

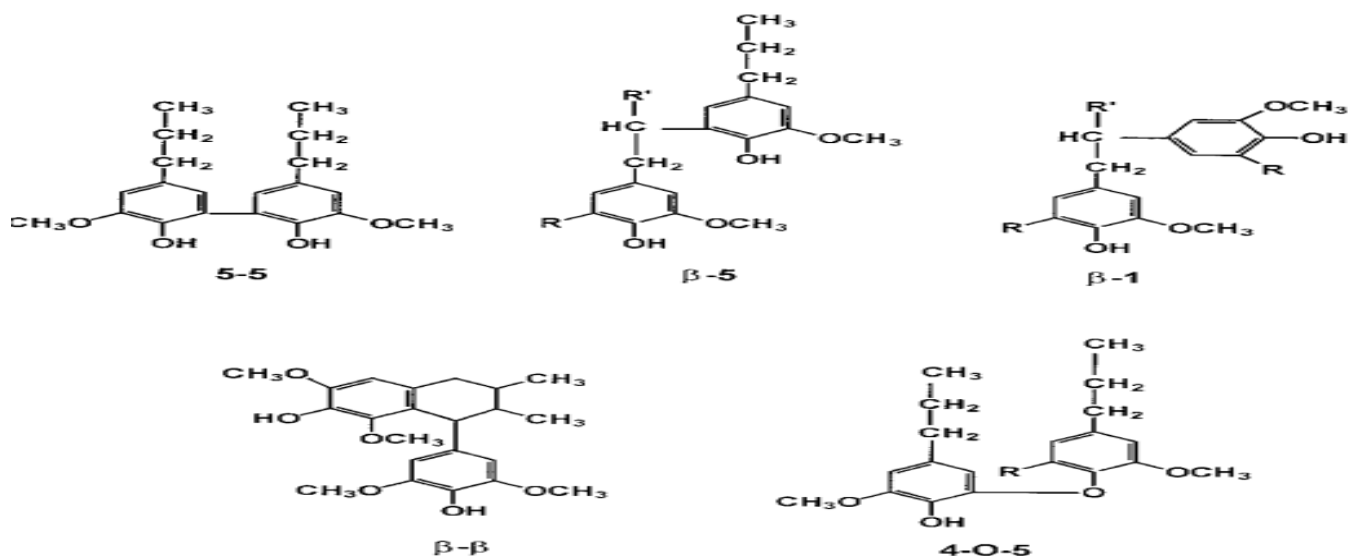


Figure1.8: Inter and intra-molecular bonds in lignin monomers and other polymers.

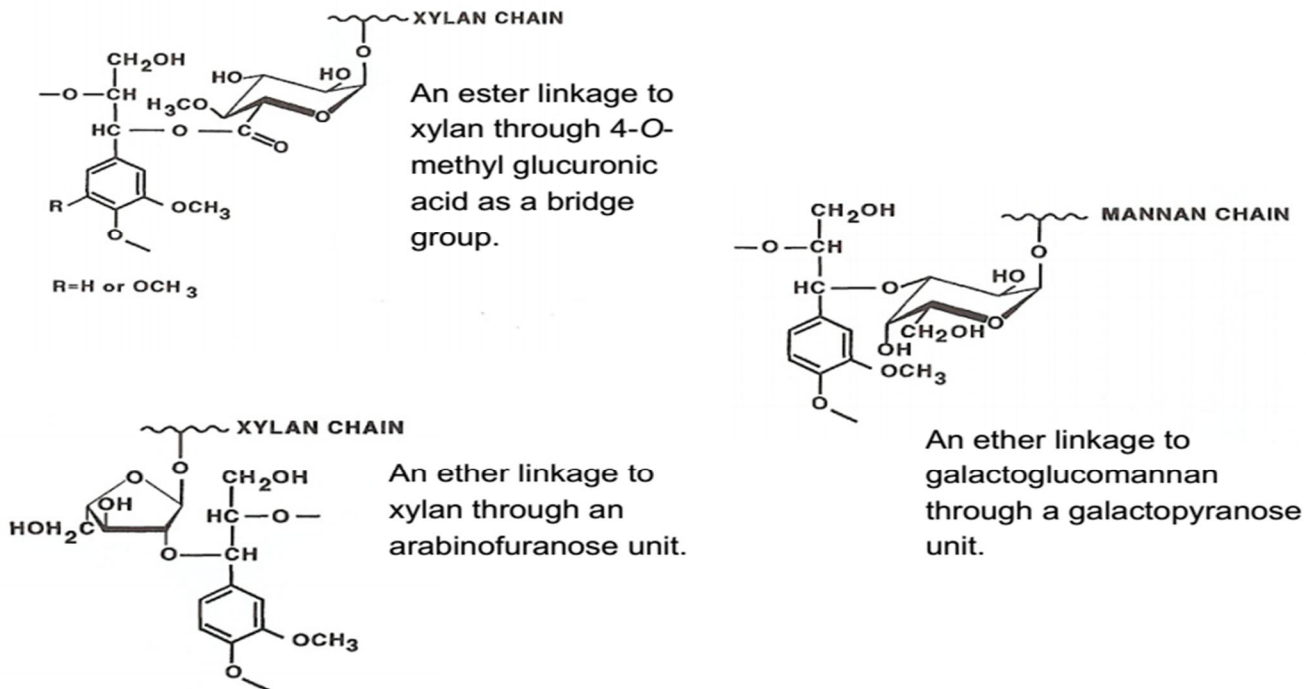


Figure1.9: Covalent bonds between lignin and polysaccharides.

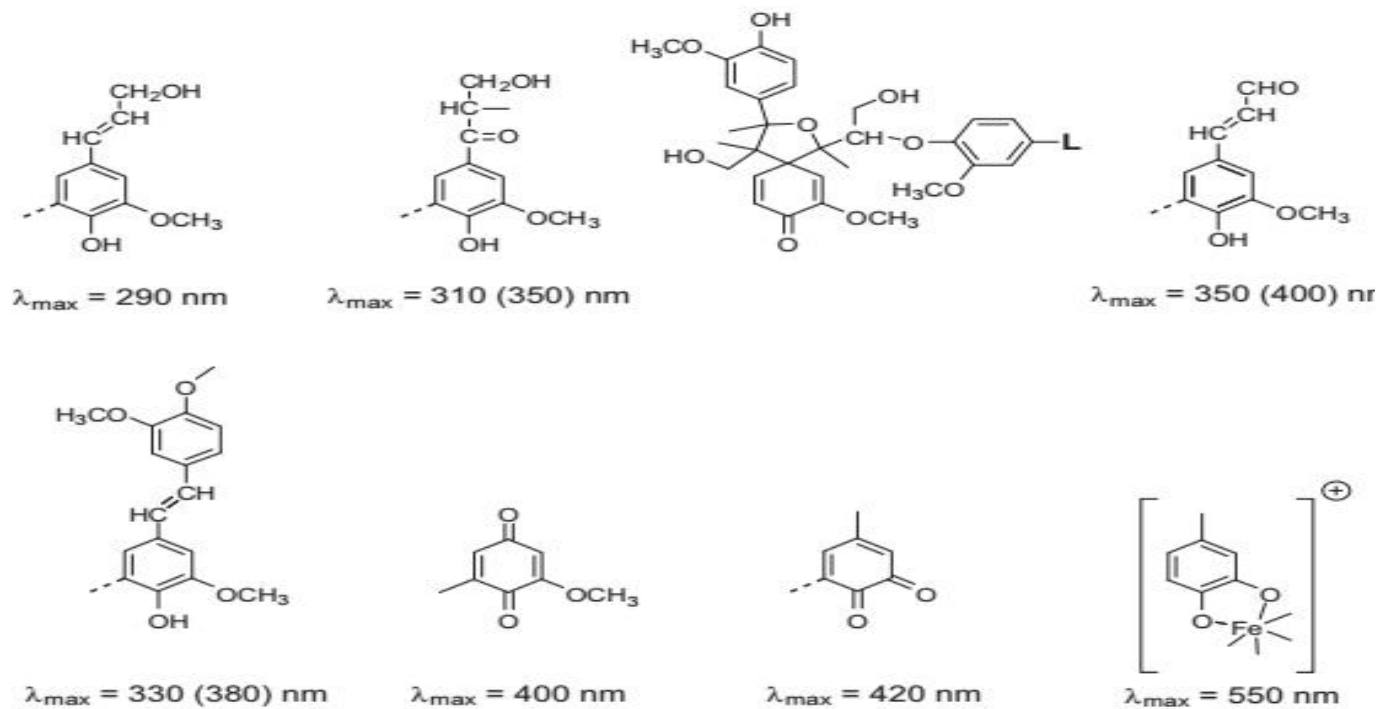


Figure1.10: The conjugated chromophore structures present in wood lignin.

1.2.3 Cellulose

Cellulose is the most abundant polymer on Earth, which makes it also the most common organic compound and the most abundant renewable and biodegradable polymer. It is a promising feedstock for the production of chemicals for various chemical industries. Annual cellulose land plants synthesis is close to 10^{12} tons (Sixta 2006). Plants contain approximately 33% cellulose whereas wood contains around 50 per cent and cotton contains 90% (Brown 1999). In plants, extended cellulose chains are aligned in sheets that are stabilized by intra and intermolecular hydrogen bonding. The stabilized sheets form a 3D-structure of cellulose called microfibrils. Subsequently, the microfibrils form larger microfibril aggregates, which are incorporated into the plant fiber cell wall with the other main components of wood. The microfibrils contain both less-ordered cellulose, and ordered regions with crystalline cellulose. Wood cells, consist of several cell wall layers with various cellulosic compositions and have different orientations of microfibril aggregates (Brown 1999). This arrangement within the cell walls is crucial for the high strength performances of the cellulose fiber. The size of microfibrils, microfibril aggregates, and the fiber are source dependent (Gellerstedt et al. 2009). For wood the microfibrils and microfibril aggregates have a lateral dimension of 2-4 nm and 10-30 nm, respectively, and the length of microfibrils can

be up to a few micrometers. The wood fiber is normally some tens of a micrometer in diameter, and 1-4 mm long (Gellerstedt et al. 2009).

1.2.3.1 Structure and reactivity of cellulose

Cellulose is a carbohydrate made up of glucose units. These have an empirical formula, $C_6H_{12}O_6$. The chemical and physical properties of cellulose can only be properly understood by acquiring knowledge of the chemical nature of the cellulose molecule in addition to its structure and morphology in the solid state (D. Klemm et al. 1998). A profound understanding of the structural properties of native cellulose is a requirement to understand the effects of different substituents on the chemical and physical properties of cellulose and its derivatives. When considering macromolecules of any kind, three structural levels must be distinguished, molecular level, supra-molecular level, and morphological level.

1.2.3.2 Cellulose molecule at the molecular level

Payen was the first to determine the elemental composition of cellulose as early as in 1838 (D. Klemm et al. 1998). He found that cellulose contains 44 to 45% carbon, 6 to 6.5% hydrogen and the rest consisting of oxygen. Based on these data, the empirical formula was deduced to be $C_6H_{10}O_5$. However, the actual macromolecular structure of cellulose was still unclear. Haworth proposed a chain-like macromolecular structure in the late 1920s, whereas Staudinger delivered the final proof of the highly polymer nature of the cellulose molecule (Liu and Sun 2010). Cellulose is a linear and fairly rigid homopolymer consisting of D-anhydroglucopyranose units (AGU). These units are linked by β -(1 \rightarrow 4) glycosidic bonds formed between C-1 and C-4 of adjacent glucose moieties. In the solid state, AGU units are rotated by 180° with respect to each other due to the constraints of β -linkage. Each of the AGU units has three hydroxyl (OH) groups at C-2, C-3 and C-6 positions. Terminal groups at the either end of the cellulose molecule are quite

different in nature from each other (Figure 1.11). The C-1 OH at one end of the molecule is an aldehyde group with reducing activity. Aldehyde groups form a pyranose ring through an intramolecular hemiacetal form. In contrast, the C-4 OH on the other end of the chain is an alcoholborne OH constituent and thus is called the non-reducing end. It has been known from the infrared spectroscopy (IR), X-ray crystallography and nuclear magnetic resonance (NMR) investigations, that the AGU ring exists in the pyranose ring, and that this adopts the $4C_1$ -chair formation which constitutes the lowest energy conformation for D-glucopyranose (Kennedy and Pons 1995). The chain length of the cellulose polymer varies depending on the cellulose source. For example, naturally occurring vascular plant cellulose has a degree of polymerisation (*DP*) higher than 10000 (Perez and Mazeau 2005). The value of *DP* is greatly dependent on the method of isolation and therefore, the cellulose used in practice has an average *DP* of between 800-3000 (Perez and Mazeau 2005). In its commonly used form, isolated cellulose is always polydisperse. Like all polymers, it is a mixture of molecules that has the same basic composition but differs in the chain length. Therefore, the molecular mass and the *DP* of cellulose can only be considered as average values. The chemical character and reactivity of cellulose is determined by the presence of three equatorially positioned OH groups in the AGU, one primary and two secondary groups. In addition, the β -glycosidic linkages of cellulose are susceptible to hydrolytic attack (D. Klemm et al. 1998).

The hydroxyl groups are responsible for the extensive hydrogen bonding network forming both, intra- and intermolecular hydrogen bonding (Figure 1.12). There are two possible mechanisms by which the OH groups in the cellulose molecule form hydrogen bonds. One is by the interaction between suitably positioned OH groups in the same molecule (intramolecular). These are located between C2-OH and C6-

OH groups and C3-OH with endocyclic oxygen (Gardner and Blackwell 1974). The other mechanism occurs when neighbouring cellulose chains (intermolecular) interact via their C3-OH and C6-OH groups. Intramolecular hydrogen bonds between the hydroxyl group at the C-3 and oxygen of the pyranose ring were first described in the 1960s by (Marchessault and Liang 1960) who claimed the existence of a second 'pair' of intramolecular hydrogen bonds between the C-6 and C-2 of the neighbouring AGUs.

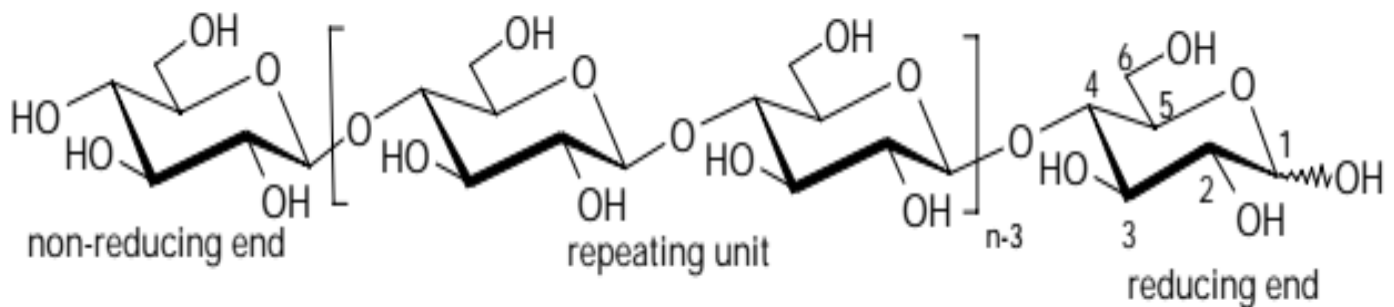


Figure 1.11 Molecular structure of cellulose representing the cellobiose units.

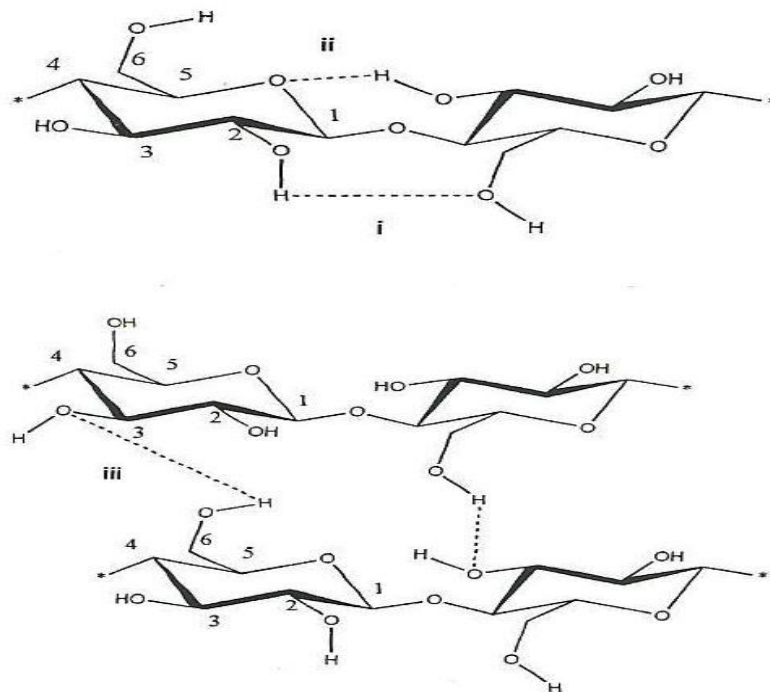


Figure 1.12: Cellulose structures with the intramolecular hydrogen bonding.

Cellulose is regarded as a semi-flexible polymer. The relative stiffness and rigidity of the cellulose molecule is mainly due to the intra-molecular hydrogen bonding. This property is reflected in its high viscosity in solution, a high tendency to crystallize, and its ability to form fibrillar strands. The chain stiffness property is further favoured by the β -glucosidic linkage that bestows the linear form of the chain. The chair conformation of the pyranose ring also contributes to chain stiffness. This is in contrast to the α -glucosidic bonds of starch (Barrows et al. 1995)

1.2.3.3 Supramolecular structure of cellulose

Cellulose chains have a strong tendency to aggregate and to form highly ordered structures and structural entities. The highly regular constitution of the cellulose molecule, the stiffness of the molecular chain and the extensive hydrogen bonding capacity favor molecular alignment and aggregation. Based on these findings, and the theories on the macromolecular structure, scientists developed the ‘fringed fibrillar’ model of the structure (Figure 1.13), which is still the prevailing accepted theory of the supramolecular structure (S. Hearle 1958).

The supramolecular model of cellulose is based on the organization of cellulose chains into parallel arrangements of crystallites and crystallite strands, which are the basic elements of the fibers. The intermolecular hydrogen bonding between C6-OH and C3-OH of adjacent chains are considered to be the major contributors to the structure of cellulose, and is regarded as the predominant factor responsible for uniform packing (D. Klemm et al. 1998). In turn, the consistency of the interchain interactions is governed by the high spatial regularity and availability of the hydroxyl groups. The order of molecules in a cellulose fiber is far from uniform throughout the whole structure, and so it can be assumed that there exist regions within the structure, that have varying amounts of order. Experimental

evidence describes a two-phase model, which clearly divides the supramolecular structure into two regions: low ordered (amorphous) and highly ordered (crystalline) excluding the medium ordered regions completely(D. Klemm et al. 1998).

Cellulose exists in several polymorph (classes I, II, III, IV) that differ in their unit cell dimensions(Table 1.2).

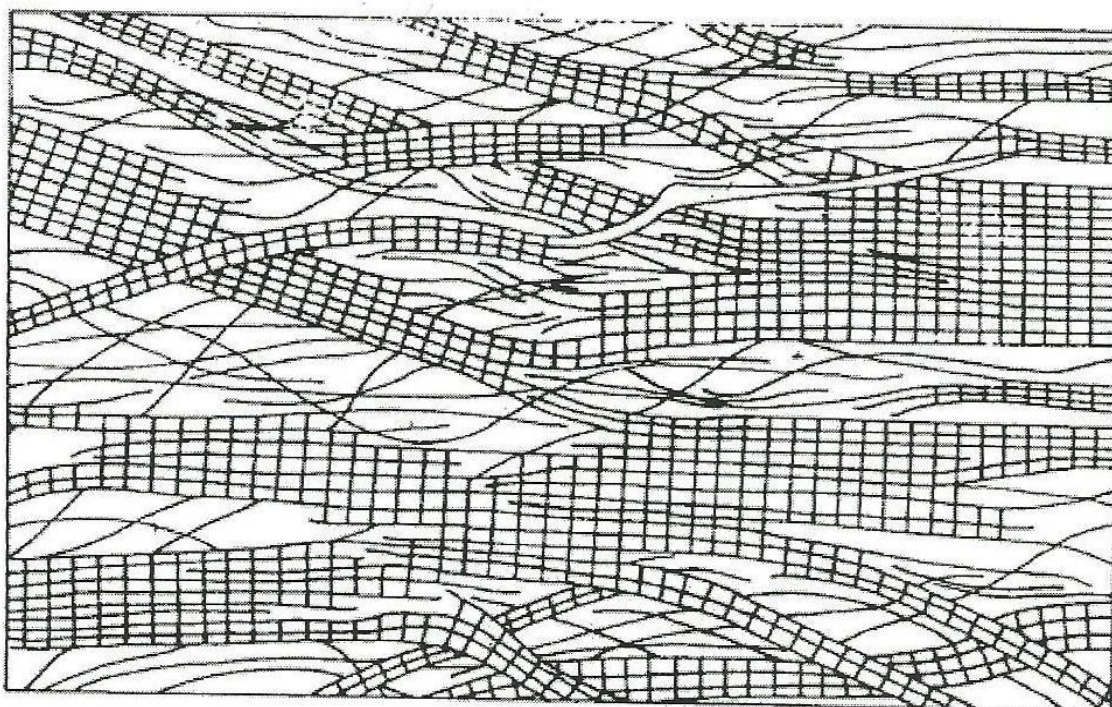


Figure1.13: Fringed fibril model of the supramolecular structure of cellulose.

Table1. 2: Unit cell dimensions of cellulose polymorphs I, II, III and Cellulose IV.

<i>a</i> -axis (Å)	<i>b</i> -axis (Å)	<i>c</i> -axis (Å)	γ (deg)a	Polymorph
7.85	8.17	10.34	96.4	Cellulose I
9.08	7.92	10.34	117.3	Cellulose II
9.9	7.74	10.3	122	Cellulose III
7.9	8.11	10.3	90	Cellulose IV

^a γ = lattice angle

1.2.3.4 Morphological structure of cellulose

The morphological structure of cellulose comprises a well-organised architecture of fibrillar elements. An elementary fibril is considered to be the smallest morphological unit with variable size between 3-20 nm depending on the source of cellulose. In native cellulose, the hierarchy of the fibrillar entities are organised in layers with differing fibrillar textures. However, the arrangement into distinct layers does not exist in regenerated cellulose fibers. These man-made fibres consist of elementary fibrils, which are positioned, quite, randomly, in the structure. A skin-core structure is typical morphology for these regenerated cellulose products. Morphology of the cellulose derivatives can be studied by electron microscopy techniques such as scanning (SEM) or transmission (TEM) electron microscopy(Liu et al. 2005).

1.2.4 Extractives

In addition to the major structural wood components, wood contains an exceedingly large number of low and high molecular weight organic compounds known as extractives (Table 1.3). These compounds can be extracted from wood with organic solvents or hot water. These include volatile oils, resins, fats, and waxes.

1.2.5 Inorganic compositions

The inorganic constituents of wood are entirely contained in ash, the residue remaining after burning the wood matter (Table 1.4). The content depends of environmental condition and location of the tree. The mineral compounds are mainly oxalates, carbonates, and glucuronates of calcium, potassium, magnesium, and sodium. In addition to some trace elements such as aluminum, zinc, copper, and nickel.

Table1. 3: wood extractives

Volatile oils	Wood resins	Fats and waxes
<i>Mainly softwoods</i>	<i>Mainly softwoods</i>	Minor, less than 0.5%
Terpentine, monoterpenes, turpentine, tropolens	Acidic diterpenes; resins of softwoods, basis of tall oil	Suberin
Tannins	Lignans	Carbohydrates
<i>Hardwoods and softwoods</i>	<i>Hardwoods and softwoods</i>	<i>Typically food reserves</i>
Hydrolyzable tannins built upon glucose and gallic acid; Condensed tannins, flavonoid-based	Optically active lignin dimers (controlled free radical coupling process)	

Table1. 4: wood inorganic composition of several wood species.

Species	Ca [%]	K [%]	Mg [%]	Mn [%]	Na [%]	P [%]	Al [%]	Fe [%]	Zn [%]
Softwoods									
<i>Abies balsamea</i>	830	770	270	127	–	–	–	13	11
<i>Picea abies</i>	1800	250	160	440	100	50	–	14	20
<i>Pinus strobus</i>	210	290	70	28	–	–	–	10	11
<i>Pinus spp.</i>	764	39	110	97	28	–	6	–	–
<i>Pseudotsuga menziesii</i>	295	–	41	25	44	–	13	–	–
<i>Tsuga spp.</i>	750	400	110	145	–	–	–	6	2
Hardwoods									
<i>Acer rubrum</i>	820	690	120	72	29	30	2	11	29
<i>Betula papyrifera</i>	740	270	180	34		150	23	10	28
<i>Fagus sylvatica</i>	1150	880	320	250	120	–	–		10
<i>Populus spp.</i>	1130	1230	270	29	–	100	–	12	17
<i>Quercus alba</i>	674	780	11	2	3	8	6	–	–
<i>Tilia americana</i>	1125	543	117	11	74	–	15	–	–

1.3 Wood pulping

The pulping processes aim first and foremost to liberate fibres from wood matrix. In principal, this can be achieved by two ways, either mechanically or chemically. Mechanical methods require electric power, but on the other hand they make use of, practically, the whole wood material, i.e. the yield of the process is high. In chemical pulping, only approximately half of the wood becomes pulp, the other half is dissolved. For a chemical process to be, economically, feasible, it has to consist of an efficient recovery system. Spent cooking chemicals and the energy in the dissolved organic material is recovered. The pulp obtained is coloured, the

degree of colouring depending on the pulping process. Pulping can be categorized to conventional and non-conventional processes.

1.3.1 Mechanical pulping

Mechanical pulping is one of the conventional pulping processes. By grinding wood or wood chips, the fibres in the wood are released and a mechanical pulp is obtained. In the process, some easily dissolved carbohydrates and extractives are lost, but on the whole the pulp yield is little affected. The pulp yield for mechanical pulp is about 90 to almost 100 %, depending on the mechanical pulping, method used. Groundwood pulp is produced by pressing round wood logs against a rotating cylinder made of sandstone. The logs are fed parallel to the cylinder axis and fibres are scraped off. Another type of mechanical pulp is refiner pulp. In which, chips are fed into the center of two refining discs, One, or both, discs rotate whereby the chips are reduced in chips and fibres abraded off (McDonald et al. 2004).

The pulp strength is enhanced if the pulp consists of a higher portion of long fibres by softening the lignin in the middle lamella, by an increase in temperature, the fracture can take place in the secondary (or primary) wall of the fibre, thus resulting in less fines formation. The chips can be pre-treated with steam, ~120 °C, before feeding to refiner. This type of refiner pulp is called thermos-mechanical (TMP) pulp (Mohta et al. 2000). By soaking the chips in a sodium sulphite solution the lignin becomes sulphonated and the lignin softening temperature is decreased. In a Chemo-Thermo-Mechanical Pulping (CTMP) process, the chemical treatment is followed by a steam pre-treatment (Theliander 2009)

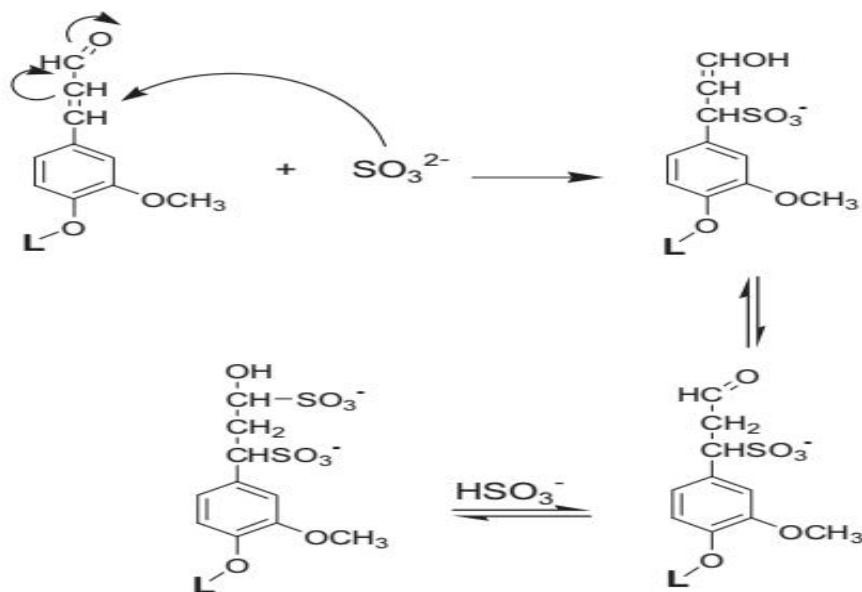
Among lignin structures, only a few are able to react with sulfite under the mild conditions of CTMP manufacturing. The most prominent of these is the coniferaldehyde structure which contains an electron deficient α -carbon atom and,

consequently, will react with a strong nucleophile such as the sulfite anion (Scheme 1.2).

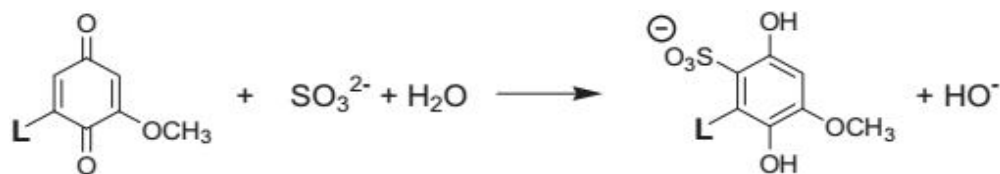
In a competing or consecutive reaction, the coniferaldehyde structure may also react at its γ -aldehyde group with formation of a hydroxy-sulfonic acid structure (Lundquist et al. 2007). In practice, only a portion of the coniferaldehyde structures seems to be eliminated. The sulfonation reaction (Scheme 1.3) will result in an increased hydrophilisation and swelling of this part of the fiber wall which promotes a more selective fiber-fiber separation. Among other reactive lignin structures, ortho- and para-quinones, being α,β -unsaturated carbonyl structures, may also react with sulfite with destruction of the chromophoric system (Theliander 2009).

1.3.2 Chemical pulping

In conventional chemical pulping, wood lignin is made water soluble by action of hydroxide (soda pulping) or hydroxide ions in combination with hydrosulphide ions (kraft pulping), known as alkaline pulping. And with the action of bisulphite ions in sulphite pulping (Theliander 2009).



Scheme 1.2: Reactions of a coniferaldehyde structure with sodium sulfite.



Scheme 1.3: Sulfonation of a quinone structure by sodium sulfite.

1.3.2.1 Kraft pulping

The selectivity of dissolution of carbohydrates and lignin during a Kraft cook proceeds in three distinct phases with the first one, merely, being an extraction of both types of components (initial phase). When around 20 % of both carbohydrates and lignin have gone into solution, the kinetics changes dramatically and a rather selective lignin dissolution takes place until approximately 90 % of all lignin has been dissolved. The final portion of the lignin can, however, only be removed with great difficulty and at the expense of a large carbohydrate loss (Gierer 1980). In practice, the cook is interrupted at the transition point to the final phase in order not to lose pulp quality or yield. The predominant loss of carbohydrates in kraft pulping is due to the fact that most of the hemicellulose components are degraded and dissolved in the alkaline liquor. Glucomannan and xylans behave differently,

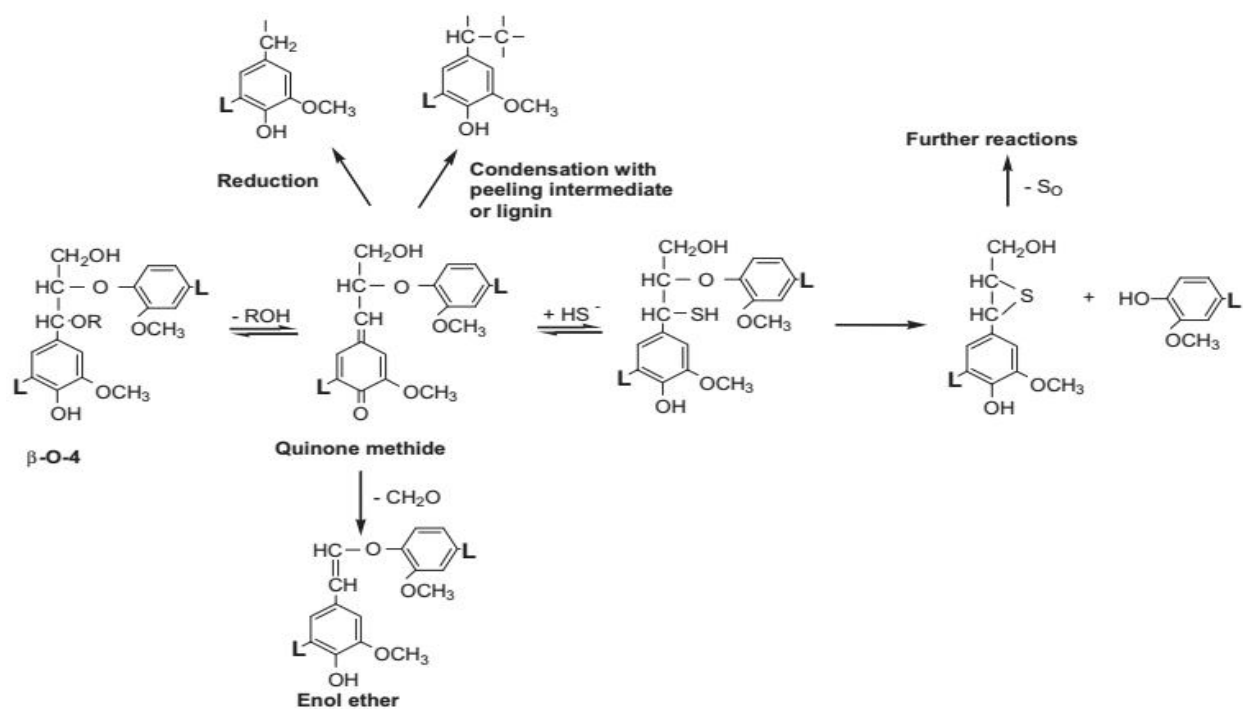
however. The glucomannan is rapidly dissolved irrespective of the charge of alkali whereas the dissolution of xylan from both softwood and hardwood becomes more extensive at a higher charge of alkali (Gustafson et al. 1983).

The delignification chemistry encountered in Kraft and soda pulping has been thoroughly investigated; the cleavage reactions take place in the predominant chemical linkage connecting the phenylpropane units together as lignin or the β -O-4 linkage, by the action of hydrosulphide ions. The phenolic β -O-4 structures are to a large extent fragmented. If no hydrosulphide ions are present, as in soda pulping, the delignification efficiency is poor and the rate of delignification becomes much lower (Tai et al. 1990).

The chemistry of cleavage of phenolic β -O-4 structures in alkaline conditions is that, the phenolic benzyl alcohol structure forms equilibrium with the corresponding quinonemethide (Scheme 1.4). In the presence of hydrosulphide ions, a further equilibrium is present resulting in a benzyl thioalcohol structure. Once formed, the latter can attack the β -carbon atom in a nucleophilic reaction with formation of a thiirane (episulphide) and a new phenolic end-group. The episulphide structure, in turn, is not stable and elemental sulphur is expelled to form polysulphide in the cooking liquor. Under the alkaline conditions, the latter will successively disproportionate and hydrosulphide and thiosulphate ions are formed (Gierer 1980).

In competing reactions, the quinonemethide intermediate, can either lose the γ -hydroxymethyl group and form an enol ether structure without cleavage of the β -ether linkage or react with other nucleophiles present in the pulping system such as lignin or carbohydrate structures, thereby, creating new stable carbon-carbon linkages. As a further alternative, a reduction of the quinonemethide with

formation of an α -methylene group may take place. In the cleavage reaction of phenolic β -O-4 structures, the primary product, the episulphide, loses sulphur and is converted, at least in part, to a coniferyl alcohol structure (Gustafson et al. 1983). Competing reactions may occur, involves elimination as well as reduction and condensation reactions. In all cases, the intermediate quinonemethide is the starting point. From this structure, an elimination of the γ -hydroxymethyl group as formaldehyde can take place giving rise to an enol ether structure which in turn is rather stable towards further reactions (Gellerstedt et al. 2004).

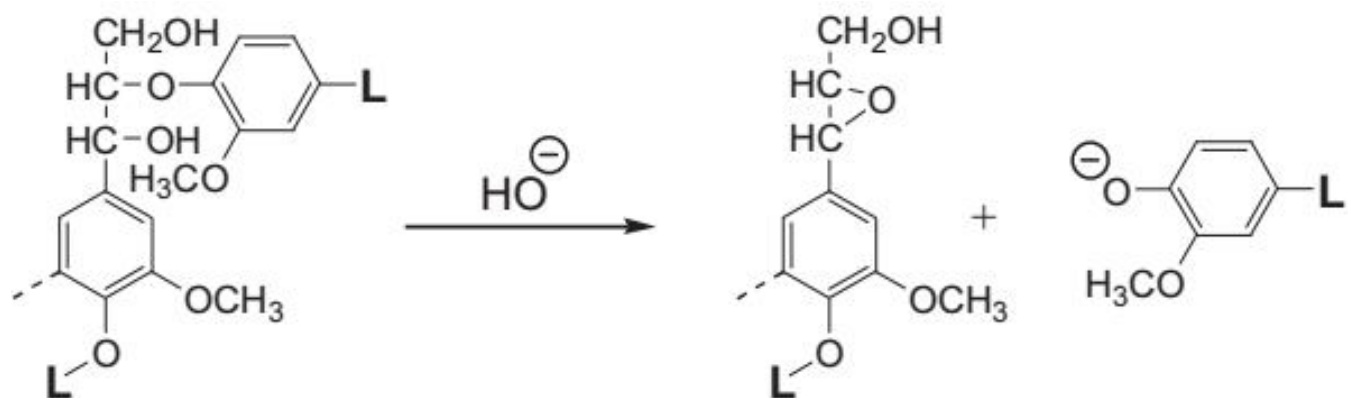


Scheme 1.4: Cleavage of phenolic β -O-4 structures in lignin during Kraft pulping conditions and competing reactions in the L denotes a lignin residue.

Non-phenolic β -O-4 structures in lignin can also be cleaved during the course of a Kraft cook (Scheme 1.5). In contrast to the phenolic type, this cleavage does not, however, involve hydrosulphide ions and the mechanism only depends on the presence of an α -hydroxyl (or a γ -hydroxyl) group which, in the alkaline cooking

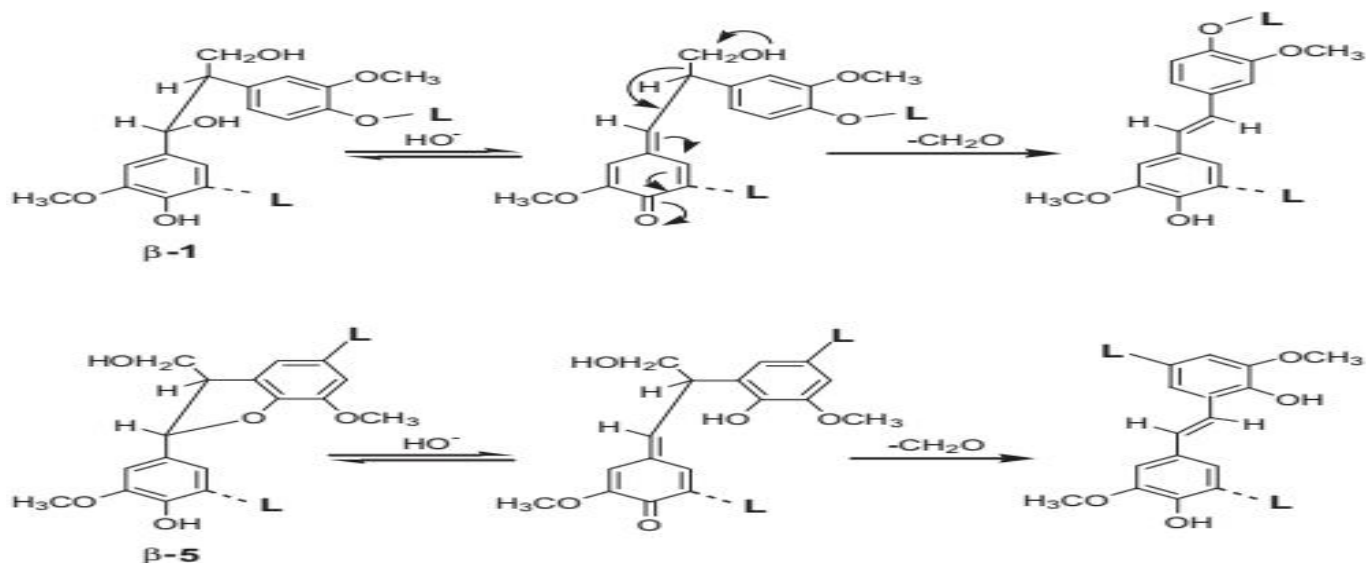
liquor, can become ionized. In analogy to the mechanism of the phenolic structure, a nucleophilic attack will result in a cleavage of the β -ether linkage and an epoxide (oxirane) structure is formed together with a new phenolic lignin end-group. The epoxide, in turn, is not stable but can react further with nucleophiles present in the cook (Crestini et al. 2000).

In other types of lignin sub-structures such as the β -5 and the β -1 structures (Scheme 1.6), the phenylpropane units are held together, with carbon-carbon linkages. The linkage between the phenylpropane units is completely stable during pulping conditions (Crestini et al. 2000). The phenolic variants of the two structures may form quinonemethide intermediates in equilibrium with the corresponding benzyl (thio) alcohol structures. The further reactions of the quinonemethide are, however, restricted to an elimination of either a proton or formaldehyde and formation of stilbene structures (Theliander 2009).

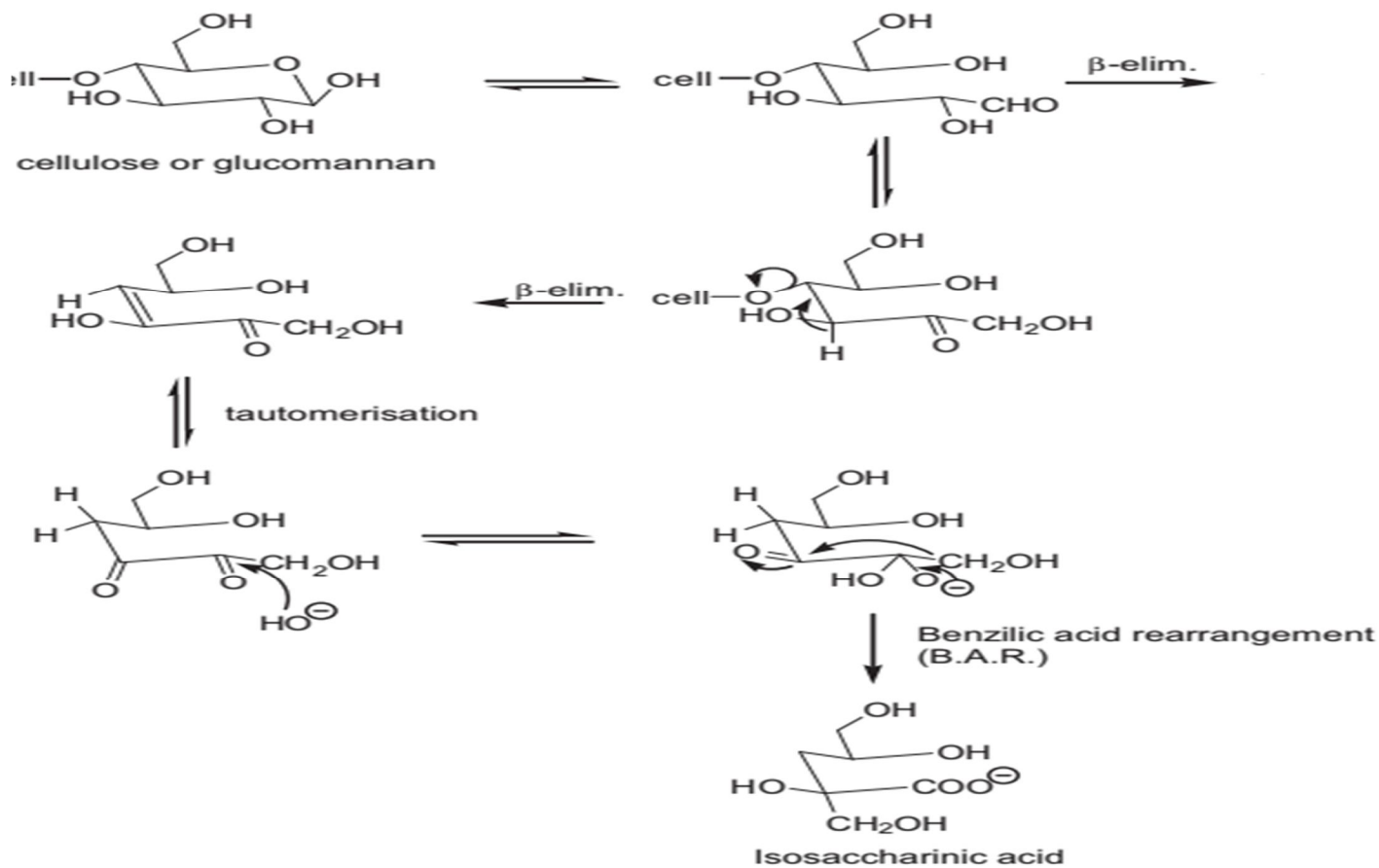


Scheme 1. 5: Cleavage of non-phenolic β -O-4 structures in Kraft pulping.

Reactions of carbohydrates in a Kraft cook are comprehensive and will result in a large yield loss, include a successive depolymerisation of the polysaccharides starting from the reducing end group (Scheme 1.7). This so called peeling reaction starts, immediately, when the wood comes in contact with the alkaline pulping



Scheme 1.6: Formation of stilbenes from β -5 and β -1 lignin sub-structures during Kraft pulping.



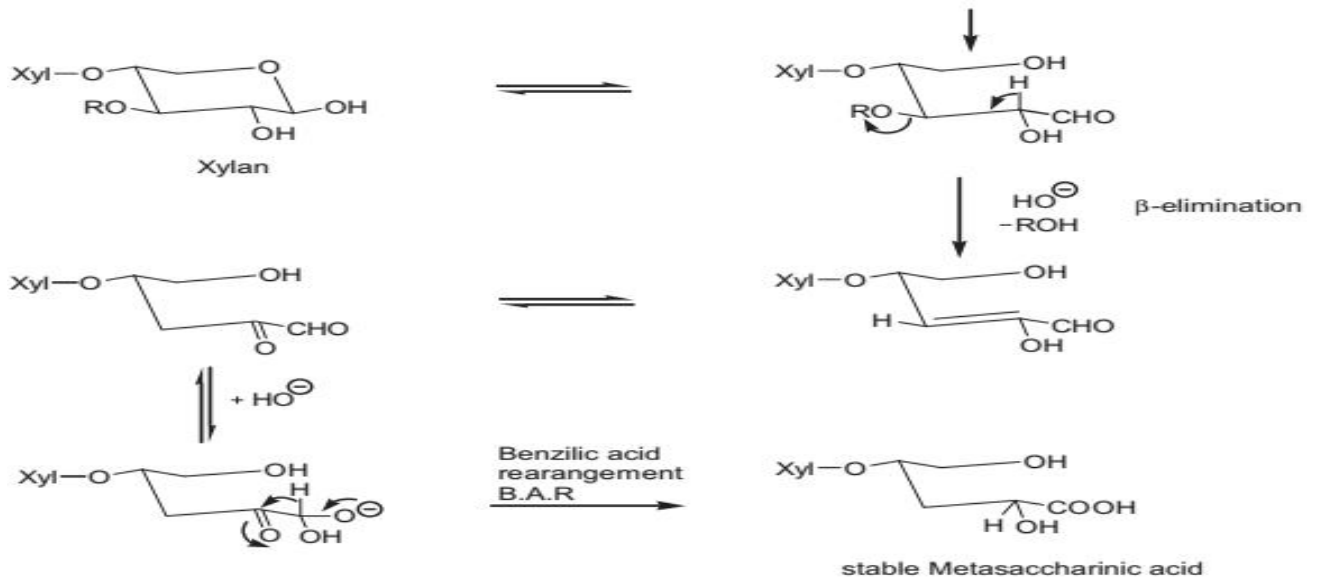
Scheme 1. 7: Mechanism for the peeling reaction in Kraft pulping.

liquor and proceeds, rapidly, at temperatures around 100 C. At, considerably, higher temperatures, ~170 C or more, random alkaline hydrolysis of glucosidic bonds, may, also take place to some extent (Gratzl and Chen 1999). The peeling reaction has a particular importance for polysaccharides containing a substituent in the 4-position like in glucomannans, xylans and cellulose. In the aqueous environment during pulping, the reducing end group in the polysaccharide will form equilibrium between the hemiacetal and the open aldehyde form.

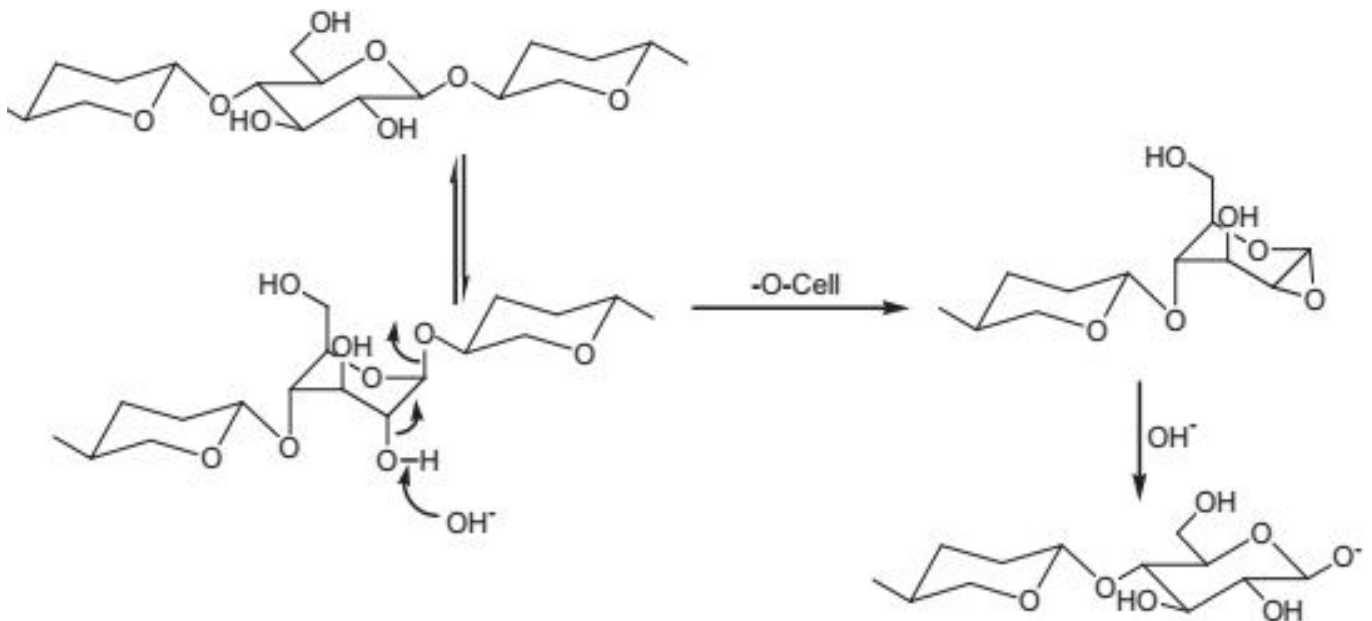
In the presence of alkali, a further equilibrium will be established between the aldehyde and the keto form. From both these forms, a subsequent β -elimination reaction may occur (Scheme 1.8). In the former case, the reaction will result in a stabilisation of the polysaccharide chain whereas the other type of reaction will give rise to a cleavage of the glucosidic bond in the 4-position. Thereby, the first sugar unit in the chain is eliminated and a new reducing end unit is liberated and able to go through the same reaction sequence again. Once, the β -elimination has taken place, the liberated product can react further via a benzilic acid rearrangement to form an isosaccharinic acid (Tai et al. 1990).

A certain further loss of cellulose may take place when the Kraft cook approaches the maximum temperature due to alkaline hydrolysis of glucosidic linkages (Scheme 1.9). The reaction is initiated by the C-2 hydroxyl group which, if ionized, can attack the C-1 carbon atom and expel the attached anhydroglucose unit. The result will be a cleavage of the cellulose chain and thus a large reduction of degree of polymerization, formation of a new reducing end group and a rapid secondary peeling reaction. It must be emphasized, however, that the alkaline hydrolysis is rather heterogeneous and preferentially occurs in the amorphous parts of the cellulose microfibrils. As a result of both peeling and alkaline hydrolysis, a

total loss of cellulose of around 10% (on wood) is generally encountered in Kraft pulping (Gratzl and Chen 1999).



Scheme 1.8: β -elimination in polysaccharide end groups resulting in a stopping reaction and formation of a metasaccharinic acid.



Scheme 1.9: Alkaline hydrolysis of a glucosidic linkage via epimerisation and epoxide formation.

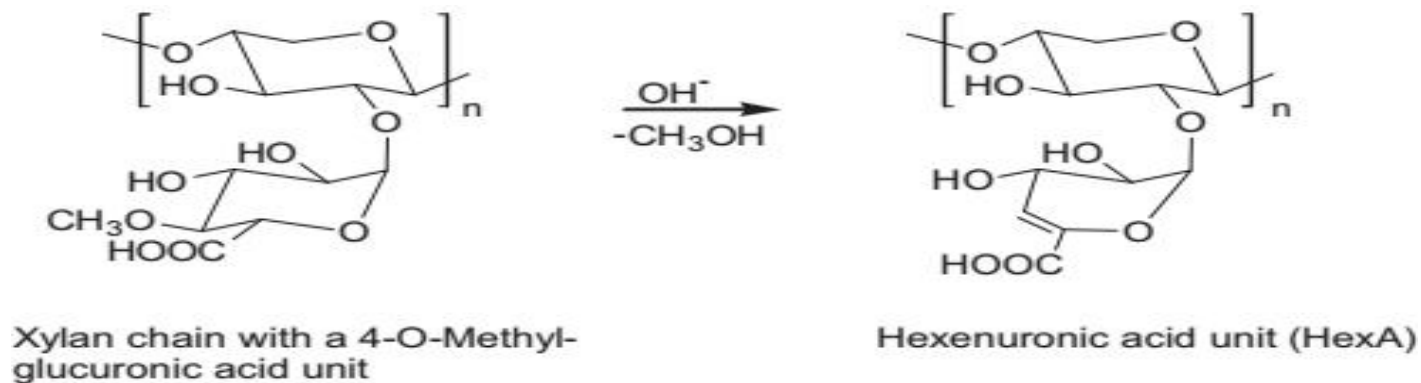
In both softwood and hardwood, the xylan chain is substituted with 4-O-methylglucuronic acid groups located in the C-2 position and linked through an α -glucosidic linkage. Under alkaline conditions, the methoxyl group can be eliminated as methanol resulting in the formation of a hexenuronic acid group (Scheme 1.10). Since the hexenuronic acid group is rather stable in alkali, the xylan that remains in the pulp after the cook will contain an appreciable amount of such groups. These will influence the pulp properties and contribute to the bleachability of the pulp (Teleman A. 2001).

1.3.2.2 Sulphite pulping

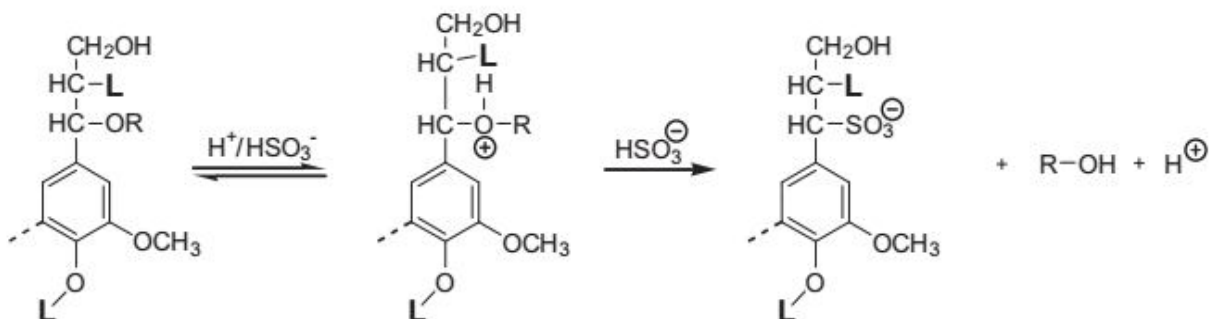
The dissolution of lignin and the liberation of cellulosic fibers by the action of bisulphite ions can be done with calcium, sodium, magnesium or ammonium as the counter ion. In the production of chemical sulphite pulps, acidic conditions are employed although alkaline sulphite pulping is a potential alternative, however, a neutral sulphite pulping liquor can be used to produce high yield fibres. The sulphite system contains two equilibrium reactions and it has been found that in acidic sulphite pulping, a certain amount of bisulphite ions must be present in the liquor at all times in order to obtain a lignin sulphonation reaction. Otherwise, the wood residue will turn dark without any dissolution of lignin due to predominance for lignin condensation reactions (Wong and Chiu 2001).

Lignin dissolution in sulphite pulping is caused by a sulphonation of the lignin reaction, and acid hydrolysis of ether linkages in lignin takes place to various extents depending on the pH (Scheme 1.11). The degree of sulfonation is also dependent on the pH of the cooking liquor. Thus, under strongly acidic conditions, high degrees of sulphonation can be achieved, whereas under neutral or slightly alkaline conditions, the sulphonation seems to reach a plateau value at around 30 sulphonate groups per 100 phenylpropane units. It can also be seen that, under

neutral conditions, a very rapid initial sulphonation takes place resulting in the introduction of around 15 sulphonate groups per 100 phenylpropane units within only a few minutes. The reaction between a phenylpropane unit and acidic bisulphite proceeds via the protonation of the benzylic hydroxyl (or ether) group followed by elimination of water and addition of the bisulphite ion. Both phenolic and non-phenolic phenylpropane units can react thus explaining the high overall degree of sulphonation that can be achieved (Theliander 2009). Under neutral or slightly alkaline conditions, on the other hand, the reaction becomes more selective and only the phenolic phenylpropane units react. In this case, the mechanism is analogous to the reaction in Kraft pulping, namely a formation of a quinonemethide intermediate followed by addition of a sulphite ion. At longer cooking,



Scheme 1.10: The elimination of methanol from 4-O-methylglucuronic acid.



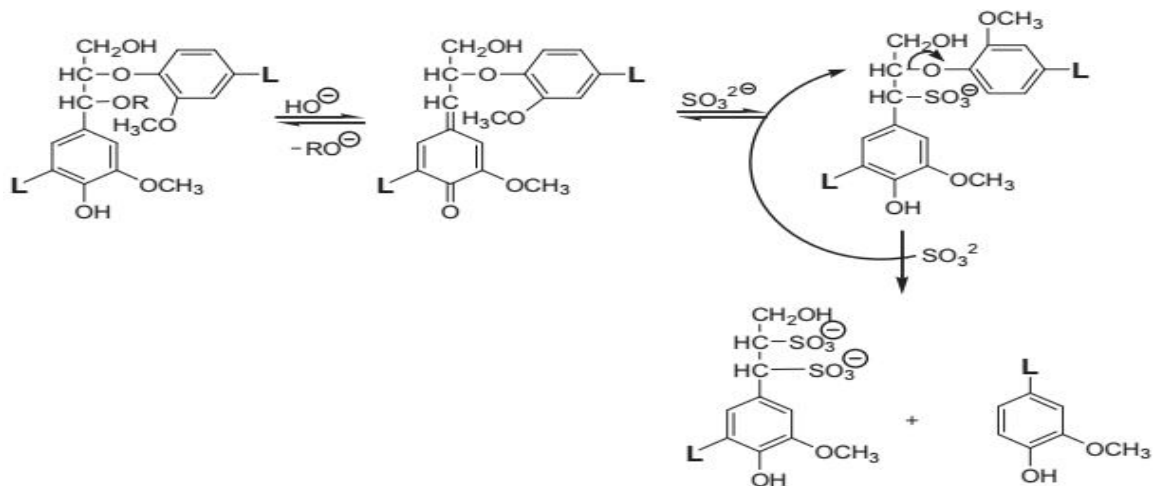
Scheme 1.11: Sulphonation of lignin in acidic sulphite pulping.

times at a neutral pH, a further slow sulphonation can take place. Sulphonated β -O-4 structures may undergo a β -ether cleavage by attack of sulphite on the β -carbon atom. Thereby, two sulphonate groups can be introduced in the same side chain (Scheme 1.12). At the same time, a new phenolic lignin end group is created which in turn may become sulphonated (Hanhikoski et al. 2016).

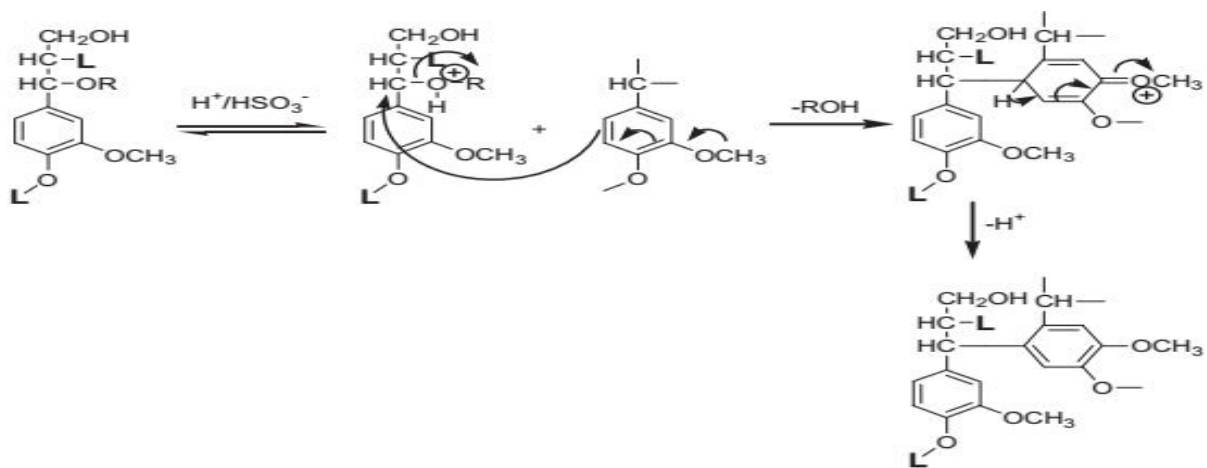
The major reaction of the polysaccharides in acidic sulfite pulping is the acid catalysed hydrolysis of glucosidic linkages resulting in the formation of large amounts of monomeric sugars in the pulping liquor (Scheme 1.13). In particular, the more easily accessible hemicelluloses are degraded and some 70 % of the glucomannan and 50 % of the xylan can be lost in a spruce sulphite pulp (Gierer 1985).

During the eighties, the addition of anthraquinone (AQ) and related compounds to the alkaline pulping process opened up new possibilities for developing novel processes (Scheme 1.14). Many studies have revealed that with the addition of AQ, the efficiency and selectivity of delignification by oxidation improve. Compared to the Kraft process, the AQ in alkaline sulfite (AS-AQ) pulping under alkaline conditions behaved selectively, providing both a higher yield and viscosity at a given kappa number. The chemistry of AQ in modified pulping starts with a rapid oxidation of the reducing end-groups in the polysaccharides. In this reaction,

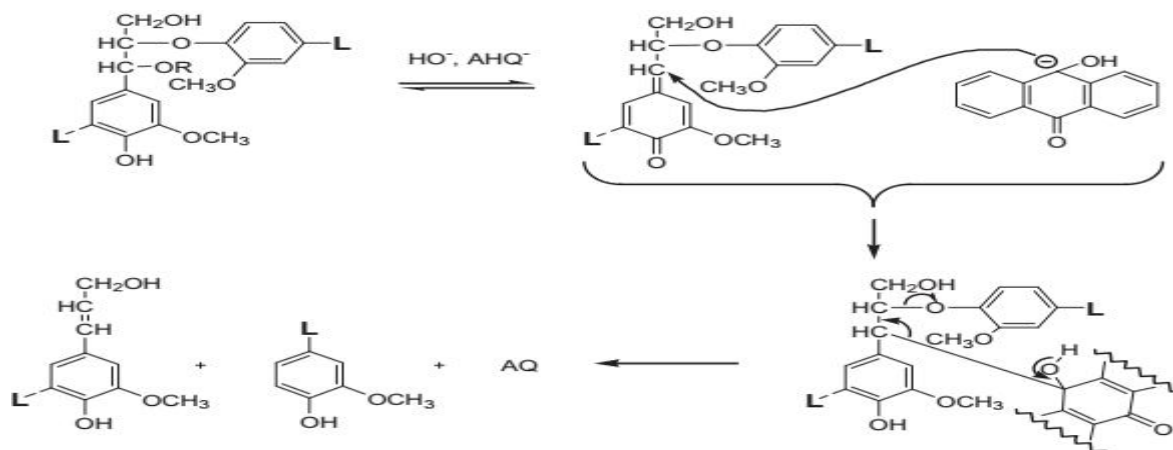
anthrahydroquinone (AHQ) is formed. The latter will react with quinonemethide intermediates formed in the lignin. When part of a β -O-4 structure, the adduct between AHQ and the quinonemethide will decompose with formation of AQ. At the same time, the β -O-4 linkage is cleaved to form coniferyl alcohol and new phenolic end-groups (Hedjazi et al. 2009).



Scheme 1.12: Sulphonation of lignin in neutral sulphite pulping



Scheme 1.13: Mechanism for the acid catalysed condensation in lignin.



Scheme 1. 14: Mechanism for the alkaline cleavage of phenolic β -O-4 structures in lignin by anthrahydroquinone.

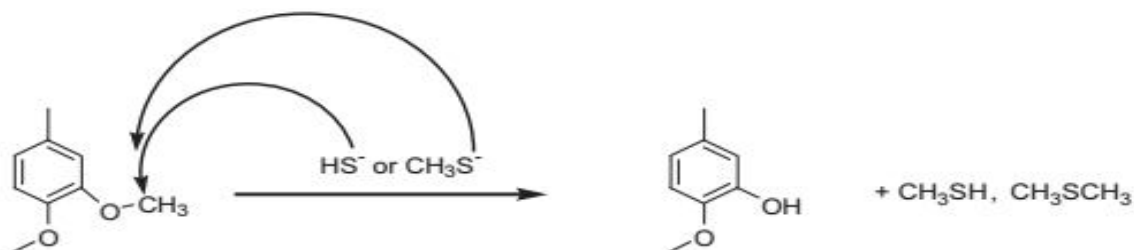
1.3.2.3 Organosolv pulping

In spite of the advantages of Kraft pulping, the process displays certain serious drawback such as emission of malodorous substances, the presence of strong nucleophiles and the high temperature employed in Kraft pulping induces a cleavage of the methyl-aryl ether linkages in lignin. Although the cleavage reaction takes place to a minor extent only, the products formed are highly detrimental from an environmental point of view since they constitute the origin of the smell from Kraftmills. The primary reaction involves an attack of a hydrosulphide ion on the aromatic methyl ether group and formation of methylmercaptan together with a phenolic hydroxyl group. Under the alkaline conditions prevailing in the cook, a methylmercaptide anion is formed and this in turn can attack a new methyl group with formation of dimethylsulfide (Scheme 1.15). Both methylmercaptan and dimethylsulfide are volatile and, in particular, methylmercaptan is also highly toxic. When exposed to air (oxygen), a portion of the methylmercaptan may become oxidized with formation of dimethyldisulfide, a further malodorous and volatile product (Theliander 2009).

Furthermore, requiring very efficient bleaching sequences, this has resulted in serious water pollution problem. In addition, the effect of peeling reaction in pulp yields. Consequently, many efforts have done for modification for the improvement of the pulping processes includes organosolv, biopulping and other chemicals, which known as nonconventional pulping (Aaltonen et al. 2016).

It was known since the last quarter of 19th century that some organic solvents can extract lignin but using organic solvents for pulp production was not considered until 1930's. The studies were made and the patents were taken about this issue between 1929 and 1939 by Aranovsky and Gortner and later by Kleinert resulted organosolv methods to develop (Akgul and Kirci 2009). The most prevalent solvents that are still used are methanol, ethanol, acetic acid and formic acid. Other organic solvents are phenols, amines, glycols, nitrobenzene, dioxane, dimethylsulphoxide, sulfolene and carbon dioxide. Various organosolv systems using all these solvents are developed, it was reported that organosolv process had advantages compared to the conventional kraft method, that is easy to bleach, minimizing environmental problems caused by waste chemical pollutants such as sulphurous, chlorinated organics (F. Olie, 2000). Additionally, the lignin removed can be recovered in the recycling operations of organic solvent, which involves stages of distillation and precipitation. The most applicable solvents are ethanol and methanol which can be obtained easily and cheaply. In recent years, various organosolv cooking systems with or without catalyst that consider alcohol as basis, were suggested. The most prominent among the processes, are those carried out by Kleinert (with ethanol or methanol, in the absence of a catalyst) – Alcell (ethanol-water), Organocell (ethanol-soda), Organocell (methanol-soda anthraquinone), ASAM (alkali-sulphite anthraquinone-ethanol), the one using sodium bicarbonate-ethanol-water and that using oxygen-alcohol. Other processes based on different

alcohols, also worthy of note, are those of ester and phenol pulping – Acetocell (acetic acid-water), Milox (formic acid-hydrogen peroxide), Formacell (acetic acid-water-formic acid), and those using formic acid, glycerol, oxygen-acetone-water, water, glycerol-acetic acid, and ammonia and amine bases (Akgul and Kirci 2009).



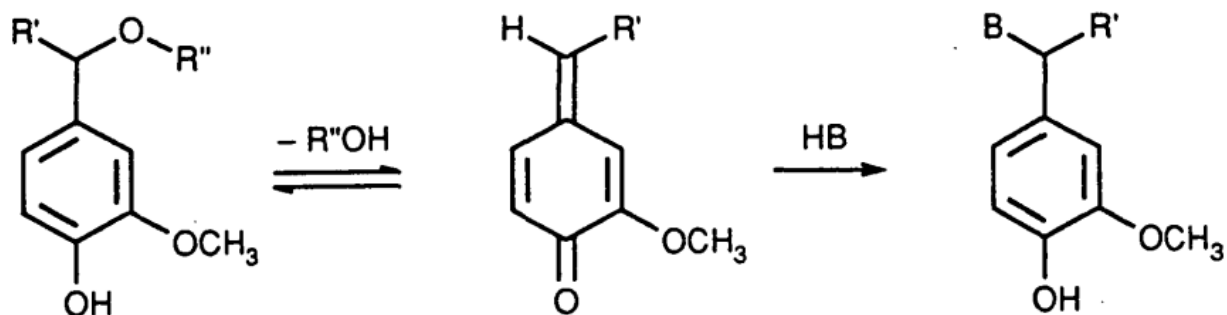
Scheme 1. 15: Formation of malodorous compounds in Kraft pulping

Numerous studies within the field of lignin chemistry have led to the conclusion that the cleavage of ether linkages is primarily responsible for lignin breakdown in organosolv processes. Easily hydrolyzable α -ether bonds are most readily broken, but it is likely that β -aryl ether bonds are also broken under the conditions of many processes. Important parameters governing the course of delignification are pH, physical properties of the solvent that govern its ability to dissolve lignin fragments, and chemical properties of the solvent that govern its ability to participate in fragmentation reactions or inhibit lignin recondensation.

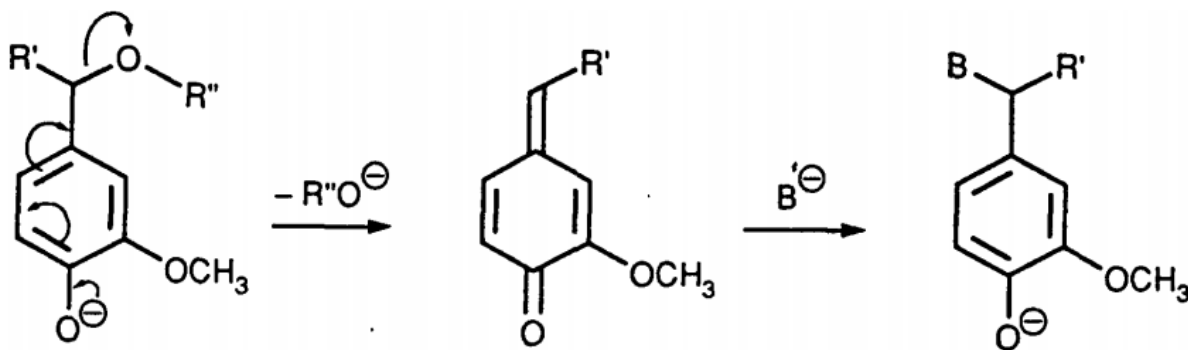
Most of the organosolv processes use neutral, acidic and alkaline solvents. In cases where no acid is added, the liquor becomes acidic as a result of release of acetic acid from the wood. In organosolv acidic or neutral systems pulping, the responsible reactions in neutral and acidic systems, which very likely occur in, are believed to consist primarily of the solvolytic splitting of α -ether linkages (scheme

1.16). An α -aryl ether linkages are more easily split than β -aryl ether linkages, especially when they occur in a lignin structural unit containing a free phenolic hydroxyl group in the para position. In this case the formation of a quinonemethide intermediate is possible (McDonough 1992).

In alkaline systems, the ionization of a free phenolic hydroxyl group facilitates its conversion to a quinonemethide in alkaline medium (Scheme 1.17), provided that a suitable leaving group is situated at the α position of the side chain. Linkage via It is generally observed that organosolv lignins have low carbohydrate contents, suggesting that the bonds anchoring lignin to hemicellulose in wood are readily hydrolyzed under acidic conditions. This is in accord with the hypothesis that these bonds consist of ether linkages between the carbohydrate and the α -carbon atoms of lignin sidechains, since such bonds are known to be readily hydrolyzed (McDonough 1992).



Scheme 1. 16: Solvolytic cleavage of a phenolic α -aryl ether linkage via a quinonemethide intermediate.



Scheme1. 17: Quinone methide formation with α -ether cleavage on free phenolic.

1.3.3 Bleaching

In Kraft or sulfite pulping, the process does not permit a complete delignification for reasons of pulp yield and quality. The colour of pulp is generally agreed to be due to the presence of strong light absorbing substances known as chromophores. Chromophores exist naturally in native lignin but may also be formed from chemical reactions during the pulping process. To obtain pulp of acceptable brightness and lignin free, it is necessary to further treat the pulp to remove the coloured compounds. This is accomplished by a series of alternating oxidation and extraction treatments ultimately leading to an almost lignin-free fiber. The chromophores can be removed by two different methods, lignin preserving bleaching and lignin removing bleaching (delignification). Lignin preserving bleaching, also known as brightening, is mainly used for high yield pulps that have high lignin content. In this process, the bleaching chemicals increases brightness by selective reaction with the chromophoric groups on the lignin, changing them into weaker light absorbing compounds, while leaving the bulk of the lignin intact. The advantage of this process is that high yields can be achieved. However, high brightness pulps are difficult to produce and brightness stability is often poor. The action of light and oxygen will cause certain groups in the pulp to be changed into coloured compounds. To produce pulps of high brightness, lignin removing

methods have to be used. This method is essentially a continuation of the pulping process although more selective chemicals are used instead. For effective bleaching, the bleaching is usually done in a series of stages known as pulping sequences. The choice of bleaching sequence will depend on the pulp species, pulp treatment, bleaching method and the end use of the pulp(Gellerstedt 2010).

Bleaching sequences generally contain two phases within each sequence, a delignification segment, whose function is to remove the lignin; and a brightening segment, whose principle function is to increase the brightness of the pulp. In the conventional multistage bleaching processes of Kraft pulp, chlorination stage (C-stage) is basically taken place as a first bleaching stage in the sequence, followed by alkali extraction stage (E-stage). Kraft pulp residual lignin is attacked by chlorine in C-stage so that the complicated structure of the lignin can be modified to form a lot of acidic group, which becomes labile to the successive alkali treatment. In E-stage, the most of modified residual lignin is dissolved in aqueous solution. Hypochlorite bleaching stage (H-stage), chlorine dioxide bleaching stage (D-stage), and hydrogen peroxide bleaching stage (P-stage) basically follow the two stages to obtain brightness required. Several of the more commonly used bleach sequences are CEDED, CEDH, CEHDED, CEH, and CED. Although these are the most prominent bleaching sequences currently in use, an increasing number of mills are now using oxygen (O-stage) in combination with alkali for extraction (E_o), and chlorine dioxide (D_o) in the chlorination stages. In addition, there are a number of unique bleaching sequences used by some mills (e.g., CEH_oDH, CEHEDP, CEDPD, CEDEHD and CEHCHDED). Chlorine dioxide is today the dominating bleaching chemical used in pulp mills worldwide. Bleaching based on chlorine dioxide and where no other chlorine based chemical like chlorine gas or hypochlorite is used is today denoted as ECF (elemental chlorine

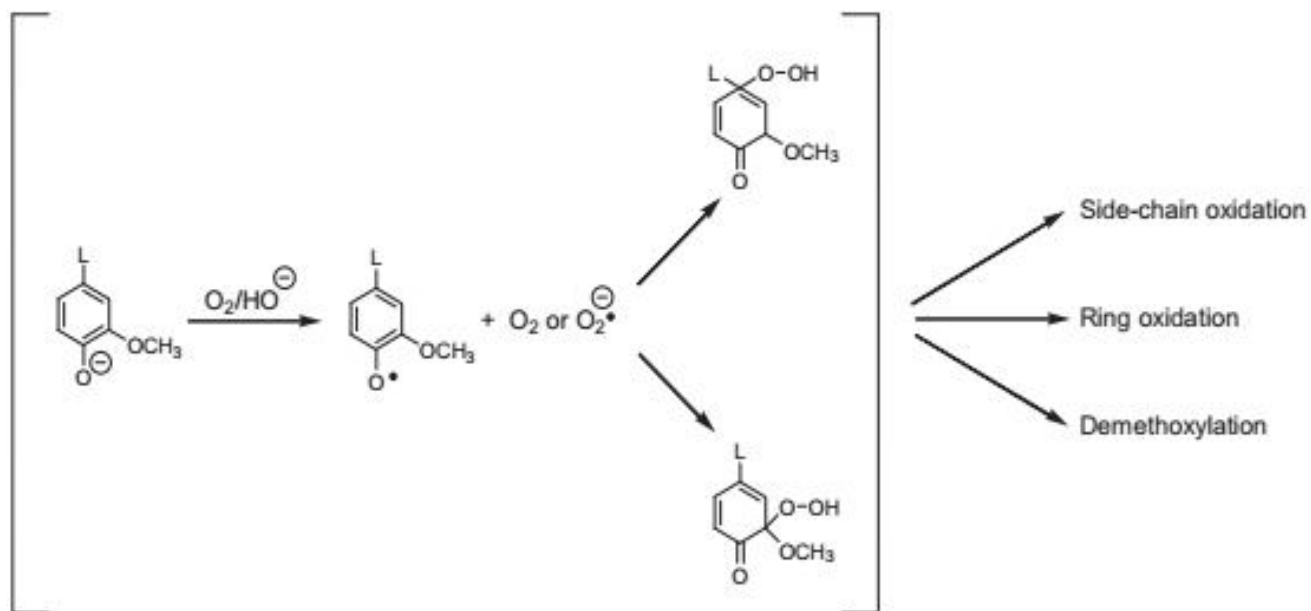
free bleaching). If chlorine dioxide is not used (and no other chlorine containing bleaching chemicals) the bleaching is instead called TCF (totally chlorine free bleaching). However, very few mills are today producing only TCF bleached Kraft pulp(Vila et al. 2004).

The remaining (residual) lignin that is present in the fibers has a chemical structure that apparently is much different from the original lignin in wood. A large decrease in the amount of remaining β -O-4 structures, an increased amount of free phenolic hydroxyl groups and chemical linkages between lignin and all the major polysaccharides, cellulose, xylan and glucomannan, almost all residual lignin present in a Kraft pulp is chemically linked to the polysaccharides with the majority being linked to the hemicelluloses(Vila et al. 2004).

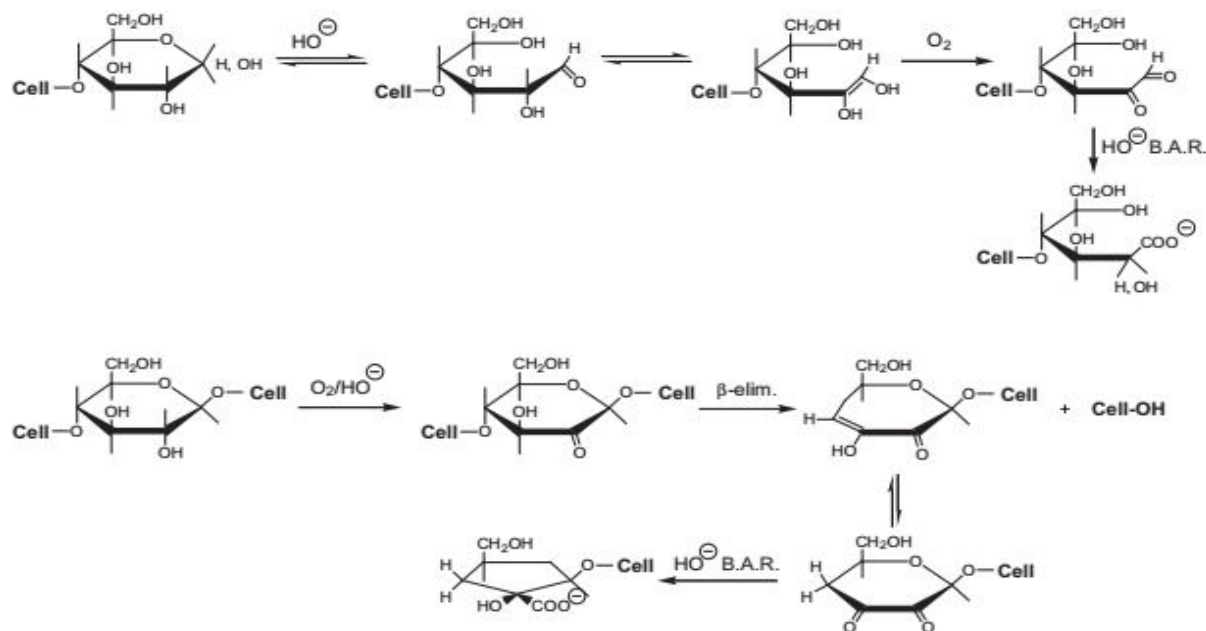
1.3.3.1 Oxygen bleaching chemistry

The alkaline oxygen oxidation of lignin has been the subject of studies with pulp, isolated lignin and with lignin model compounds. These studies clearly reveal that the major reaction is an oxidation of aromatic units in lignin having a free phenolic hydroxyl group (Scheme 1.18). The primary reaction step, formation of a phenoxyradical, is followed by attachment of a superoxide radical or possibly an oxygen molecule to any of the resonance structures and formation of an organic hydroperoxide. The hydroperoxide structures are not stable and will undergo different types of secondary reactions. Among these, the oxidative cleavage of the aromatic ring and formation of acidic groups must be regarded as the most important since that reaction will render the lignin more hydrophilic. A certain decrease of the molecular size of the lignin may, however, also play a role since the oxidized lignin must be able to diffuse out of the fiber wall(Germgård and Larsson 1983). The yield of pulp after oxygen bleach is high demonstrating that lignin is the predominant component being dissolved.

The major carbohydrate reactions in oxygen bleach is oxidative stabilization (Scheme 1.19) of a reducing end group (upper reaction) and oxidative cleavage of a polysaccharide chain (lower reaction). Despite the fact that the reaction is carried out in an alkaline medium, the peeling reaction, prevalent during kraft pulping, is of a minor importance. During oxidative conditions, any reducing end group present in the polysaccharides will rapidly become oxidized to the corresponding aldonic acid group thereby preventing the endwise degradation from taking place (Gamelas et al. 2005).



Scheme 1. 18: Oxidation of a phenol with oxygen in alkaline media.



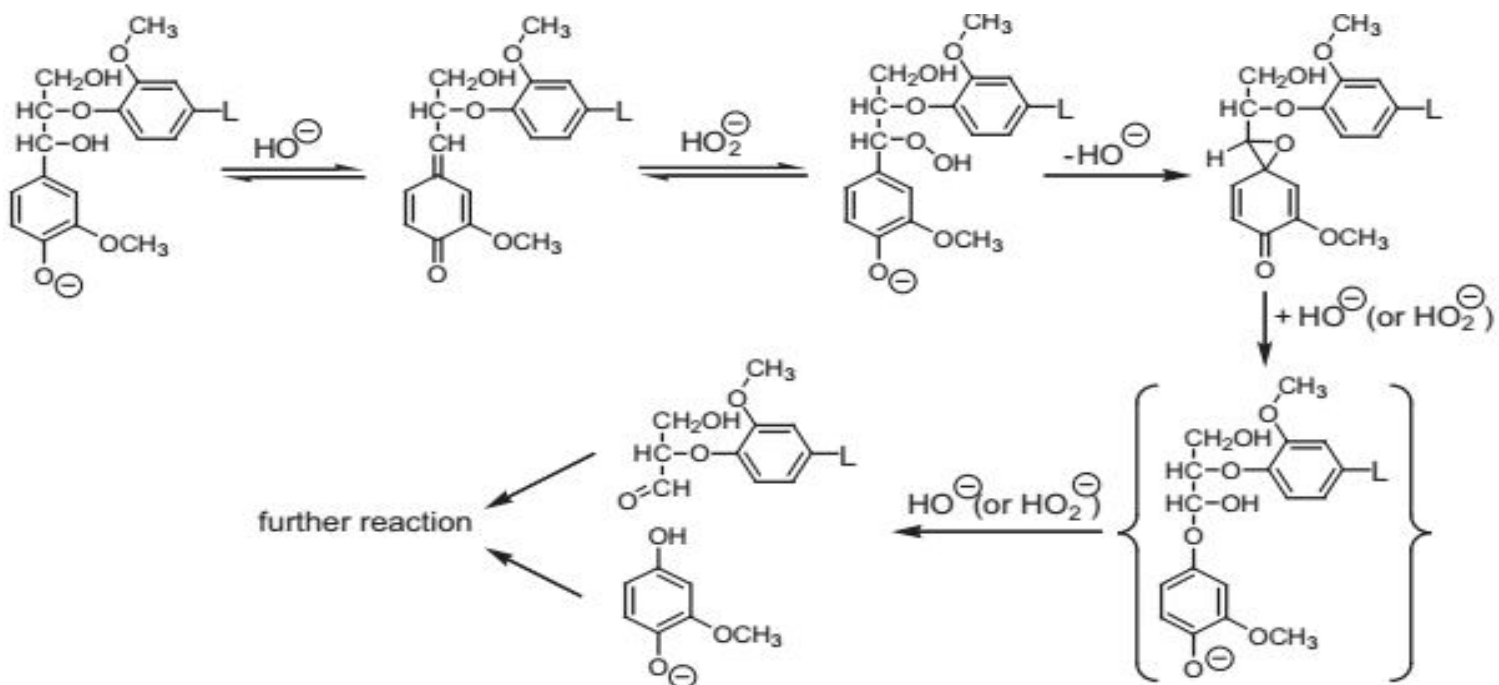
Scheme 1.19: Major carbohydrate reactions the oxygen bleaches. B.A.R. = benzilic acid rearrangement.

1.3.3.2 Hydrogen peroxide bleaching

Hydrogen peroxide in alkaline media has been used for the bleaching of mechanical pulp. When it is required that only the chromophoric structures present in the pulp are removed but virtually without any loss of pulp yield. The bleaching liquor must also contain sodium silicate in order to stabilize the peroxide and to provide a buffering capacity to the bleaching system.

The high temperature required results in formation of a quinonemethide from phenolic benzylalcohol structures. Thereby, a nucleophilic addition of a peroxy anion is made possible and, in subsequent reaction steps, a lignin side chain cleavage and fragmentation (Scheme 1.20) may occur (Chen et al. 2003).

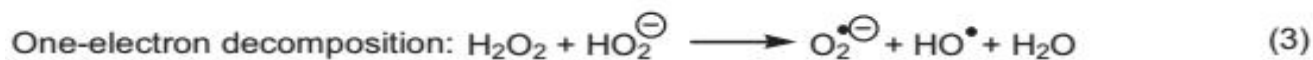
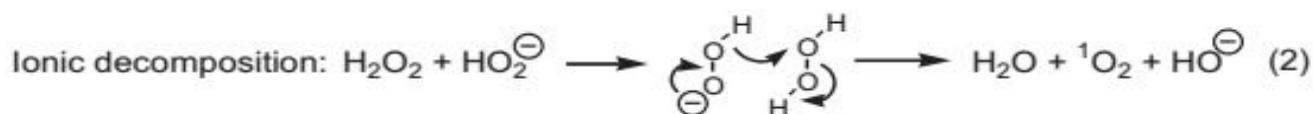
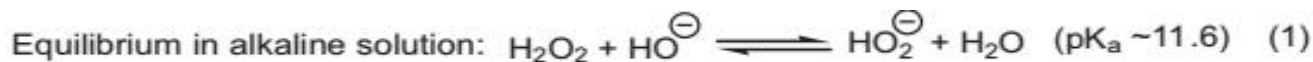
Acertain decomposition of hydrogen peroxide through spontaneous and/or metal catalysed reactions is unavoidable, however. These reactions will result in the formation of oxygen and water via the intermediate formation of hydroxyl and superoxide radicals(Scheme1. 21).The radical species present in Hydrogen peroxide bleaching will contribute to the oxidation of lignin (scheme 1.22) but also to a certain oxidation of the polysaccharides. (Maes and Delcour 2001).



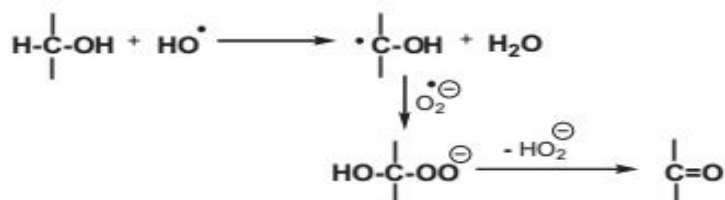
Scheme1.20: Chain cleavage of a phenolic β -O-4 structure in lignin on oxidation with alkaline hydrogen peroxide

1.3.3.3Chlorine dioxide bleaching

The reaction of chlorine dioxide with lignin can be divided to pre bleaching stage and final bleaching stage. In pre bleaching stage, there are two reaction route of chlorine dioxide with lignin viz phenolic and non-phenolic.. For both types of structures, the initial reaction is a one-electron transfer reaction giving rise to a phenoxy radical and a radical cation respectively.



Scheme1.21: Decomposition reactions of hydrogen peroxide in alkaline solution. Influence of transition metal ions.

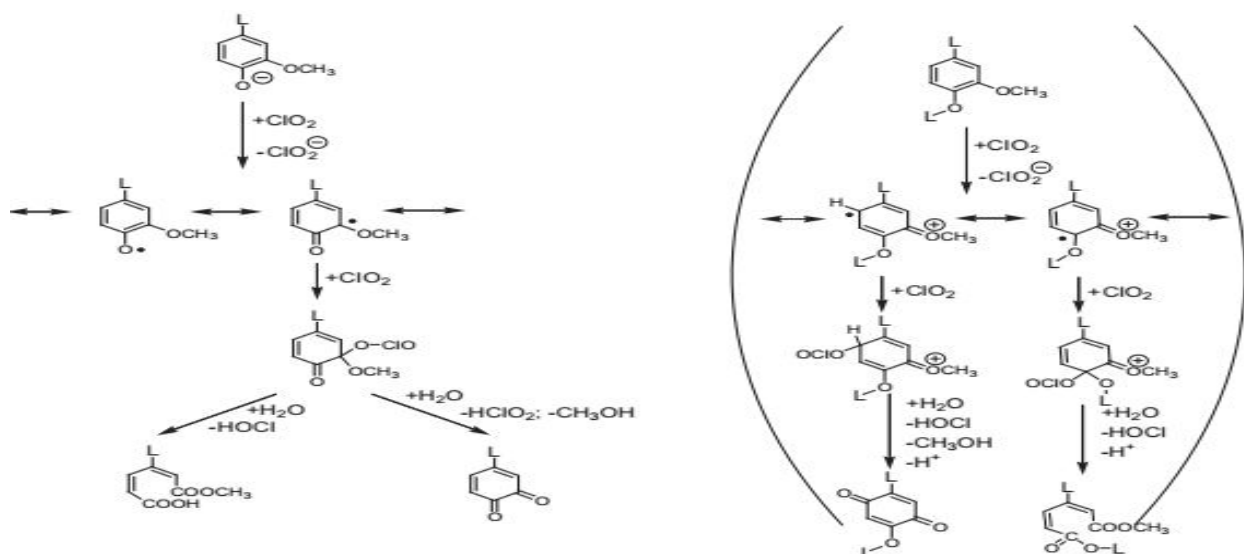


Scheme1.22: Possible modes of formation of carbonyl groups in carbohydrates on oxidation with oxygen in alkaline media.

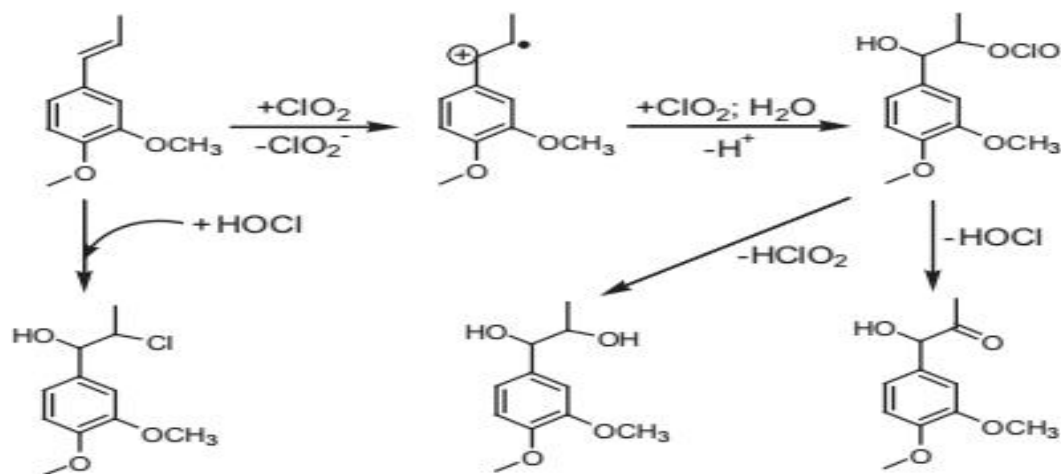
The chlorine dioxide is reduced to chlorite ion. In the next reaction step, a second molecule of chlorine dioxide is added to the radical species with formation of esters of hypochlorous acid. These, in turn, are hydrolysed and, depending on the type of leaving group, give rise to acids of the muconic acid type and to quinones (Scheme 1.23). In these reactions, hypochlorous acid and chlorous acid together with methanol are liberated (Kolar et al. 1983).

In order to remove the remaining pulp lignin and to increase the brightness to a value around 90 %, either two further D-stages or, alternatively, one D-stage known as final bleaching stage, oxidation of various non-phenolic aromatic and conjugated aromatic structures (Scheme 1.24) thus giving rise to both lignin dissolution and non-specified chromophore elimination (Lindgren 1979).

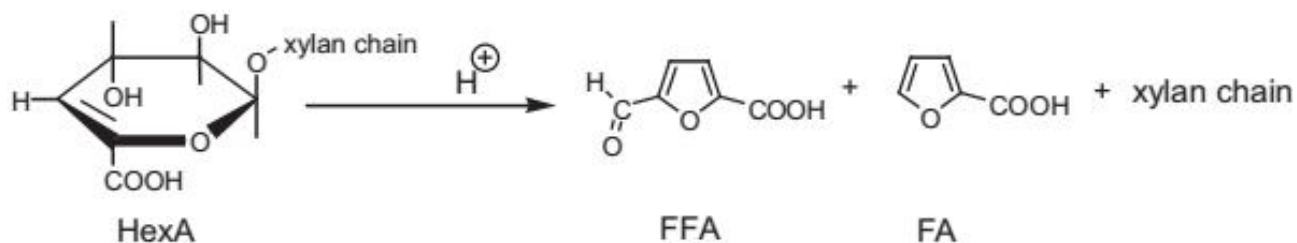
Bleaching of chemical pulp with chlorine dioxide is very selective and unless the pH is very low and/or the temperature very high, the polysaccharide chains are left virtually intact. At the more extreme conditions, acid hydrolysis may take place (Scheme 1.25). Furthermore, the hexenuronic acid groups attached to the xylan can be degraded by hydrolysis and/or by oxidation. The latter reaction may proceed, rapidly, in the presence of hypochlorous acid/chlorine and more slowly when only chlorite remains as active chlorine species in the bleaching liquor. In the latter case, the actual oxidizing species may in fact be chlorine dioxide, formed through the slow disproportionation of chlorite (Kolar et al. 1983)



Scheme1. 23: Reactions between a phenolic (left) and a non-phenolic (right) lignin structure respectively with chlorine dioxide under acidic conditions.



Scheme1. 24: Reactions between a conjugated aromatic structure and chlorine dioxide under mild acidic conditions.



Scheme1. 25: Acidic hydrolysis of hexenuronic acid resulting in the formation of 5-formylfuroic(FFA) acid and furoic acid(FA).

1.3.3.4 Chlorine and Hypochlorite bleaching

In aqueous chlorine system, active chlorine can exist in three different forms, depending on the pH of the solution (Figure 1.14). These are molecular chlorine (Cl_2), hypochlorous acid (HOCl) and its anion (OCl^-). In the region up to pH 5, a concentration dependent equilibrium exists between molecular chlorine and hypochlorous acid, while at higher pH values hypochlorous acid and its anion are both present in proportions, directly, determined by the pH of the solution. Two pH regions are of particular interest for bleaching chemistry.

The reactions between pulp lignin and aqueous chlorine (Scheme 1.26) may proceed by, several, different pathways which seem to occur extremely fast and more or less simultaneously. It should be noted that, in addition to chlorine, hypochlorous acid is, usually present in the bleaching liquor. The major products from these reactions are aromatic substitution, either directly on the aromatic ring or through a side chain displacement reaction, hydrolysis of ether linkages, and oxidation of aromatic rings to quinones and carboxyl groups. The first of these reactions will give rise to, a variety of, chlorinated aromatic structures with one or more chlorine atoms attached to the same aromatic ring. These, in turn, are sensitive to oxidation, presumably by the hypochlorous acid present and both quinones and various carboxyl groups are formed thus rendering the oxidized lignin soluble in alkali (Solomon 1996).

Hypochlorite bleaches the pulp by destroying and removing residual native lignin and lignin derivatives formed from the pulping stage. The reaction between hypochlorite and lignin involves a series of complicated reactions, the mechanics of which have, still, not being fully understood. However, the reactions can, basically, be categorized into three types; inorganic reactions, lignin reactions and carbohydrate reactions. The latter two reactions are influenced by the first reaction,

which in turn is determined by the pH of the reaction(Sarkanen 2010.).In the same way as molecular chlorine, hypochlorous acid react as substituted agent, that, it can cause electrophilic displacement reaction. Hypochlorous itself is rather un reactive in acidic solution, but chloronium ion is, very, effective substituted agent in reaction with reactive phenol and their ether. In the neutral and alkaline regions,

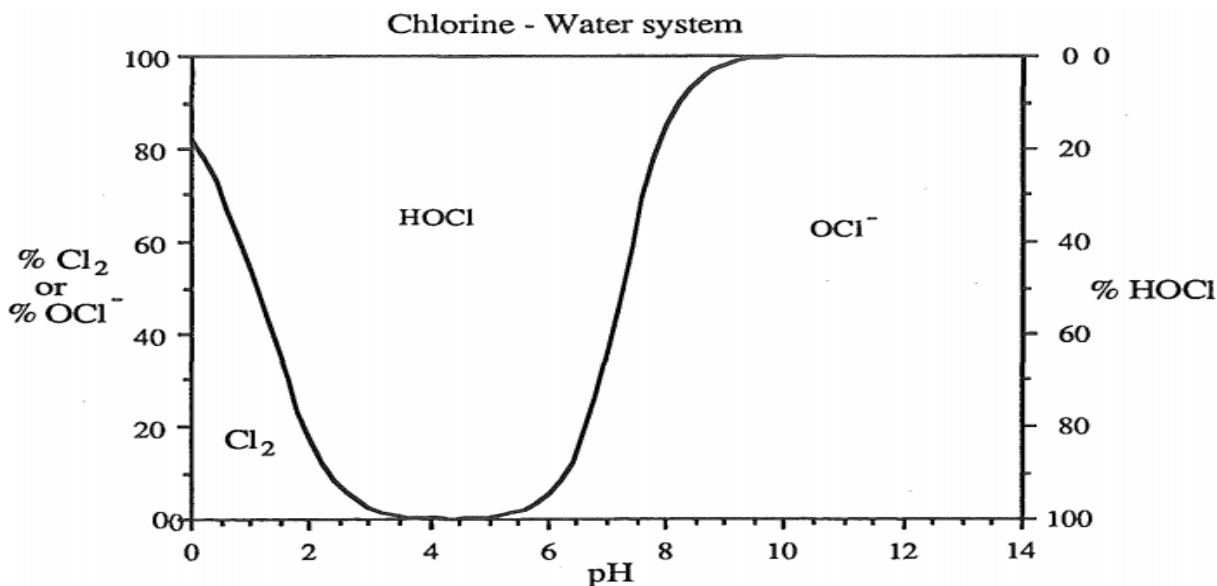
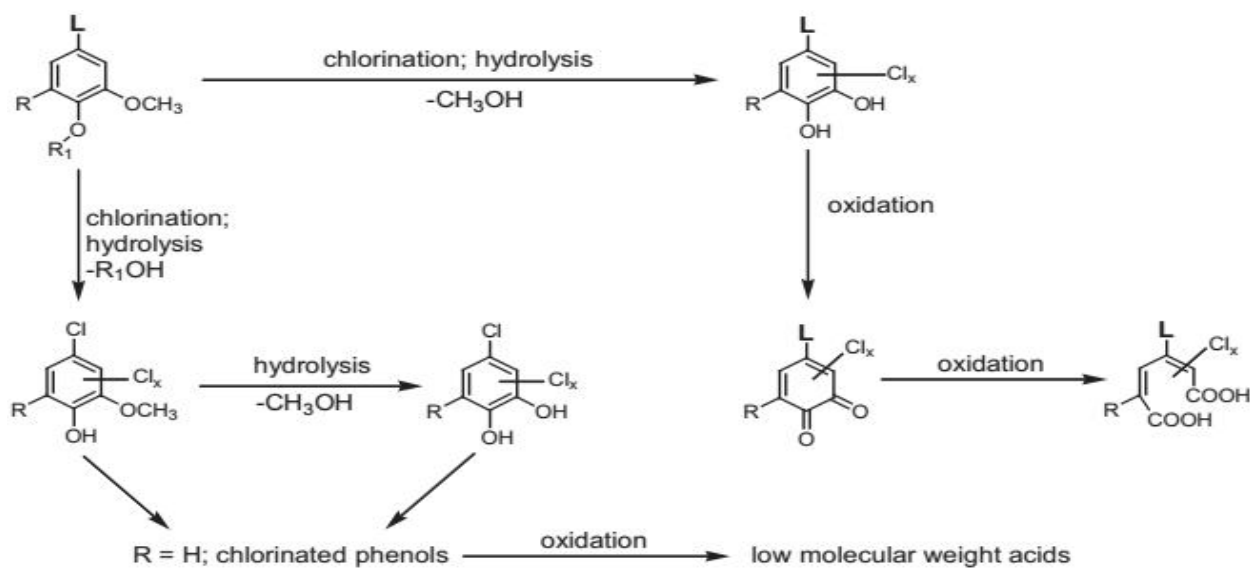


Figure 1.14: composition of chlorine –water system at different PH.



Scheme 1. 26: Reaction modes of lignin, in pulp bleaching with aqueous chlorine.

hypochlorous acid itself as reactive species, but is only capable of reacting with, negatively, charged ions. The reactivity ratio between lignin and carbohydrate in hypochlorous oxidation is of substantial interest, because of its degrading effect on cellulose on hypochlorite bleaching. Maximum attachment on cellulose occurs at PH 7. Hence the hypochlorite bleach should be around PH 9 to minimize cellulose degradation (T.J. McDonough 1991).

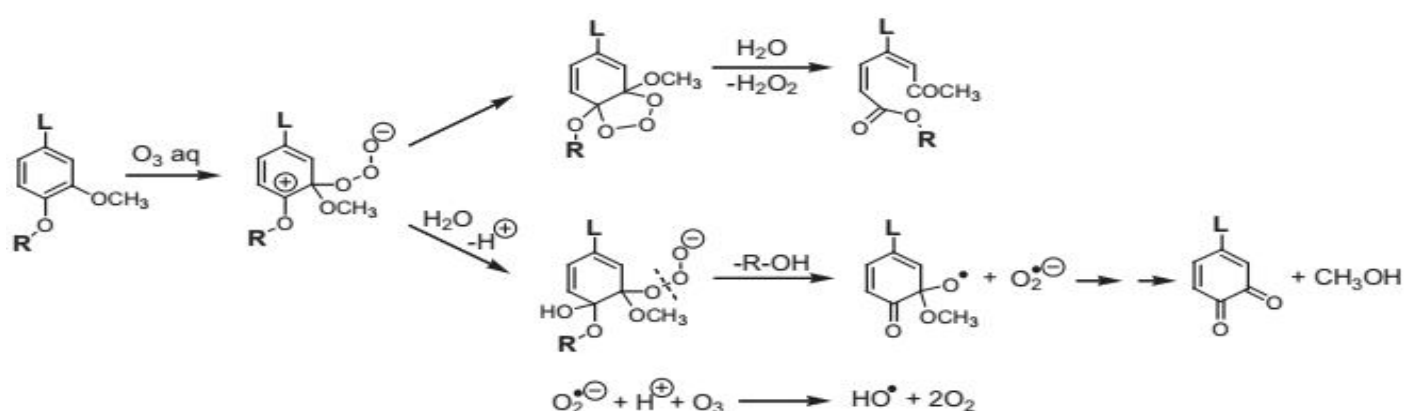
1.3.3.5 Ozone bleaching chemistry

The ozonolysis reaction has to be carried out under slightly acidic conditions since; otherwise, a rapid decomposition of ozone into hydroxyl and superoxide radicals will accompany the desirable oxidation reaction. The presence of these radicals is detrimental and will affect the quality characteristics of the pulp in a negative way (Bajpai 2012). Initial intermediate in the addition of ozone to the lignin, a trioxide, may decompose homolytically instead of forming the desired ozonide. In the latter case, the Criegee reaction, a ring opening reaction will follow whereas in the former case, superoxide radical is formed together with a quinol radical (Scheme 1.27). In the presence of ozone, the superoxide (hydroperoxy) radical will rapidly react further with formation of oxygen and hydroxyl radical (Bajpai 2012).

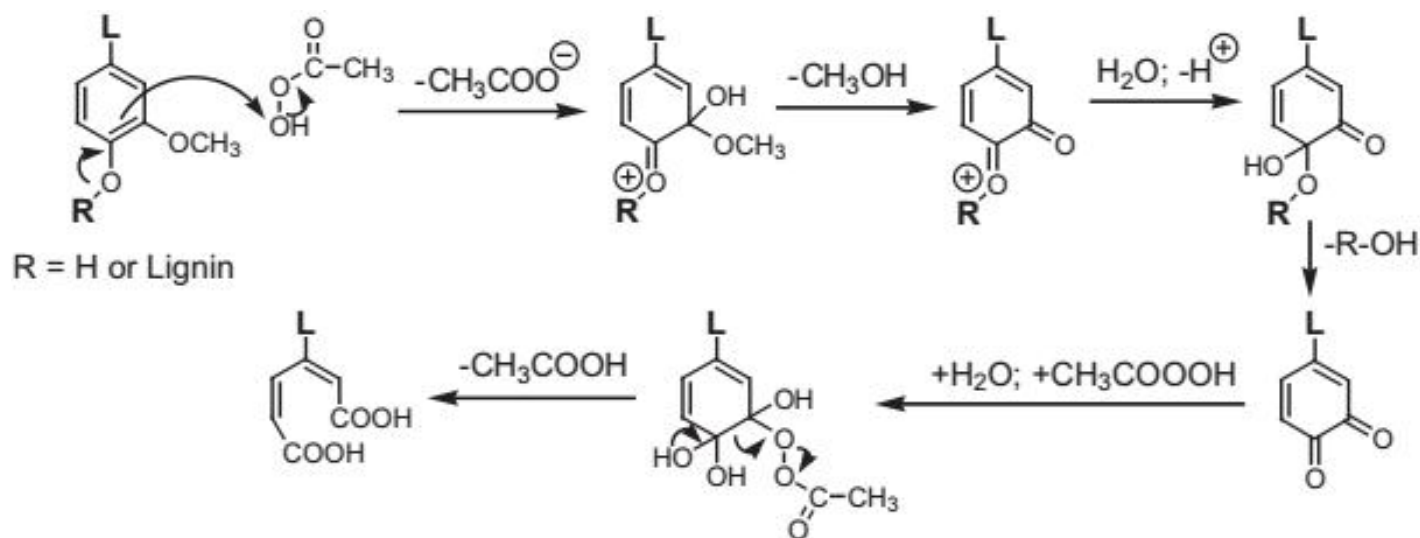
1.3.3.6 Peracetic bleaching

Peracetic acid has been known since a long time as an efficient and selective bleaching agent for both mechanical and chemical pulps. Thus, at weakly alkaline conditions (pH ~8), an elimination of chromophoric structures in mechanical pulps can be achieved without any substantial loss of yield (Hickman 2002). For chemical pulps, on the other hand, a comprehensive lignin oxidation and dissolution is obtained at neutral-slightly acidic pH-values. The major reaction between peracetic acid and lignin (Scheme 1.28) is a nucleophilic addition of peracetic acid to electron-rich aromatic systems resulting in a successive oxidation to muconic acid

structures via an intermediate formation of quinones. The reaction takes place with phenolic as well as with non-phenolic aromatic structures albeit with large differences in reaction rates. Overall, however, the rate of oxidation with peracetic acid is rather low. In addition to oxidation of aromatic rings, peracetic acid may also induce a side-chain cleavage by oxidation of benzylalcohol structures. Despite the selective reactions of peracetic acid, it has not been used commercially for bleaching purposes due to the high manufacturing costs (Jiménez et al. 2008).



Scheme 1.27: Oxidation of aromatic structures.

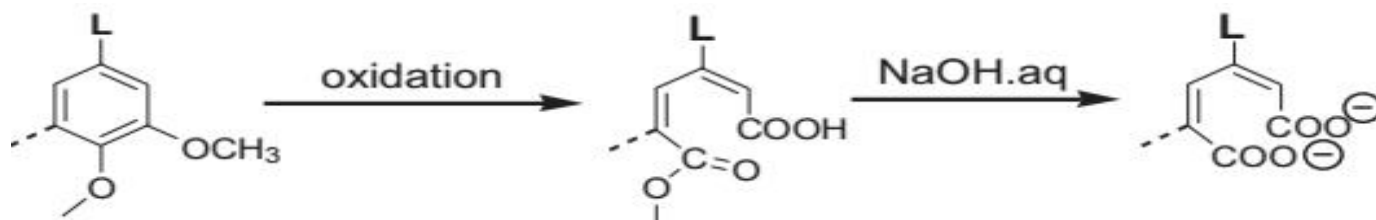


Scheme 1.28: Reaction sequence for the oxidation of aromatic lignin structures with peracetic acid.

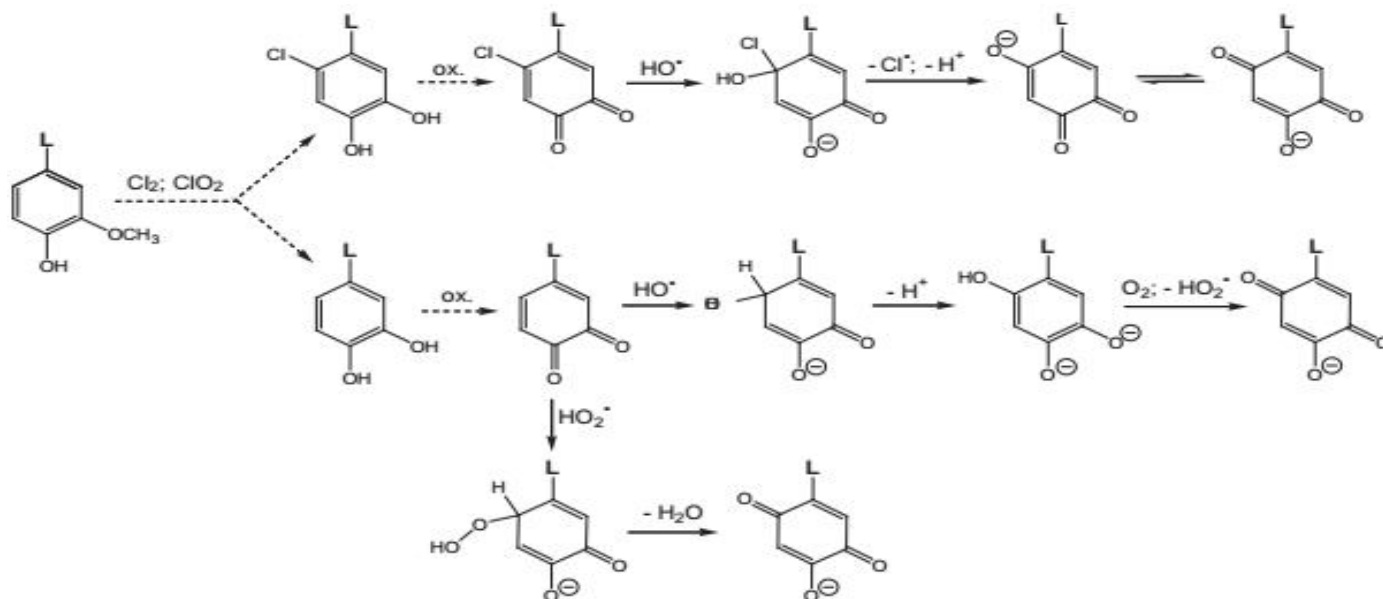
1.3.3.7 Alkaline extraction

Treatment of the pulp with aqueous sodium hydroxide is usually done at a temperature of 70–95 °C and with a retention time of one hour. Normally, an oxidant like oxygen, hydrogen peroxide or both is added in order to further increase the extent of lignin removal and/or to reduce the charge of chlorine dioxide. The major reaction encountered in an alkaline extraction stage is the neutralization of carboxyl groups (Scheme 1.29) thereby strongly increasing the water solubility of the oxidized lignin.

A comprehensive elimination of organically bound chlorine and formation of chloride ion takes place. In the presence of oxygen and/or hydrogen peroxide, an increased (Scheme 1.30) formation of quinones and an increased oxidative degradation of such structural units will occur (Runge et al. 1998).



Scheme 1.29: Neutralization of carboxyl groups in alkaline extraction stage.



Scheme 1.30: Lignin reactions in an alkaline extraction stage.

1.3.4 Dissolving pulp

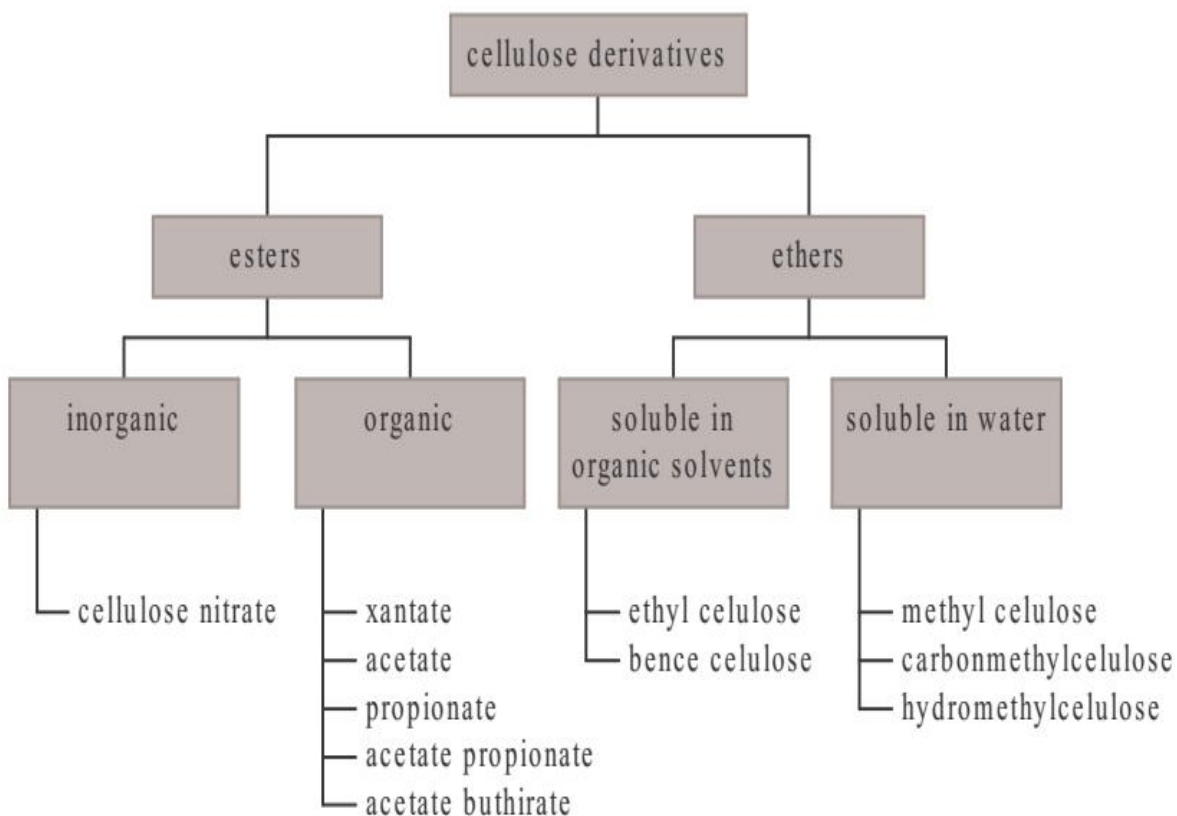
Dissolving pulp is a chemical pulp intended primarily for the preparation of chemical derivatives of cellulose. It is utilized for the chemical conversion into products such as microcrystalline cellulose, cellulosic ethers, and cellulosic esters. The unbleached pulp that results after pulping is used as raw material for dissolving pulp production. Lignin and hemicelluloses in the unbleached pulp are considered to be contaminants and are removed in order to produce high purity dissolving pulp (Batalha et al. 2012). The bleaching sequence can either be Chlorine dioxide – Alkali extraction – Chlorine dioxide – Hypochlorite or Chlorine dioxide – Alkali extraction – Chlorine dioxide – Peroxide stages depending on the desired end product i.e. 91%, 92% or 96% α -cellulose dissolving pulp (Ek 2010).

1.4 Cellulose derivatives

The OH groups of cellulose are relatively inert because of extensive intra and intermolecular hydrogen bonding where the three OH groups of anhydroglucopyranose of each cellulose unit are responsible for most of the interactions with organic and inorganic substances (Kumar et al. 2012). Purified cellulose shows semi-crystalline behavior and is insoluble in water and common organic solvents. In spite of its high crystallinity, cellulose decomposes before it undergoes melt flow. Therefore, cellulose is, generally, converted into derivatives such as ethers and esters because these derivatives are water soluble (Kumar et al. 2012).

Commercial cellulose derivatives (Scheme 1.31) are either ethers or esters that are soluble in water or organic solvents. The three free hydroxyl groups react with various functional substitution groups. The resultant substituents therefore disturb the inter- and intra-molecular hydrogen bonds in cellulose, reduce the hydrophilic character of the, numerous, hydroxyl groups, and increase the hydrophobicity.

Introducing ester and ether groups separates cellulose chains so that the fiber structure is either altered or destroyed (Cash and Caputo 2010). The solubility of a cellulose derivative in a solvent or in water depends on the type of substituents, the degree of substitution and the molecular weight. These cellulose derivatives are grouped according to the processes and chemical substituents. Cellulose derivatives are, usually, produced from cotton or wood-dissolving pulps, and have diverse physicochemical properties. They are mainly used, therefore, as additives of fine/special chemicals, such as cement additives, cosmetic additives, pharmaceutical components, diet additives, textile-treatment additives, painting additives, package materials and membrane materials (Granström and Kilpeläinen 2009).



Scheme 1. 31: Cellulose derivatives

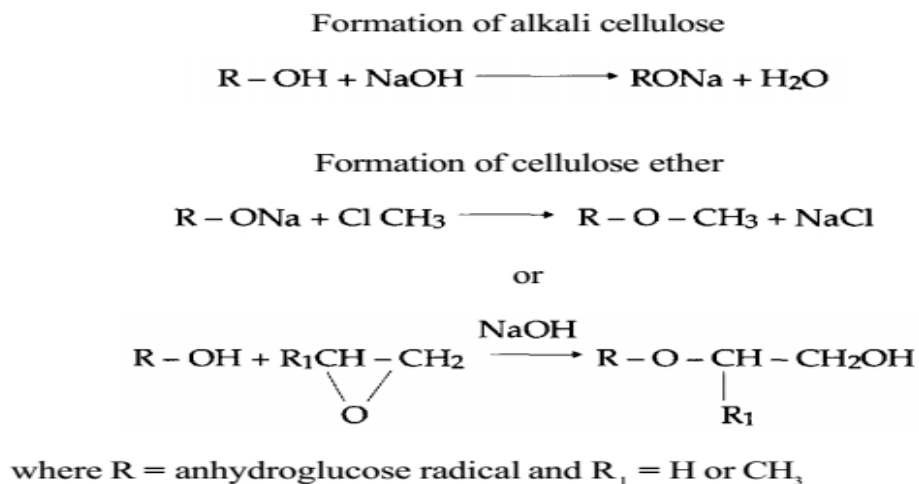
Cellulose ethers are important cellulose derivatives. They can be dissolved in water or in organic solvents. Cellulose ethers have various substituents, degrees of substitution, degrees of polymerization and even various mixed substituents, which make them suitable for a wide range of applications in various industries, such as the food industry, the recovery of oils, paper, cosmetics, pharmaceuticals, adhesive, agriculture, ceramics, textiles and construction (Majewicz and Podlas 2000). Cellulose is mercerized with aqueous alkaline solution to yield swollen alkali cellulose, which is etherified under alkaline conditions.

There are two important types of etherification (Scheme 1.32) depending on the amount of alkali. The first is a Williamson etherification (Brandt, 1986) in which an organic halide is used as the etherification reagent to react with the alkali cellulose. Alkali is consumed stochastically. On purification, the residual alkali must be washed out as salts. The second is a Michael addition (Brandt, 1986). The alkali functions as a catalyst during the addition of epoxides to the hydroxyl groups. No alkali is consumed although sufficient alkali must be retained during the etherification process. The alkali in the crude products must be neutralized before the purification stage (Nishimura and Sarko 1987).

The etherification can be carried out in heterogeneous or homogeneous systems as continuous or batch reactions. The cellulose ethers in heterogeneous system are produced by the following three steps: mercerization, etherification and separation or purification. In modern mercerization processes, 30–70 % NaOH solution is sprayed onto dry cellulose powder in fast-turning, dry-mixing aggregates (Brandt, 1986). The cellulose powder can also be impregnated with an inert organic solvent (Budtova and Navard 2016). The optimum parameters often control ageing time, temperature, NaOH concentration and the presence of catalytic amounts of iron,

cobalt, or manganese salts, which catalyze the oxidative depolymerization(Cerqueira et al. 2007)

Etherification is, preferably, produced in slurry systems. Most reactions are carried out in organic systems in order to produce final slurry in which solid ethers can, easily, be recovered. Another reason for this is that etherification is an exothermic reaction. In slurry, the heating and cooling can be,easily, controlled. Organic solvents are selected in order to produce the most uniform alkali cellulose and be unreactive towards the reagents and products.Some unreactive surfactants and amines have been added to improve penetrationinto organic systems and swelling, respectively (Fox et al. 2011).



Scheme1. 32 : synthesis of cellulosic ether derivatives.

1.4.1 Carboxymethylcellulose (CMC)

Carboxymethylcellulose (Figure1.15) is one of the most important cellulose derivatives, which have an immense importance to the industry. CMC is a linear, long chain, water soluble, anionic polysaccharide derived from cellulose (Yan et al. 2009). In addition, the purified cellulose is a white to cream colored as well as tasteless, odorless, and it is a free-flowing powder. Furthermore, due to its water-soluble heteropolysaccharides with high molecular weight properties, thus CMC is

often blended with starch to provide desirable texture, enhanced product quality and stability, control moisture and also water mobility (Feddersen and Thorp 2012)

Several methods have been used to synthesized CMC, including homogeneous carboxymethylation(Qi et al. 2009), fluidized bed technique(Murray and Fletcher 1994), sheet carboxymethylation , rotating drum technique, solvent-less method using a double screw press , a paddle reactor and heterogeneous slurry carboxymethylation(Schlufte and Heinze 2010).

In the slurry method, cellulose is mercerized by suspending in a mixture of NaOH-water-alcohol systems with an excess of alcohol(Scheme1.33). The liquid phase (water-alcohol mixture) which acts as a solvating agent dissolves the NaOH and distributes it evenly to the cellulose hydroxyl groups forming alkali cellulose. Aqueous NaOH penetrates the crystalline structure of cellulose, which then solvates its hydroxyl groups and, thus, makes them available for etherification reaction by breaking the hydrogen bonds (Gurd 1967). Furthermore, the alkali cellulose produced is reactive towards monochloroacetate acid (MCA) which is added in the second step either as free acid, or its salt, sodium monochloroacetate acid to form carboxymethyl cellulose ethers. NaOH reacts, simultaneously, with MCA to form two by-products, which are sodium glycolate and sodium chloride (Klemm et al., 1998).

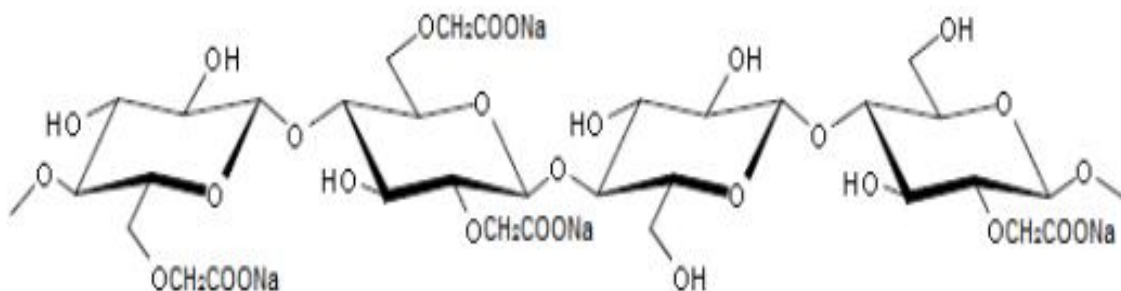
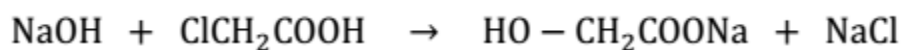
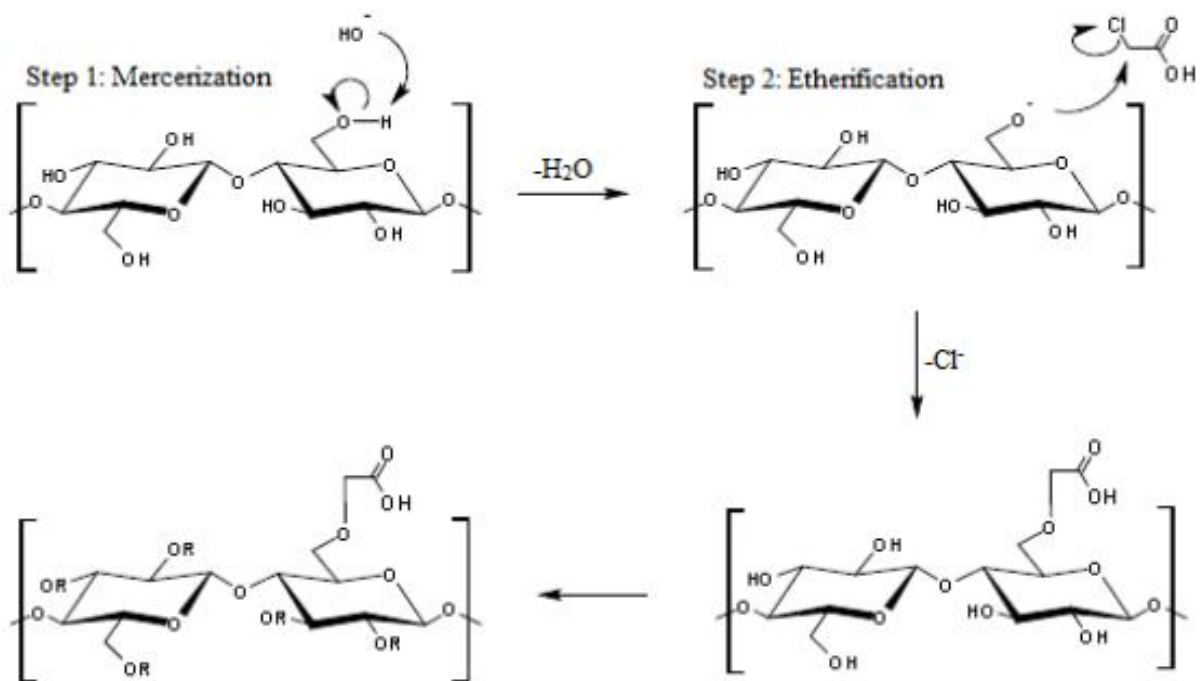


Figure1.15:Structure of carboxymethylcellulose.

Furthermore, in this carboxymethylation process, NaOH is consumed; thereby the initial charge of NaOH has to be high to maintain the alkaline pH throughout the reaction. If the pH during the etherification reaction is acidic, an internal etherification will occur and causes CMC molecules to be cross-linked. Therefore, pH in the reaction system is important during etherification reaction. According to (Klemm et al., 2001) the reaction requires at least 0.8 mole of NaOH per molecule of AGU to maintain the alkalinity if the etherifying agent used is NaMCA. However, if MCA is used instead, thus extra mole of NaOH per mole of AGU must be added to neutralize the acid. Based on (Olaru et al. 1998), the rate of mercerization reaction in ethanol is lower than isopropanol since sodium hydroxide is more favorable to dissolve in ethanol.



Scheme 1.33: Reaction mechanism of synthesizing carboxymethylcellulose.

The use of ethanol during mercerization stage will give a homogeneous NaOH-water-ethanol system. Whereas using isopropanol, a heterogeneous system will occur and forms a layer around the fiber composed of ,highly, concentrated NaOH-water phase due to the low solubility of NaOH in a non-polar system. Therefore, only small amounts of Na⁺ and OH⁻ ions will enter the alcohol phase of isopropanol and favoring a higher concentration of NaOH in the surrounding area of cellulose, which results in a significant decrystallization of cellulose and changes of polymorphism from cellulose to Na-cellulose during mercerization. In addition, it is also reported that different solvent system will affect the characteristic of CMC during synthesis. The use of isopropanol in CMC synthesis is reported to generate fewer amounts of sodium glycolate byproduct, as MCA is enriched in less polar solvent while NaOH in the aqueous phase (D. Klemm et al. 1998) . The efficiency of carboxymethylation increases as the polarity of the aqueous medium decreases (Barai et al. 1997), thus isopropyl alcohol is used since it has a lower polarity than water. The most common reaction diluents used for this process are isopropyl alcohol, t-butyl alcohol or ethyl alcohol (Majewicz and Podlas 2000).

Industrial applications of CMC polymer are due to its high viscosity, non-toxic, non-allergenic, biodegradability as well as production at lower cost. It is a most important water soluble derivative with various applications (Table 1.3) in paper, food, detergents, cosmetics, and textiles (Tasaso 2015).

Table 1.5: Applications of CMC

Industry	Application	Function
Paper	Internal additive	Water binder
Detergents	Laundry	Soil anti-redeposition aid
Cosmetics	Toothpaste	Thickener, suspension aid
Textiles	Printing paste, dye	Water binder, thickener
Foods	Frozen desserts	Inhibit ice crystal growth

1.4.2 Hydroxypropylcellulose(HPC)

Hydroxypropylcellulose (HPC) is an alkyl-substituted hydrophilic cellulose derivative that not only has a particular phase transition behavior in aqueous solution, and in some solvents, but also has many advantages such as excellent film forming properties, degradability, biocompatibility (Reddy et al. 2013).(Figure 1.5)

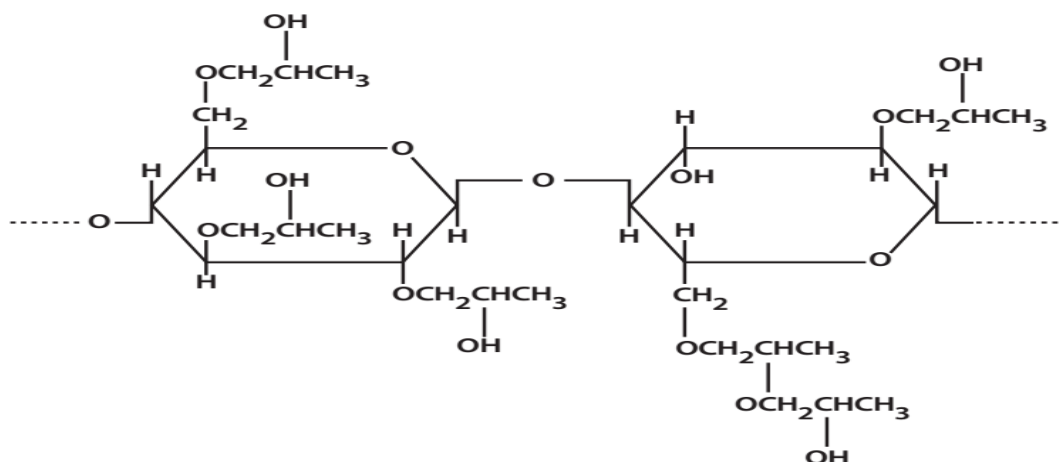
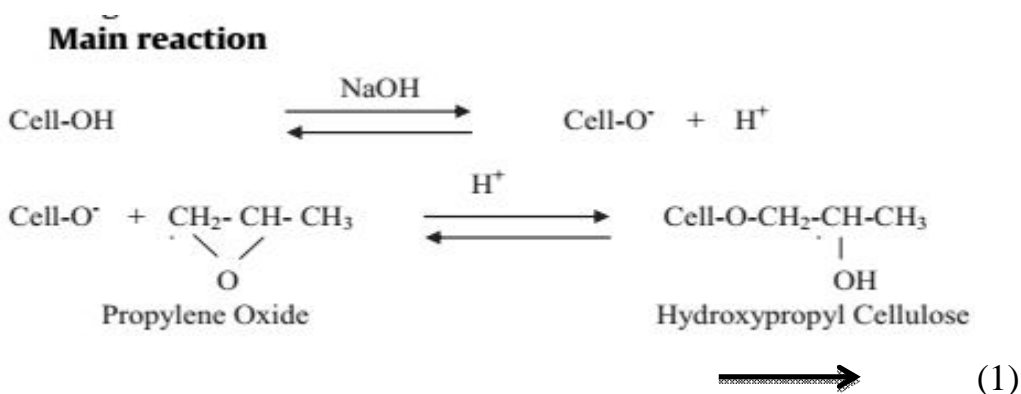


Figure 1.16: Structure of Hydroxypropylcellulose

HPC has been a focus of research because of these unusual and desirable properties, and its prospects in industrial applications. HPC is obtained by treating mercerized cellulose with propylene oxide (Reaction 1) in dispersing medium like isopropyl alcohol in a heterogeneous medium (Bhatt et al. 2011).



1.4.3 Methylcellulose (MC)

Methylcellulose (MC) is the simplest cellulose derivative, (Figure 1.17) where methyl groups (-CH₃) substitute the hydroxyls at C-2, C-3 and/or C-6 positions of anhydro-D-glucose units (Nasatto et al. 2015). MC is usually synthesized through a heterogeneous route in a two-phase system. More specifically, since cellulose is insoluble in water and in most common organic solvents, an alkaline medium (NaOH) is used to swell cellulosic fibers and obtain the alkali-cellulose. This alkali-cellulose reacts with an etherifying agent such as iodomethane, chloromethane, or dimethyl sulfate. Then, purification and removal of by-products is applied by washing in hot water, followed by drying and pulverization of the prepared MC. Sometimes acetone, toluene, or isopropanol are also added, after the etherifying agent, in order to increase substitution (Nasatto et al. 2015).

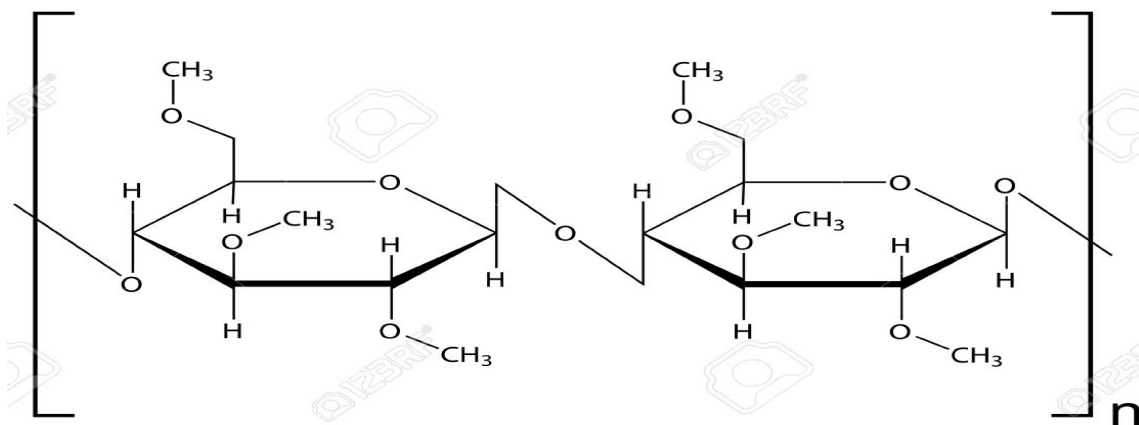


Figure 1.17: Structure of methylcellulose.

Methylcelluloses function as surfactants in aqueous systems by reducing surface tension and supporting emulsification of two-phase layers. The amphiphilic character is due to the presence of both hydrophilic OH and hydrophobic OCH₃ groups in a single methylcellulose molecule. Their viscosity is excellent during long-term storage due to resistance against fungi and bacteria attack. Methylcelluloses improve the properties of cement-based products and ceramic extrusions thanks to their lubricant and water-retention properties. Methylcelluloses function as thickening additives and improve adhesion degree of formulations, and form clear, tough, flexible films that have excellent barrier properties to oils and greases (Grover 2012). They also enhance the stability of suspension throughout the solution due to the formation of hydrogen bonds. They are soluble in some binary organic and organic-water solvent systems because they are hydrophobic (Vieira et al. 2009). Methylcelluloses dissolve more easily in cold water than in hot water. They can reduce water-loss when its formulations are applied to water-absorbing surfaces. They have excellent water-retention properties, being used in cement and gypsum formulations and in water-based paints and wallpaper adhesives, where the cohesiveness of the products is also important. Water retention increases as the number of hydrophilic groups and the

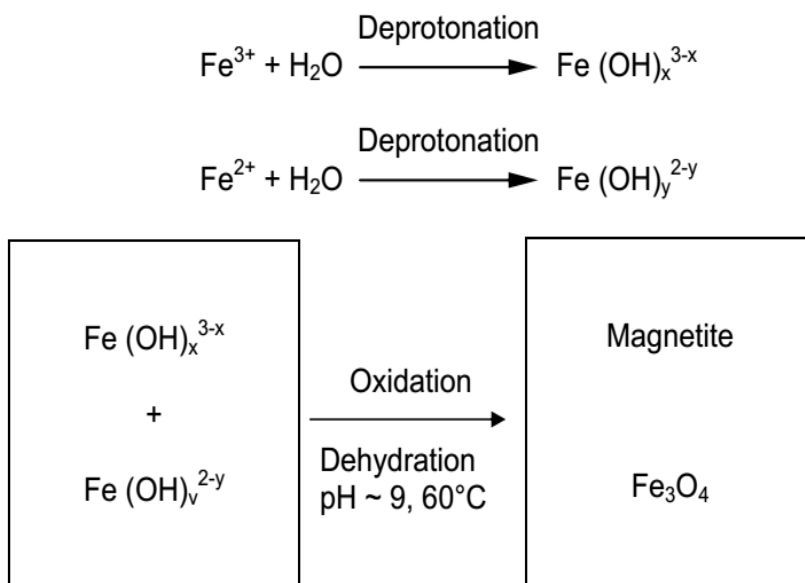
viscosity increase(Stimers and Greminger Jr. 1983). Typical applications for methylcelluloses are gels and fine or special chemicals in the pharmaceutical industry, foods, construction, paints, ceramics, detergent, agriculture, polymerization, adhesives, cosmetics, and tobacco(Viera et al. 2007).

1.5 Magnetite nanoparticles

Current and growing interest in nanostructures results from their numerous potential applications such as in materials development, biomedical sciences, electronics, optics, magnetism, energy storage, and electrochemistry(Hu et al. 2004; Majewski and Thierry 2007). Nano-sized materials display properties that differ from their respective bulk counterparts. Magnetic nanomaterials constitute one of the most interesting classes because of current and potential biological, biomedical and environmental applications like their use as adsorbents for the removal of dyes from polluted waters and the heavy metal uptake in water treatment procedures (Morel et al. 2013). The low toxicity, biocompatibility, cost-effectiveness and high surface area to volume ratios, as a function of particle size, when combined with their ability for surface chemical modification, represent major advantages compared to other nanoparticles (Hu et al. 2004) .There are several methods used to produce magnetic iron oxide nanoparticles. However, the common fundamental approach, currently, being used to synthesize magnetite nanoparticles is aqueous co-precipitation (scheme 1.34).

Conventionally, magnetite is prepared by adding a base to an aqueous mixture of Fe^{2+} and Fe^{3+} at a 1:2 molar ratio. The precipitated magnetite is black in color(Mascolo et al. 2013). A complete precipitation of Fe_3O_4 is expected between pH 9 and 14, while maintaining a 2:1 molar ratio of $\text{Fe}^{3+}:\text{Fe}^{2+}$ under an oxygen free environment. If the oxygen free environment is not maintained, Fe_3O_4 might be further oxidized (Eq.2). This would, critically, affect the physical and chemical

properties of the magnetic particles (Gupta and Curtis 2004). In order to prevent them from possible oxidation in air as well as from agglomeration, Fe₃O₄ nanoparticles are usually protected by adding organic or inorganic surfactants as a coating agent during the precipitation process. Successful approaches to the synthesis of stable magnetic nanoparticles use capping stabilization agents which may be simple molecules or polymer. Among the polymeric, capping, agents, biopolymers such as polysaccharides are of special interest due to their biocompatibility and biodegradability (J. Ngenefeme et al. 2013).



Scheme 1.34: Reaction mechanism of iron oxide formation in the presence of a strong base.



In term of magnetic nanoparticles removal of dyes from polluted waters and heavy metal uptake in water treatment procedures, adsorption kinetics and isotherms are very essential to determine the adsorption equilibrium time and to investigate the adsorption mechanism. These parameters are important for the optimization of the

waste water treatment process with Fe₃O₄nanoparticles. Pseudo-first and pseudo-second order models (Eqs3 and 4) and Langmuir, Freundlich(Eqs5 and 6) are applied to explain the experimental data of adsorption kinetics and isotherms respectively (Wong et al. 2004).

$$\log(q_e - q_t) = \log(q_e) - \frac{K_1}{2.303} t \quad (3)$$

$$\frac{t}{q_t} = \frac{t}{q_e} + \frac{1}{K_2 q_e^2} \quad (4)$$

$$\frac{C_e}{q_e} = \frac{1}{Q_0 b} + \frac{C_e}{Q_0} \quad (5)$$

$$\log q_e = \log k_f + 1/n \log C_e \quad (6)$$

In the above equations, in Eq. 3 and 4, the parameters q_t and q_e (mg/g) are the adsorption capacity at time t and at equilibrium, respectively; k_1 (min^{-1}) and k_2 ($\text{g mg}^{-1} \text{min}^{-1}$) are the corresponding rate constants of adsorption.

Where in Eq. 5, C_e is the concentration of solution (mg L^{-1}) at equilibrium, Q_0 gives the theoretical monolayer adsorption capacity (mg g^{-1}) and b is related to the energy of adsorption (mg L^{-1}). In Eq. 6, k_f and $1/n$ are the constants that can be related to adsorption capacity and the intensity of adsorption respectively.

1.6 Cellulose derivatization

Heinze and Pfeiffer, (1999) prepared CMC using a completely heterogeneous procedure in an isopropanol/water slurry and checked the influence of the reaction conditions on the pattern of functionalization within the anhydroglucose repeating unit as well as due to the formation of the four main repeating units. The reaction

with sodium monochloroacetate leads to a high degree of substitution (DSCMC) of 1.24 at a NaOH concentration of 15% and 5 h reaction time. And they found that no influence of the reaction time between 2 h and 6 h using 30 % NaOH.

Claudia *et al.*, (2002) synthesized carboxymethylcellulose from non-wood fiber (abaca, jute, sisal, linen and *Miscanthus sinensis*) and studied the accessibility of cellulose fiber, by one and two successive reaction steps in aqueous medium under identical conditions. They concluded that, the degree of substitution (DS) of CMC was found to depend upon the source of the cellulose pulp, but generally it was close to 1 with one etherification treatment and around 2 after the second. The molar mass of CMC depends on the initial intrinsic viscosity of the cellulose pulp. The weight average molar mass of our CMCs ranged from 1.5×10^5 to 2.8×10^5 . Increasing the DS up to 2 improved the CMC solubility, but viscosity slightly decreased due to a slight degradation of the polymer.

Latif *et al.*, (2006) synthesized carboxymethylcellulose from rayon grade wood pulp and cotton linter by two step etherification and concluded that the etherification could, generally, increase the degree of substitution in case of cotton cellulose to 1.9.

Hutomo *et al.*, (2012) synthesized sodium carboxymethylcellulose from pod husk of Cacao. And determined the optimum condition for synthesis by the response surface methodology (RSM). And showed that, the optimum condition was 15% NaOH and 4 g NMCA, at 55.93 °C for 3h. Extracted Na-CMC had 0.75° of substitution (DS), 3.73 g/g water holding capacity (WHC), 2.12 g/g oil holding capacity (OHC), 56.61 lightness, 206.10 cps viscosity, and 141.60% yield.

Haleem *et al.*, (2014) isolated cellulose from cotton gin waste and synthesized carboxymethylcellulose by etherification using sodium monochloroacetic acid and sodium hydroxide. They showed that the optimum condition was found to be 20 g/100 mL NaOH which provided the highest viscosity and degree of substitution (DS = 0.874). and characterized cellulose and CMC using Fourier transform infrared spectroscopy (FT-IR) and scanning electron microscopy (SEM). FT-IR analysis, and revealed that the produced cellulose was of very good quality.

Tasaso., (2015) synthesized carboxymethylcellulose from oil palm fronds using response surface methodology (RSM). He found that the optimum conditions were: 52 % NaOH and 10.7 g of MCA, at reaction temperature of 50 with 3 h of reaction time, and the highest yield of 170.1 % CMC. He characterized the synthesized CMC and found to have a DS of 1.1, purity 97.3 %, viscosity of 1% w/v CMC solution was 685 cP. And categorized it as technical grade CMC.

Onigbinde and Vivian., (2015) prepared carboxymethylcellulose from agricultural wastes such as sugarcane bagasses, maize cob, palm kernel cake, palm oil empty fruit bunches banana pseudo stem and orange mesocarp. They extracted cellulose from raw materials by 8% sodium hydroxide and bleaching using 3.85% NaOCl at 30 °C and then etherified by monochloroacetic acid. They characterized the physical properties of NaCMC in terms of degree of substitution, viscosity with FT-IR spectroscopy. They found it has a viscosity of 14.0 cPs at 29.8 °C and DS 1.02 and therefore were categorized as technical grade with medium viscosity. After optimization and scaling up of the production process they concluded that, the NaCMC synthesized will be a useful and cheap raw material for the industries.

Yeasmin and Monda., (2015) synthesized food grade carboxymethylcellulose from corn husk agro waste by extraction of alpha cellulose by 30% (w/v) NaOH and etherification by 120%(w/v) mono chloroacetic acid using ethanol as supporting solvent with reaction time of 3.5 h at 55°C. The synthesized CMC characterized in term of DS and physical properties were compared with CMC available in the international market. And they found that, the purity of the prepared CMC was higher, at 99.99% well above the purity of 99.5% for standard CMC. High purity CMC showed a yield 2.4 g/g with DS 2.41, water holding capacity 5.11 g/g, oil holding capacity 1.59 g/g. And then concluded that, the obtained product is well suited for Pharmaceutical and Food Industries.

Yeasmin and Mondal., (2015) synthesized highly substituted carboxymethyl cellulose depending on cellulose particle size using sodium hydroxide (NaOH) and monochloroacetic acid (MCA), in aqueous ethanolic medium, under heterogeneous conditions. Optimized the carboxymethylation reaction as to the NaOH concentration, MCA concentration, reaction temperature, reaction time and cellulose particle size. And determined the degree of substitution (DS) using chemical methods. Then identified, the produced, CMC by FTIR and the crystallinity of the CMC by XRD. They found that the CMC product had an optimized DS of 2.41 and the optimal conditions for carboxymethylation were NaOH concentration, 7.5 mol/L; MCA concentration, 12 mol/L; reaction temperature, 55°C; reaction time, 3.5 h and cellulose particle size, 74 µm. A highly substituted CMC with higher yield, 2.40 g/g, and concluded that it could provide plenty of opportunities for its many applications.

Viera et al., (2007) produced methylcellulose from cellulose extracted of sugar cane bagasse, using dimethyl sulfate in heterogeneous conditions. Studied the effect of using toluene and acetone during the synthesis. Without using the solvent,

the degree of substitution (DS) of the methylated sample was 0.70, reaching a DS of 1.2 when using acetone. The produced methylcellulose presents chemical and physical properties that increase its range of application and aggregate value to this agro-industrial residue.

Kumar *et al.*, (2012) synthesized methylcellulose (MC) from chemically purified cellulose extracted from sugarcane bagasse with dimethyl sulfate (DMS) in the presence of sodium hydroxide and acetone as solvent under heterogeneous conditions and characterized the products by FT-IR, ¹H-NMR, and ¹³C-NMR and found that the degree of substitution (DS) is 1.44.

Vieira *et al.*, (2012) produced methylcellulose from the fibers of mango seeds by heterogeneous methylation, using dimethyl sulfate and iodomethane as alkylating agents, respectively. And characterized the product for their thermal properties (DSC and TGA), crystallinity (XRD) and Degree of Substitution (DS) in the chemical route. Employed MC as mortar additive in order to improve mortar workability and adhesion to the substrate and concluded that the polymers can be used to produce adhesive mortars.

Oliveira *et al.*, (2015) prepared methylcellulose from bacterial cellulose (BC), using dimethyl sulfate in a 3 h and 5 h reaction time under heterogeneous conditions. And characterized the products by FT-IR, SEM, ¹H-NMR and ¹³C-NMR. The 3 h methylcellulose showed a degree of substitution (DS) of 2.26 ± 0.13 and 5 h methylcellulose showed a DS of 2.33 ± 0.05 .

Bhatt *et al.*, (2011) prepared hydroxypropylcellulose from *L. camara* isolated alpha cellulose with propyleneoxide in presence of sodium hydroxide under different reaction conditions. The optimum conditions for (DS 1.42) were 23.18 M/AGU

propyleneoxide and 1 M/AGU sodium hydroxide at 70 °C for 3 h. evaluated the optimized product with IR, SEM, TGA/DTA and WAXDs.

Marseno et al.,(2014) synthesized hydroxypropylcellulose from oil palm empty fruit bunches using propylene oxide. The optimum condition were, alkalization using 10% NaOH and etherification using 1.4% (v/w) PO.

Chen *et al.*, (2014) synthesized hydroxypropyl cellulose (HPC) from bacterial cellulose with propylene oxide under different reaction conditions while diluted by toluene. The optimized product exhibited cold-water solubility and hot-water gelatinization in aqueous medium. Further, studied the product with FTIR, TGA, XRD, SEM and ¹³C-NMR for characterization.

Garza-navarro and Gonz, (2011) developed a method to obtain nanocomposites of chitosan/magnetite with high magnetite content (75 wt %) and narrow particles size distribution which observe a mean diameter of about 7 nm. The nanocomposites were structurally and morphological studied by X-ray diffraction and transmission electron microscopy, and magnetically characterized by magnetometry. The nanocomposites show a congruent behaviour with the actual magnetic theory on single domain particles, presenting superparamagnetic character at room temperature and ferromagnetic properties at 2 K.

Pham *et al.*, (2016) synthesized anti-cancer drug curcumin-loaded superparamagnetic iron oxide (Fe₃O₄) by chitosan nanoparticles was modified (CS), using reverse micro-emulsion (water-in-oil) method. Characterized the magnetic iron oxide nanoparticles by XRD, FTIR, TG-DTA, SEM, TEM, and VSM technique. And concluded that the modified magnetic nanoparticles can be used as drug delivery carriers on target in the treatment of cancer cells.

S *et al.*, (2016) investigated the use of polymer derived from oleic acid for coating iron oxide nanoparticles. The average diameter of the coated and uncoated nanoparticles obtained by transmission electron microscopy was around 13 nm and 11 nm and the average diameter of crystallite by X-ray diffraction was around 8 nm and 12 nm respectively. The vibrating magnetometer indicated that coated nanoparticles remain magnetic, with increasing saturation magnetization value, when a magnetic field was applied.

1.7 Problem statement

In modern world, the consumption of disposable materials has increased and hence, the load on the environment has increased dramatically. Consequently, the demand for bio-based materials with renewable, low-cost and sustainable properties has increased. Cellulose-based materials of plants such as mesquite which is known to cause agricultural problems can potentially provide products to meet this demand. In addition, the chemical modification of cellulose-based materials could be developed to meet the requirements set for environmental legislation. Cellulose as raw material has several useful attributes; it is abundant, bio-based and renewable just to mention a few. Furthermore, cellulose has proved to be a versatile material due to its unique chemical structure, which provides a superior platform for several new biomaterials. However, the efficient use of this versatile material has been hampered by its insolubility in organic solvents and in water. However, modification opened up more possibilities for using. This research is aim to study the potential of synthesizing of cellulosic ether derivatives from mesquite as available cellulose source.

1.8 Objectives of the study

- To extract cellulose from mesquite plant
- To synthesize cellulose ether derivatives and optimize etherification of products.
- To characterize the synthesized products.
- To investigate thermal stability of the products.
- To investigate novel uses of the prepared products.

Chapter two

Materials and Methods

2 Materials and Methods

2.1 Raw materials

Mesquite wood was collected from different locations in Khartoum state, washed, crashed, and milled, sieved to suitable size, washed, and air dried at room temperature..

2.1.1 Determination of moisture content

10 g sample of ground mesquite was, accurately, weighed in a dry Petri dish and dried at 105 C for 3 h. The sample is allowed to cool in a desiccator, reweighed and the weight is recorded. The drying-cooling-weighing procedure is repeated until the weight is constant. The moisture content is measured using the following equation:

$$\text{Moisture content \%} = \frac{W_1 - W_2}{W_1} \times 100$$

Where W_1 is the weight of the moist mesquite sample and W_2 is the weight of the dry mesquite sample.

2.1.2 Determination of ash content

Porcelain crucible was weighed accurately (A g). About 3 g of ground mesquite was put in the crucible and the crucible with the sample was weighed accurately (B g). The sample was ashed in an electric muffle furnace, at 850 ± 25 C overnight, cooled in the desiccator for 15 min and the crucible containing the ash was weighed (Cg). The ash content is calculated using the following equation.

$$\text{Ash content \%} = \frac{C - A}{B - A} \times 100$$

Where:

A = weight of empty crucible (gram)

B = weight of crucible and sample (gram)

C = weight crucible and ash (gram).

2.1.3 Lignin content determination

Ground mesquite was extracted at first with ethanol – benzene mixture (1:1) and dried. About 1 g (accurately weighed) was then treated with 20 ml 72% sulfuric acid, drop-wise with constant stirring. After complete disintegration the sample was allowed to stand covered with a watch glass and left overnight at room temperature. The sample was then transferred quantitatively to one-liter round flask, diluted to 3% sulfuric acid and boiled for 4 h under reflux. The lignin was filtered on a pre-weighed filter paper and washed with hot distilled water till neutrality. The lignin was then dried at 105 C for 6 h and gravimetrically estimated according to the following equation:

$$\text{Lignin content \%} = \frac{\text{Weight of lignin}}{\text{Weight of sample}} \times 100$$

2.1.4 Determination of hemicelluloses

Accurately weighed ground mesquite sample (X) was extracted with 10% KOH using a material to liquor ratio of 1:20 for 10 h at 50 C; the system was allowed to cool and filtered. The filtrate was made acidic using glacial acetic acid until pH 6 is attained. The filtrate is then mixed with a solution of 2 volumes ethanol. The precipitate, formed, was recovered by filtration, and freeze-drying and weighed (Y). The hemicelluloses content (%) was calculated using the following equation:

$$\text{Hemicellulose content \%} = \frac{Y}{X} \times 100$$

2.2 Preparation of dissolving pulp

Mesquite wood grindings were introduced to pre hydrolysis using HCL 4% at 120 C for one hour and liquor ratio of 1:8 (Hashem et al. 2005). Then the fiber was introduced to modified Kraft pulping using 20, 25, 30, 35, 40 and 45% NaOH, 5% Na₂S, and 0.04% anthraquinone at 180 C for 3 hours (Fišerová and Opálená 2014). The obtained pulp was bleached by treating with NaOCl 5% at 30 C, PH of 11, consistency of 5% for 3 hours within two sequences, washed by water till the odor of NaOCl is no longer detected and screened. The bleached pulp was treated by 17.5 % NaOH for 1 hour and washed several times with water then steeped in 10% acetic acid for 10 minutes, finally the cellulose was washed by water until neutral extract and dried(Hashem et al. 2006).

2.3 Determination of alpha cellulose in bleached pulp

3.00 g of oven dried pulp was weight in 400 ml beaker. 25 ml of 17.5 % NaOH was added and left for 1 minute then pressed by glass rode. Another 25 ml 17.5 % NaOH was added and stirred to form homogeneous paste and left for 35 minutes. 100 ml of distilled water was added and the mixture was neutralized by 10% acetic acid. The remaining alpha cellulose was filtered and washed using sintered glass and dried(Schuerch 1968). Percentage of alpha cellulose was calculated using the followed formula:

$$\text{Alpha cellulose} = \frac{\text{Weight of alpha cellulose}}{\text{Initial weight of pulp}} \times 100$$

2.4 Preparation of carboxymethyl cellulose.

Carboxymethylation was carried out by suspending 5 g of cellulose in 150 ml of isopropanol. 15 ml of 20, 25, 30, 35, 40, 45% NaOH with continous mechanical stirring over a period of 30 minutes at room temperature was added. 3, 4, 5, 6, 7, 8 gm of monochloroacetic acid was added over a period of 30 min. the mixture was

left with continuous stirring for 3.5 hours at 55 C. After the end of the reaction, the product was precipitated by adding methanol followed by neutralization with 10% acetic acid, filtered and washed with 70% ethanol. The precipitate were washed with absolute methanol and dried at 60 C. The degree of substitution of the synthesized sodium carboxymethylcellulose was estimated by acid wash method (Schuerch 1968). 4 g of synthesized carboxymethyl cellulose were agitated with 10 ml of 2 M nitric acid for 2 min. The supernatant liquid was decanted. The precipitate was heated to 60C to remove nitric acid. 1 g of carboxymethyl cellulose mixed with 100 ml distilled water and 25 ml 0.3 N NaOH solution. The excess amount of sodium hydroxide was titrated with 0.3 N HCl. The degree of substitution was calculated as follows:

$$A = \frac{BC - DE}{F}$$

$$\text{Degree of Substitution}(DS) = \frac{0.162A}{1 - 0.058A}$$

Where:

A= milliequivalent of acid consumed per gram of sample.

B= milliliters of NaOH solution added. C = normality of NaOH solution.

D= milliliters of HCl required for titration of excess NaOH. E= normality of HCl.

F= grams acid carboxymethylcellulose used. (162 = gram molecular weight of the anhydroglucose unit of cellulose. 58= net increase of anhydroglucose for any carboxymethyl group substituted).

2.5 Preparation of methylcellulose (MC)

MC was prepared by mercerization of (3.0 g) purified cellulose of mesquite using 60 mL of 50% NaOH solution for 1 hour at room temperature. Excess NaOH was removed by filtration. And acetone (27.0 mL) was added. Dimethyl sulfate (DMS) (50%, 100%, 150%, 200%, 250% and 300% (v/w) based on weight of oven dried cellulose was added drop-wise at 50 °C with constant stirring. After 1 hour of reaction, the system was filtered and fresh reagents were added (acetone and DMS), maintaining the same previous proportions. The same procedure was repeated for 2, 3, 4, 5 and 6 hours reaction time. Methylcellulose, obtained, was neutralized using acetic acid (10% v/v), filtered, and washed with acetone (three times) and dried at 50 °C (Kumar and Walia 2014; Oliveira et al. 2015). The degree of substitution (DS) of methylcellulose was calculated (Bhatt et al. 2011; Kumar et al. 2012).

$$DS = \frac{\% \text{ Weight hike} \times \text{mol. wt. of anhydroglucose unit}}{\text{Mol. wt. of methyl unit (CH}_3\text{—)} \times 100}$$

2.6 Preparation of hydroxypropylcellulose (HPC)

Purified mesquite cellulose was activated by standard slurry method. 2 g of cellulose were suspended in 40 ml isopropanol and stirred vigorously, 5.65 g of 40% NaOH (w/w) were added one word over two hours at room temperature, and washed with distilled water until neutral (PH 7). After vacuum filtration, the activated cellulose was dried at 80 °C for 24 hours, suspended in 19.6 ml toluene and swept in N₂ for 5 minutes. Hydroxypropylation was conducted by adding 1.2, to 3.2 ml/g cellulose of propylene oxide. The mixture of optimum 2.8 ml/g cellulose was placed in water bath at 70 °C for 2, 3, 4, 5, 6 and 7 hours with stirring, cooling below 30 °C. The mixture was filtered, suspended in 50 ml of 80% (v/v) methanol and neutralized with acetic acid. The product was washed three times with 350 ml of 80% (v/v), 350 ml methanol and dried at 60°C (Chen et al. 2014).

The degree of substitution (DS) of hydroxypropylcellulose was calculated (Bhatt et al., 2011 ; Kumar et al., 2012; Reddy et al. 2012).

$$DS = \frac{\% \text{ Weight hike} \times \text{mol. wt. of anhydroglucose unit}}{\text{Mol. wt. of hydroxypropyl (CH}_3\text{C}_2\text{H}_2\text{O-)} \times 100}$$

2.7 Synthesis of magnetite nanocomposite

The synthesized CMC/MC/HPC has been tested for the preparation of CMC, MC, HPC/Fe₃O₄ hybrid by co-precipitation method (J.Ngenefeme et al. 2013). 0.15 g of CMC/MC/HPC and 5.2 g of ferric chloride was dissolved in 12.5 ml of deoxygenated distilled water separately and mixed in 100 ml beaker while stirring. Also, 0.15 g of CMC/MC/HPC, and 2.674 g of ferrous sulfate was dissolved in 12.5 ml of deoxygenated distilled water separately mixed in 100ml beaker while stirring and both solutions stirred overnight then mixed in the next day and deoxygenated again for 10 min. Ammonium solution 1.5 M was then added dropwise using a syringe till the solution became, completely, black indicating the formation of magnetite. The resultant, black, residue obtained was filtered and washed several times with distilled water until the pH dropped to 7. The precipitate was then freeze-dried and characterized.

2.8 Application of the carboxymethyl cellulose/Fe₃O₄ nanocomposite for methylene blue (MB) adsorption from aqueous solution

Aqueous solutions with different concentrations of methylene blue MB (25–1500 ppm) were prepared by stock dilution with water. Batch adsorption experiments were conducted in 50 ml glass bottles with 50 mg of dried adsorbents. The solutions were mixed well with magnetic stirring and maintained for a fixed time at 25 C. To determine the adsorption capacity at various pHs, the pH of the dye solutions was adjusted with 0.1 M HCl and 0.1 M NaOH aqueous solution. After adsorption for a desired time, the solution was separated from the adsorbents with

a syringe filter and the dye concentration was measured. The amount of MB adsorbed on the hybrid at adsorption equilibrium, q_e (mg/g), was calculated according to the following equation:

$$q_e = \frac{(C_0 - C_e)V}{W}$$

Where C_0 and C_e are the initial and equilibrium dye concentrations (mg/L), V is the volume (L) of the dye solution used in the adsorption experiment and W is the weight of nanocomposite (g).

2.9 Characterizations

FT-IR of HPC and cellulose was conducted using (Mattson 5000 FTIR spectrometer) in the range of 4000-400 cm^{-1} (Kumar et al. 2012). Thermogravimetric analysis of methylcellulose and cellulose was conducted using (SDT Q600 V20.9 Build 20) to determine the weight loss at different temperatures in range 20-850 C at a rate of 20 C per minute (Hivechi et al. 2015). X-Ray patterns were taken using CuK radiation source by supplying 40 kV and 40 mA to X-ray generator. The patterns were recorded at $2\theta^\circ$ from 5° to 80° (Haleem et al. 2014). NMR analysis was performed on a Bruker 400 NMR spectrometer equipped with dual probe (^{13}C and ^1H) in DMSO solvent (Oliveira et al. 2015). Methyl blue (MB) concentration was determined, calorimetrically, by measuring at maximum absorbance at 668 nm (JASCO V-650) spectrophotometer.

Chapter three

Results and discussion

3 Results and discussion

Table 3.1: shows the results of mesquite wood analysis and were within the limits of known results analysis of common wood with a high cellulose content of 45% that qualify mesquite plant wood to be as source of cellulose. These results were agreed with studies of (Khattak, T.M. and Mahmood 1986 ; Nasser 2008).

Table 3.2: shows the effect of NaOH concentration on unbleached pulp properties. The best NaOH concentration for good yield and holocellulose content was found to be 20% based on dry weight of wood. That because NaOH affect both lignin and carbohydrates (Gierer 1980).

Table 3.3: shows the results of mesquite wood bleached pulp properties. The extracted pulp has a high percentage of alpha cellulose, acceptable reject and yield, which makes the mesquite wood as usable source for producing dissolving pulp by this method.

Table 3.1 Mesquite woods analysis

Moisture content %	Ash content %	Lignin content %	Cellulose %	Hemicellulose %	Extractives %
3.7	2.56	22.75	45	23	2.99

Table 3.2 Effect of NaOH concentration on unbleached pulp properties.

NaOH concentration %	Pulp yield %	Holocellulose %
18	75	65
20	70	85
25	60	70
30	55	80
50	40	85

Table 3.3 Extracted mesquite bleached pulp properties.

rejects	α -cellulose content	Yield
2.5 %	92%	36%

Figure 3.1A: shows the effect of DMS concentration on the DS of methylcellulose. The DS value was found to increase, significantly, when the concentration of DMS is increased up to 300% (v/w), thereafter it remained unchanged. The increase in DS is probably due to the greater availability of the methyl ions at higher concentrations close to cellulose molecules, and after 300% (v/w) it turned to un limiting factor(Abdel-Halim 2014).

Figure 3.1B: shows the effect of reaction time over degree of substitution of methylcellulose. The methylation reaction was carried out at the optimum DMS concentration of 300 % (v/w). The maximum DS value attained was 1.68 at 5 h. Further increase in time resulted low DS.The increase in DS value at longer reaction times could be due to the effect on the diffusion and absorption processes

of the reactants, with improved contacts between DMS and cellulose. The decrease in DS after 5 h of methylation may be due to atmospheric oxidative degradation of MC (Mansour et al. 1994).

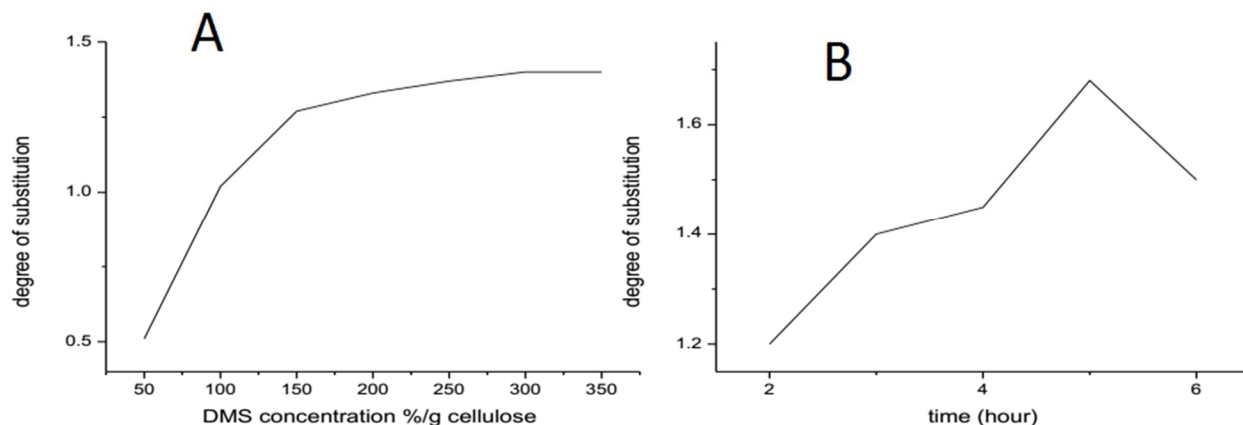


Figure 3.1 : (A) Effect of DMS on DS of MC, (B) Effect of reaction time on DS of MC.

Figure 3.2A: shows the effect of NaOH concentration as function of degree substitution of carboxymethylcellulose (CMC). The NaOH concentration plays an important role in the production of CMC and by-products. The carboxymethylation process was carried out at different concentrations of NaOH ranging from 20 to 45% (w/v), while other parameters were kept constant. The DS value was found to increase significantly when the concentration of NaOH increased up to 40% (w/v), thereafter it decreased. According to Sarmina et al., (2015), the higher concentration of alkali is not preferable as a higher concentration of sodium hydroxide reacts with monochloroacetic acid to form sodium glycolate.

Figure 3.2B: shows the effect of concentration of monochloroacetic on DS of CMC. There was an increase in the DS with amount of monochloroacetic acid up to 7.0 g. The increase probably was due to the greater availability of the acetate ions at higher concentrations in the closeness of cellulose molecules. At a concentration higher than 7.0 g, glycolate formation seems to be preferential and the reaction

efficiency decreases. These findings were supported by reports of (Latif et al. 2006; Hutomo et al., 2012).

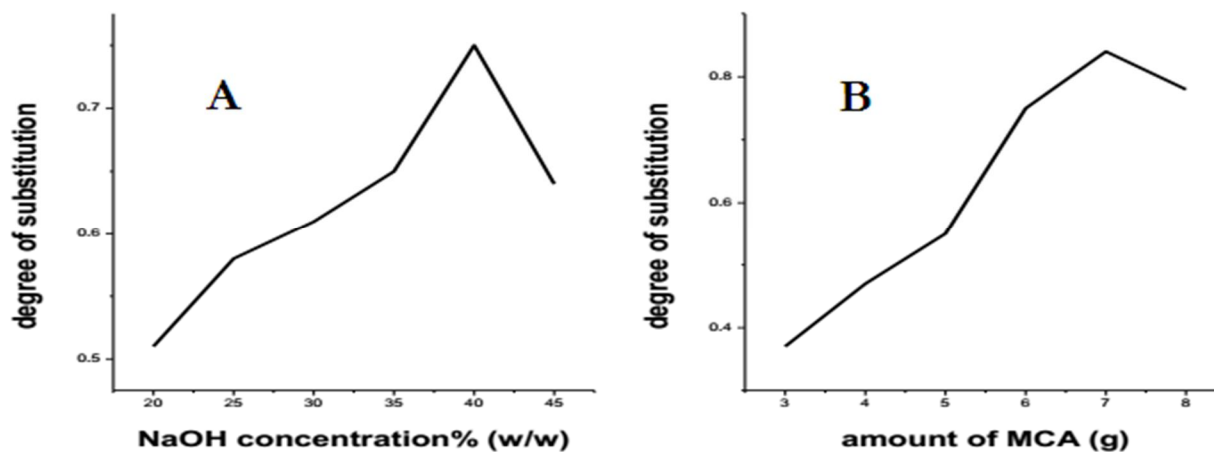


Figure 3.2: (A) Effect of NaOH concentration of DS CMC, (B) Effect of amount of MCA on DS of CMC.

Figure (3.3A) shows the effect of propylene oxide (PO) concentration on the degree of substitution of HPC. The DS value increase proportionally with increase in PO concentration up to 2.8 ml /g cellulose. The increase in DS was due to was due to the greater availability of the propylene oxide at higher concentrations close to cellulose molecules, after 2.8 ml /g cellulose it turned to un limiting factor (Marseno et al., 2014).

Figure 3.3B: shows the effect of reaction time on the degree of substitution of HPC. The DS value was found to increase significantly with time up to six hours then decrease. According to Bhatt et al., (2011), the increment in DS on increase of duration of hydroxypropylation up to six hours, is a direct consequence of the favorable effect of time to induce better contact between PO and the low rate of hydroxypropylation. Significant decrease in DS on prolonging

hydroxypropylation time may probably, be due to the deactivating effect of the additional hydroxypropoxyl group, or degradation of HPC.

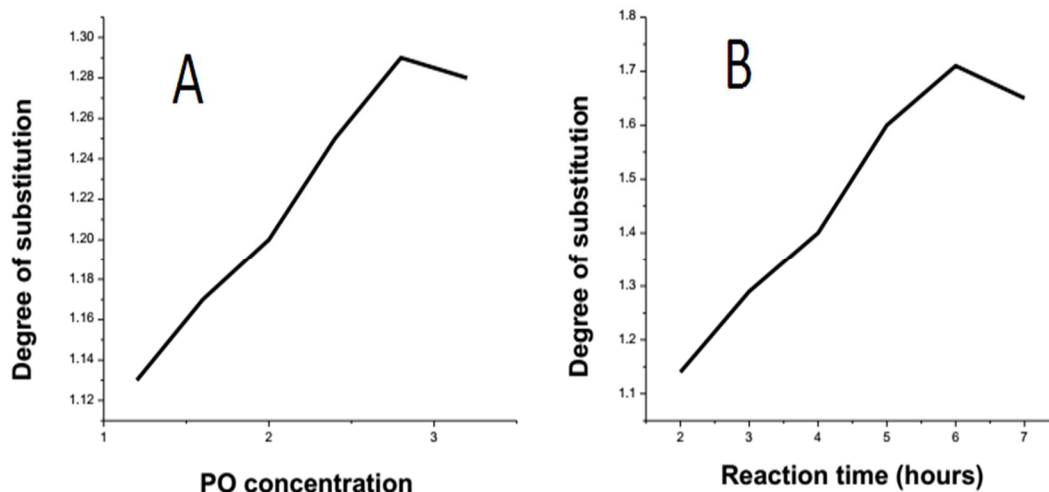


Figure 3.3 : (A) Effect of PO concentration on DS of HPC, (B) Effect of reaction time on DS of HPC.

Figure 3.4: shows FT-IR spectrums of cellulose and cellulosic ether derivatives. For cellulose, showed absorption band at 3439.42 cm^{-1} is due to the stretching frequency of the -OH groups as well as the intramolecular and inter molecular hydrogen bonds in cellulose. Peak at wave number of 1057.76 cm^{-1} is due to $\text{CH}_2\text{-O-CH}_2$. C-H stretching vibration shown at 2916.81 cm^{-1} . Other proof of cellulose are that of -CH_2 scissoring and -OH bending vibration at 1421.28 and 1318.11 cm^{-1} respectively (Onigbinde and Vivian 2015).

For methylcellulose, the main differences between methylcellulose and mesquite cellulose spectrum, were the decrease in the intensity observed for the 3440 cm^{-1} band is attributed to stretching of the O-H groups of cellulose, due to partial

substitution of hydrogen groups by methylation reaction. Furthermore, an increase is observed for the bands around 2900 cm^{-1} assigned to the C–H stretching, due to the presence of the CH and CH_2 groups of cellulose and CH_3 of the methylcellulose. Methylcellulose spectra showed bands at 1458, 1376, 1318 and 945 cm^{-1} attributed to C–H stretching of CH_2 and CH_3 groups as finger print characteristic of methylcellulose. The presence of an intense band around 1113 cm^{-1} indicates the presence of C–O–C bonds, characteristic of cellulose ethers (Viera et al. 2007). The change in the profile of the band assigned to the stretching O–H frequency and the region assigned to stretch C–H confirms the efficiency of the methylation process.

The CMC spectrum showed the broad absorption band at 3427.85 cm^{-1} is due to the stretching frequency of the OH group. A band at 2921.63 cm^{-1} is attributable to C–H stretching vibration. The presence of a new and strong absorption band at 1611.23 cm^{-1} confirms the stretching vibration of the carboxyl group (COO^-), 1422.24 cm^{-1} is assigned to carboxyl groups as the sample salts. The bands around 1327.75 cm^{-1} and 1114.65 cm^{-1} are assigned to OH bending vibration and C–O–C stretching, respectively (Haleem et al. 2014 ; Yeasmin and Mondal 2015).

For HPC, the IR spectra displays bands at 3398 and 1059 cm^{-1} and a shoulder at 2944 cm^{-1} which are assigned to –OH stretching, $-\text{CH}_2-\text{O}-\text{CH}_2$ stretching and –CH stretching of the methyl group characteristics of the hydroxypropyl group but absent in cellulose indicating the formation of hydroxypropylcellulose (Bhatt et al. 2011).

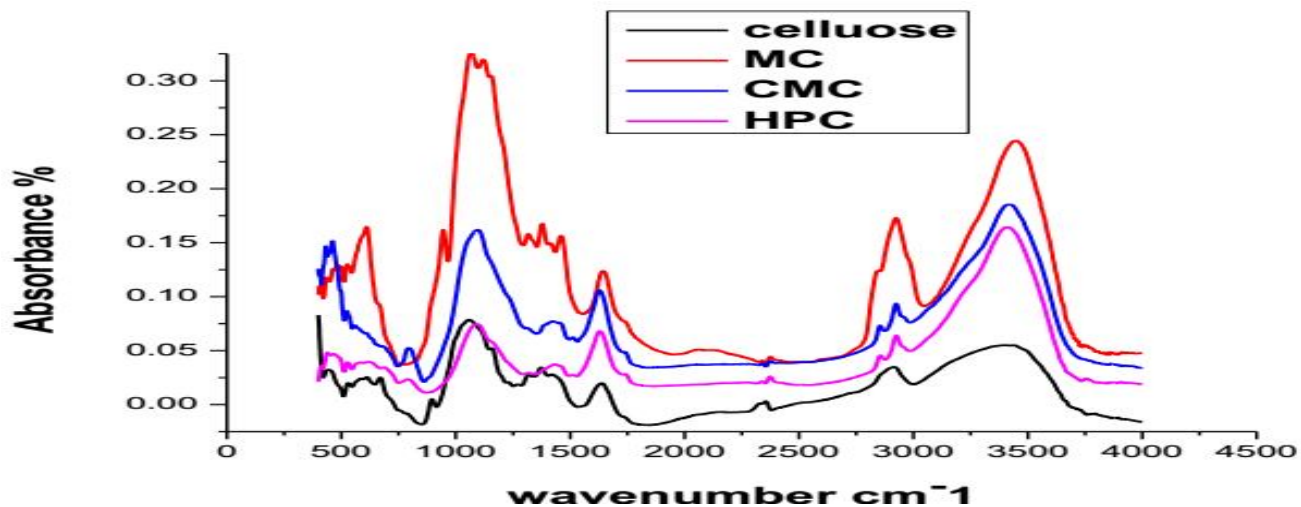


Figure 3.4 FT-IR spectrums of cellulose and cellulose and cellulosic ether derivatives.

Figure 3.5: shows the XRD spectroscopy's patterns of cellulose and cellulosic ether derivatives. The observed diffraction peaks for cellulose and cellulosic ether derivatives which attributed to crystalline scattering, and the diffuse background to disordered regions.

Cellulose showed main diffraction peaks at 12.43° , and 21.13° 2θ angles, which according to (Oliveira et al., 2015) are attributed to the interplanar distance characteristic of the phases $I\alpha$ and $I\beta$ cellulose crystalline structure. These were agree with (Rangelova et al., 2011) .

Methylcellulose showed maximum diffraction peaks at 8.58° and 20.48° 2θ angles. Comparing the XRD patterns of MC and cellulose, its observed that the peak around 8° is not present in cellulose, which according to (Filho et al., 2007) is an evidence of cellulose modification. The position of this peak (8°) indicates an increase in the inter-planar distance compared to the original cellulose diffraction pattern, due to generation of disorder when cellulose is modified. The projection of the substituting groups along the axis (methyl groups) is associated with an increase in the interfibrillar distance. Oliveira et al., (2015) reported a maxima,

around 20° , in MC is known as van der Waals halo, which appears for all polymers and corresponds to the polymeric chain packing due to van der Waals forces. Whereas the maxima around 10° , which is known as the halo of low van der Waals, occurs for some amorphous polymers due to the existence of regions with aggregates segments of parallel chains. Kumar et al.,(2012) postulated that the $2\theta=8^\circ$ peak represents the degree of cellulose modification.

X-ray diffraction (XRD) pattern of CMC shows two relatively intense reflections at 8.3° and 20.1° and additional bands at 34.6° and 44.6° . This phenomenon may be due to change in crystallinity by broadening or cleavage of hydrogen bonds by carboxymethyl substitution at the hydroxyl groups of cellulose(Mondal et al. 2015).Kumar et al., (2012)postulated that the $2\theta=8^\circ$ peak represents the degree of, cellulose, modification.

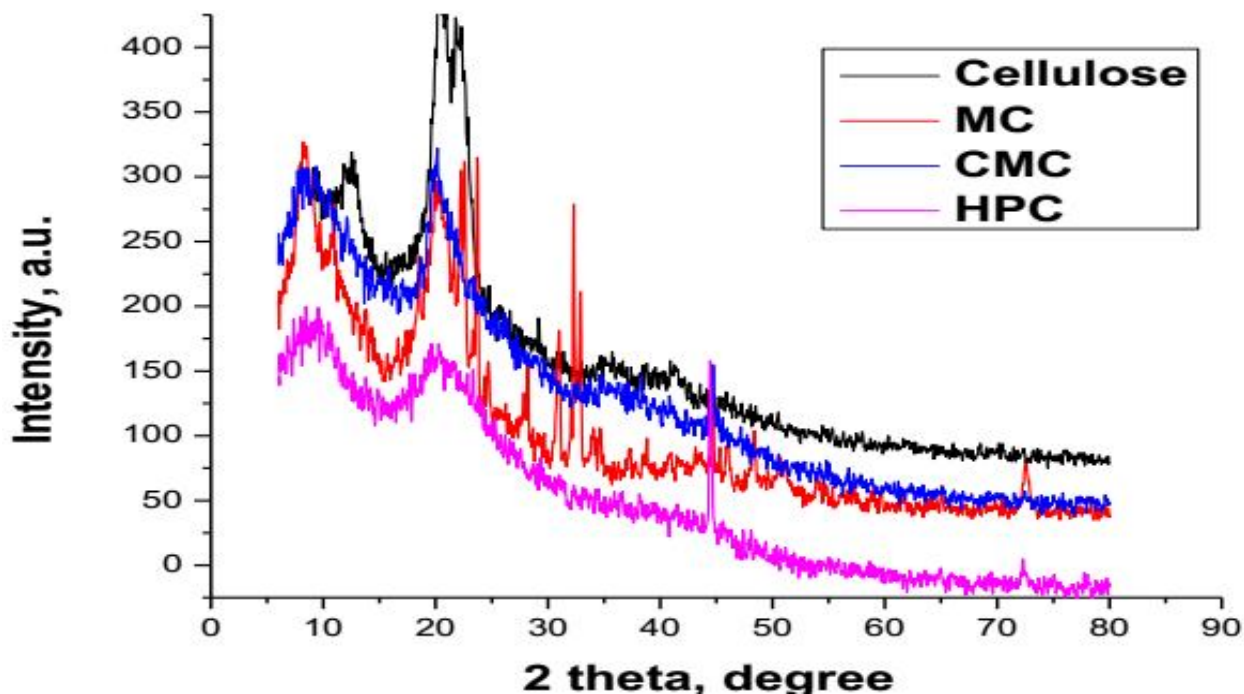


Figure 3.5 XRD patterns of cellulose and cellulosic ether derivatives.

XRD pattern of HPC showed peaks at $2\theta = 9.23^\circ$ and $2\theta = 20^\circ$ and $2\theta = 44.6^\circ$, these agree with (Reddy et al. 2012; Marseno et al., 2014).They are postulated that,

these changes were due to the lowering of crystallinity. This phenomenon was supposed to be the cleavage of the broadening hydrogen bonds due to hydroxypropyl substitution at the hydroxyl groups of cellulose due to mercerization.

Figure 3.6A: shows the TGA curve of cellulose and cellulosic derivatives. Cellulose and all cellulosic derivatives showed two mass loss steps. The first at 47 -100 C is associated with the loss of adsorbed water, while the second, for cellulose is between 220 and 400 C attributed to, the actual, pyrolysis and decomposition.

For methylcellulose, mass loss is between 300 and 400 C associated with decomposition. Oliveira et al., (2015) suggested that decomposition results in the formation of H₂O, CO and CH₄.

For carboxymethylcellulose (CMC), mass loss is between 250 and 300 C, due to the loss of CO₂ from the polysaccharide. As a result of decarboxylation of COO₂ group in this temperature range. The rate of weight loss is increased with increase in temperature (Biswal and Singh 2004).

For hydroxypropylcellulose, what is between 250 to 302C attributed to pyrolysis and volatilization of hydroxypropyl group and the residue was left showing that the left amount of the product is stable at 800 C (Bhatt et al. 2011).

Figure 3.6B: shows the DTG curves of cellulose and cellulosic ether derivatives. The maximum weight loss of dehydration and degradation states of cellulose happen at 67.48 C and 345 C respectively.

It obvious that, methylcellulose (MC) showed a smaller weight loss than cellulose in the dehydration stage at 55.43 C. And higher maximum weight loss of degradation at 350.57 C. The difference can be explained as a function of the

substitution of hydroxyl groups by methoxyl groups, during the synthesis of MC, reducing the number of hydroxyls available to interact with water molecules and increasing the molecular weight of polymer, which indicates the modification of cellulose into methylcellulose. Maximum weight loss of dehydration stage of CMC is 64°C, while the weight loss of degradation is 288.5°C, less than that of cellulose (Biswal and Singh 2004).

Maximum weight loss of dehydration stage of hydroxypropylcellulose (HPC) occurred at 71°C higher than that of cellulose, and this could be due to increased number of hydroxyl groups responsible for water hydrogen bonding to the polymer as a result of hydroxypropylation. While the maximum weight loss of degradation stage occurred at 290°C, and this could be due to acquired thermal stability after modification of cellulose.

Figure 3.6C: shows the DTA thermal analysis of cellulose and cellulosic derivatives. Cellulose degrades immediately with one endothermic between 333.09 to 400°C (Poletto et al. 2012). The presence of the endothermic event around 254°C in methylcellulose and absence of this event in cellulose, confirm that the endotherm is mainly attributed to the fusion and fast rearrangements in the structure of the polymer, however, this phenomenon is accompanied by degradation up to 400°C (Vieira et al. 2012). And this, again, confirms the modification of cellulose into methylcellulose.

CMC showed endothermic peaks at 52.12°C, due to decomposition of the main chain and depolymerisation, which proceeds due to the cleavage of glycosidic linkages. And exothermic peak at 293.04°C due to the combustion of the degraded products (Biswal and Singh 2004).

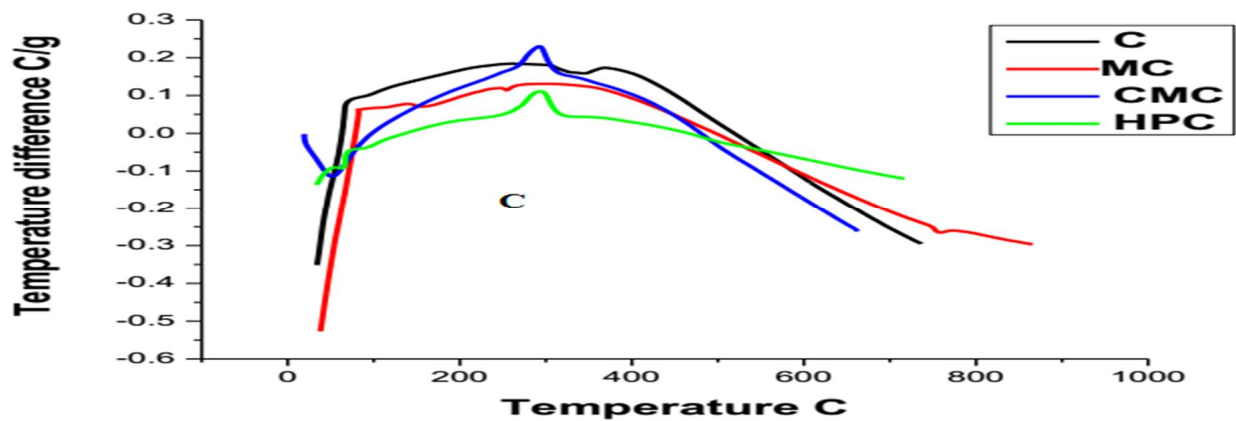
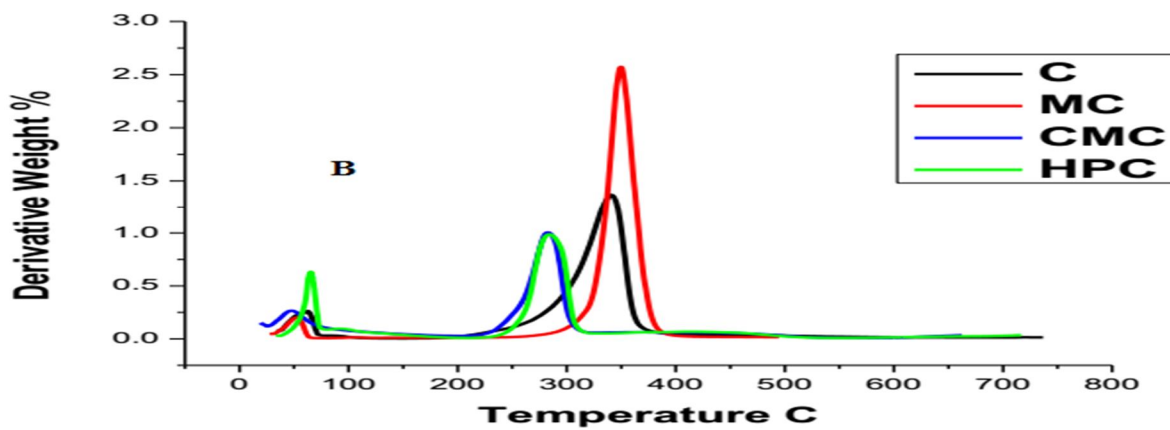
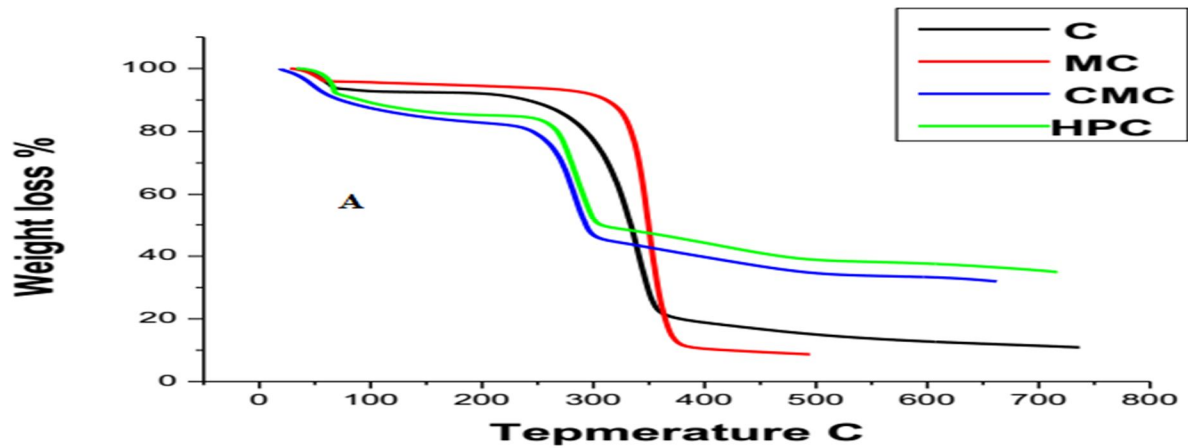


Figure 3.6 Thermal analysis curves (A) TGA, (B) DTG, (C) DTA of cellulose and cellulosic derivatives.

Hydroxypropylcellulose shows two endothermic and exothermic peaks are at 92.1 C and 293.1 C. These peaks are due to semi-melting and decomposition of the hydroxypropyl molecule (Bhatt et al. 2011). And these confirm the modification of cellulose into hydroxypropylcellulose.

Figure 3.7A: shows the ^{13}C spectrum of methylcellulose. The region between 50 and 60 ppm, signals correspond to the methyl substituents at C-2, C-3 and unsubstituted C-6 positions. The region from 74.24 to 84.30 ppm signals correspond to Carbons C2, C3, C4 and C5 and substituted C6. The signal at 103.60 ppm signal associated with C1(Oliveira et al., 2015). According to (Kamitakahara et al.,2005 ; Oliveira et al. 2015), ^{13}C spectrum of unmodified cellulose shows resonances at 70-80 ppm which is associated with C2, C3 and C5 carbons, signals around 60 ppm are assigned to C1, C4 and C6 carbons and signal at 105 is for C1 carbon. Comparing to the spectrum of unmodified cellulose confirms the modification of cellulose to methylcellulose.

Figure 3.7B: shows the ^1H NMR of methylcellulose with signal at 2.51 for DMSO, intense signals at 3.28–3.45 ppm corresponding to the overlapping of methyl protons at C-2 and C-3, signal at 3.1 ppm attributed to methyl protons at C-6 and signal at 3.36 ppm, 7.11ppm, 7.24 ppm for 6-OH, 2-OH and 3-OH protons respectively(Kumar et al., 2012 ;Nasatto et al., 2015;Oliveira et al., 2015). And are in good agreement with (Nasatto et al., 2015).

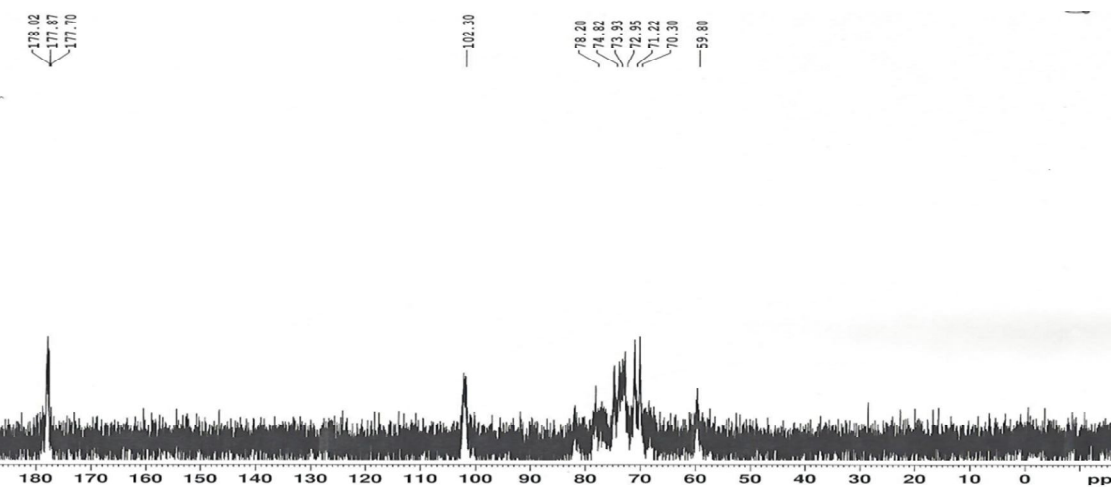


Figure 3.8: ^{13}C NMR of carboxymethylcellulose in DMSO.

Figure 3.9: shows the ^{13}C NMR spectrum of hydroxypropylcellulose. Signal at 16.5 ppm is assigned to HP- CH_3 end carbon, signals around 60 ppm assigned to unsubstituted C6 carbon, signal at 66 ppm and 73 ppm assigned to HP-CH end and internal carbon, signal at 72 ppm and 75 ppm assigned to HP- CH_2 end and

internal carbon, 71 ppm assigned to HP-C6 carbon, signal at 76.2 assigned to C4 carbon, signal at 76.5 assigned to C2-5 carbon, signal at 79 ppm assigned to C2s- 3s carbon, and 102 for C1 carbon (Ibbett et al. 1992; Cheng & Neiss 2012). Comparing to the spectrum of un modified cellulose confirms the modification of cellulose to HPC.

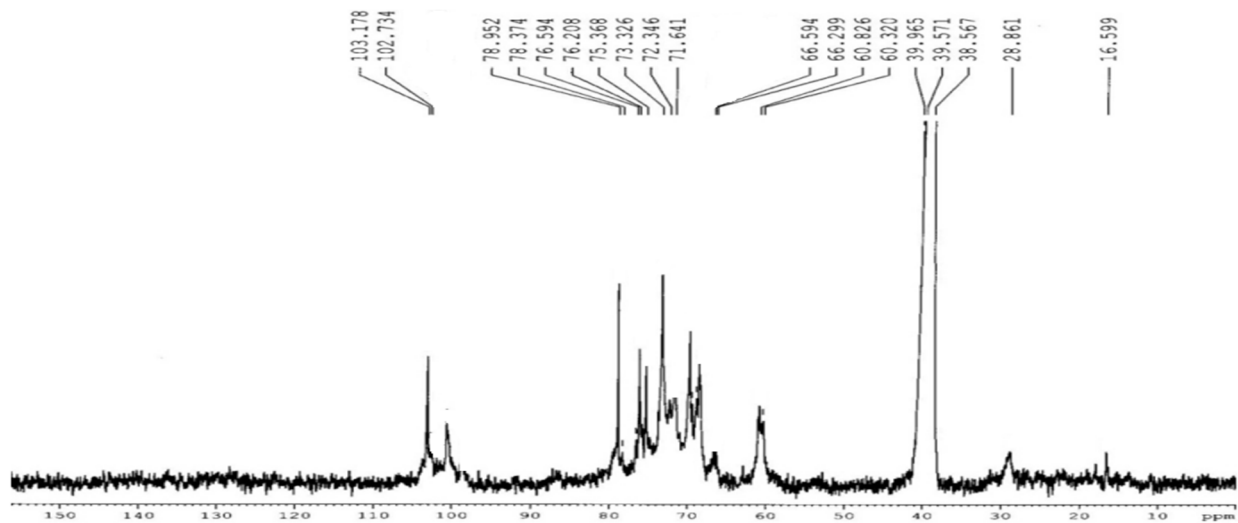


Figure 3.9 ^{13}C NMR of hydroxypropylcellulose in DMSO.

Figure 3.10: shows the FT-IR spectrum of stabilized magnetite and their stabilizers. From all the spectra, except for that of HPC and CMC it is possible to see a deep peak at about 571 cm^{-1} characteristics of the Fe–O bond absorption. This confirms the presence of the magnetic core and thus it is more pronounced in the bare magnetite nanoparticles. In addition to band at 529 cm^{-1} characteristics for MC finger print (figure 3.10B). The absorption peak at about 3400 cm^{-1} is observed in all spectra. This may be originated by hydroxyls (OH) present in water and polysaccharides.

The presence of polymer in the $\text{Fe}_3\text{O}_4/\text{HPC}$ magnetite was successfully confirmed by means of FT-IR, characteristic vibration bands of $-\text{CH}_2-\text{O}-\text{CH}_2$ stretching

appear at 1038 cm^{-1} (Figure 3.11A). No clear absorptions bands of MC appeared in $\text{Fe}_3\text{O}_4/\text{MC}$ nanoparticles. The presence of polymer in the $\text{Fe}_3\text{O}_4/\text{CMC}$ magnetite (figure 3.10C) was successfully confirmed by means of characteristic vibration bands appear at 1611.23 cm^{-1} confirms the stretching vibration of the carboxylgroup (COO^-), 1422.24cm^{-1} is assigned to carboxyl groups as salts (Haleem et al. 2014 ; Yeasmin and Mondal 2015).

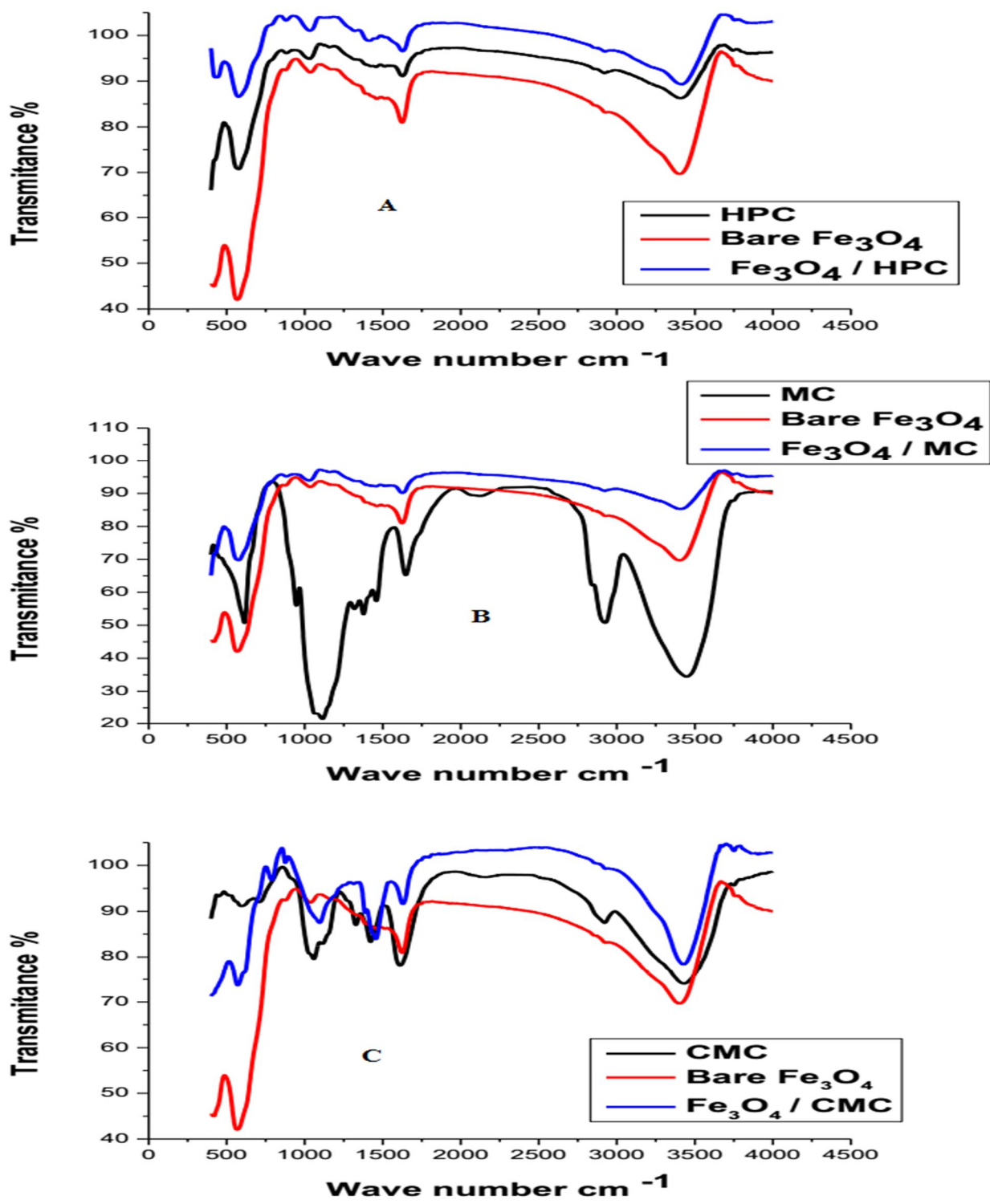


Figure 3.10: FT-IR spectrum of stabilized magnetite nanocomposite and their stabilizer. (A) HPC/ Fe_3O_4 (B) MC/ Fe_3O_4 (C) CMC/ Fe_3O_4 .

Figure 3.11: shows the XRD spectrum patterns of stabilized magnetite and their stabilizers. Bare and stabilized magnetite showed five patterns. At 2θ equal to 30.15° , 35.63° , 44.30° , 57.18° , and 62.97° for bare magnetite, 30.78° , 35.63° , 43.68° , 57.50° And 65.68° for Fe_3O_4 /HPC stabilized magnetite (3.11A), 29.3° , 34.6° , 43.5° , 56.2° , and 61.8° for Fe_3O_4 /CMC stabilized magnetite (figure3.11B), 30.40° , 35.63° , 43.68° , 56.87° , and 63.30° for Fe_3O_4 /MC stabilized magnetite (figure 3.11C). According to (Ngenefeme et al., 2013; Ashrafi et al. 2017) Are indexed to the cubic spinel phase of Fe_3O_4 . Comparing the values of bare and stabilized magnetites patterns, one can notice little deference as consequence of deferent crystallinity and indicating the effect of the HPC/ CMC/ MC on stabilized magnetites.

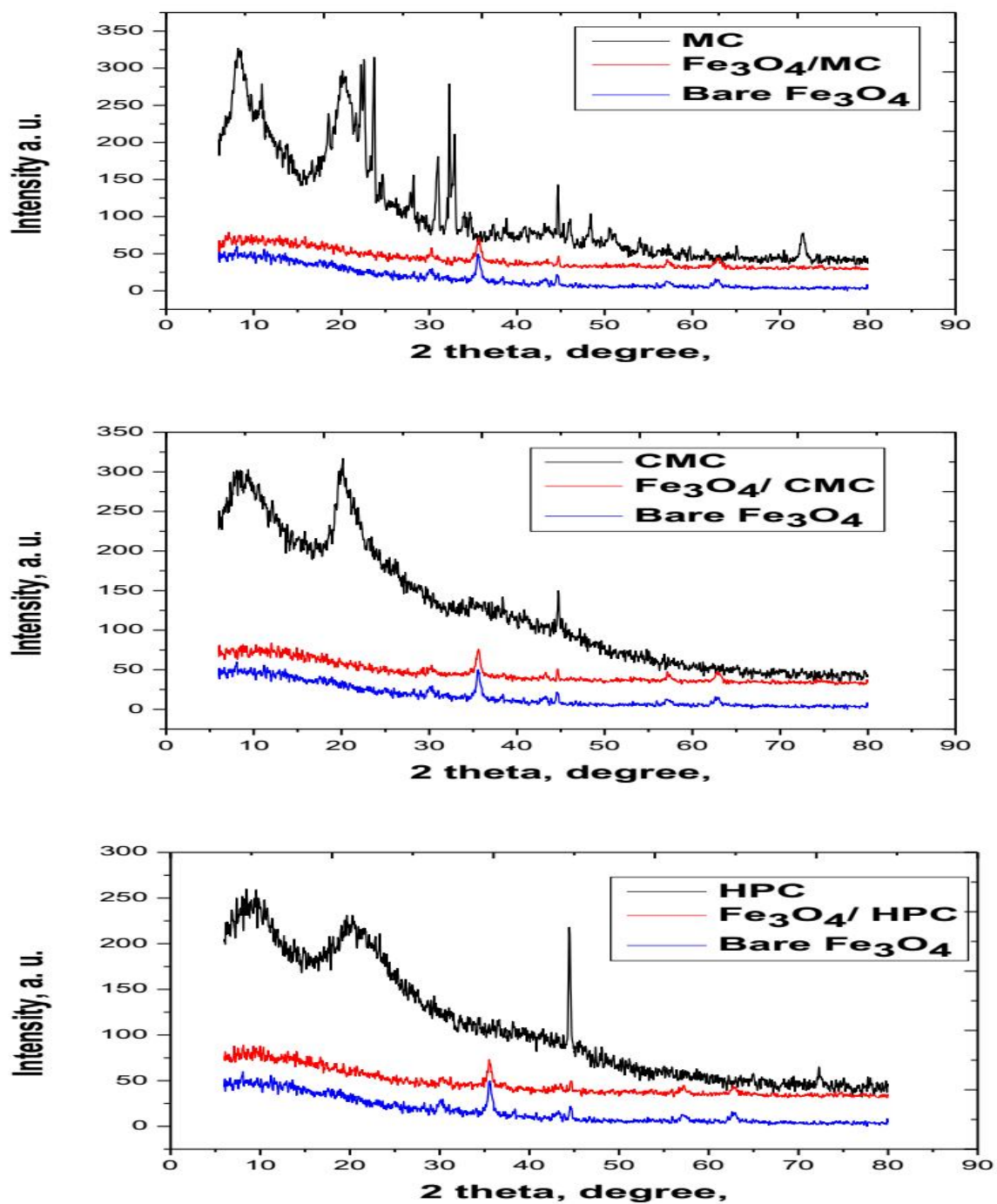


Figure 3.11: XRD spectrum patterns of stabilized magnetite and their stabilizer.

Figure 3.12: shows TGA curves of stabilized magnetite nanoparticles and their stabilizer. The TGA of pure magnetite showed no significant change in mass with increase in temperature except that of moisture (J. Ngenefeme et al. 2013), while stabilized Fe₃O₄/HPC magnetite showed a mass drop between 207.5 C and 387.70 C (figure 3.12A). This mass drop might be attributed to the thermal degradation of the HPC in the nanoparticles since pure HPC degraded between 250 and 302 C.

Fe₃O₄/MC stabilized magnetite showed a mass drop between 290 C and 336.44 C (figure 3.12B). This mass drop might be attributed to the thermal degradation of the MC in the nanoparticles since pure MC degraded between 290 and 383 C.

Fe₃O₄/CMC stabilized magnetite showed a mass drop between 253.75 C and 348.12 C (figure 3.12A). This mass drop might be attributed to the thermal degradation of the CMC in the nanoparticles since pure CMC degraded between 242.5 C and 324.37 C.

Solubility of the products in cold water was tested and was found to be 6%, 3%, 7% for carboxymethylcellulose, methylcellulose and hydroxypropylcellulose respectively.

The viscosity of the products was investigated and found to be 2500 cPs, 2000 cPs, and 1500 cPs for carboxymethylcellulose, hydroxypropylcellulose and methylcellulose respectively for 2% solution at 20 C, and consequently all products can be classified as high viscos.

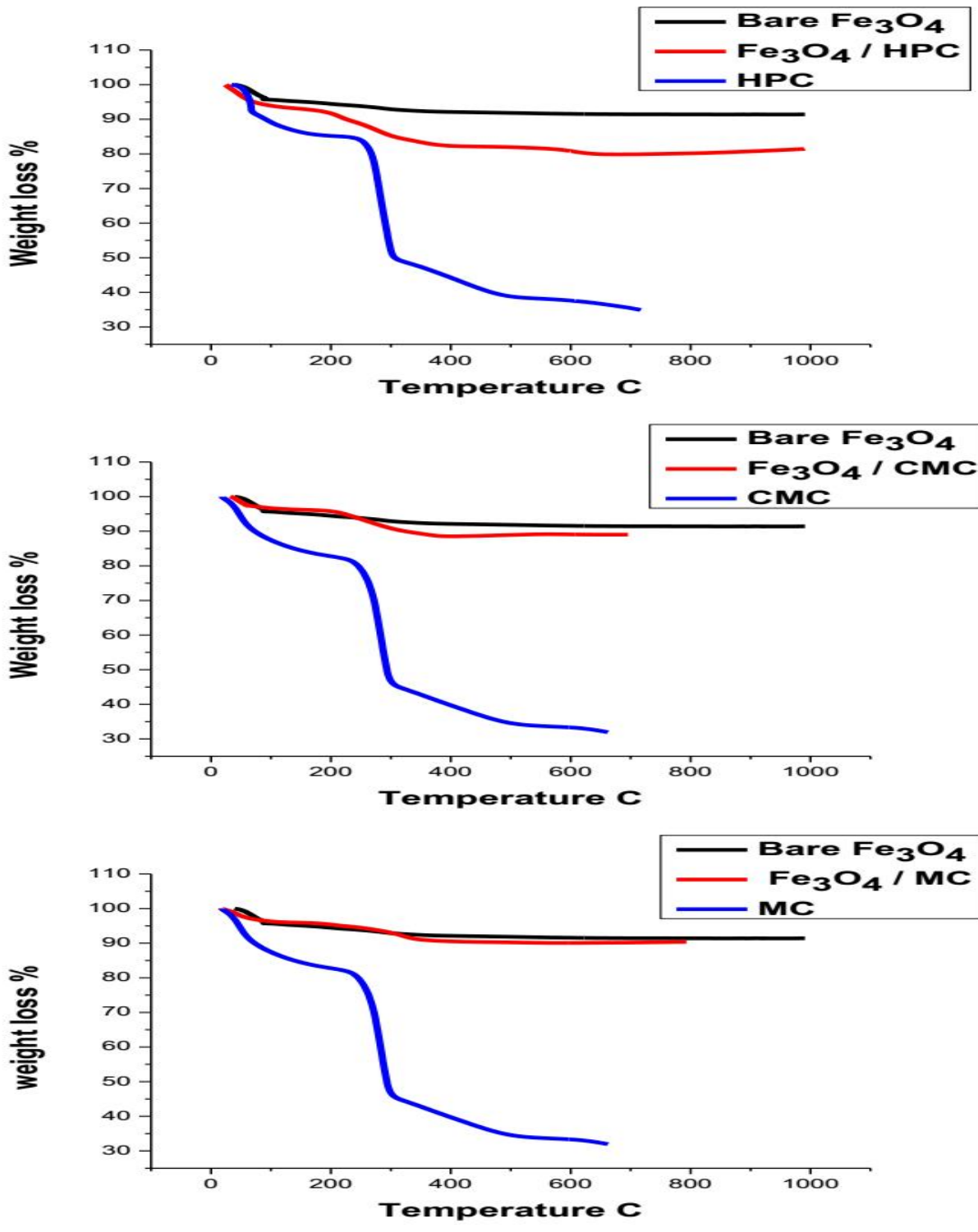


Figure 3.12 TGA curves of stabilized magnetite nanoparticles and their stabilizer.

Figure 3.13: shows the effect of PH on adsorption capacity of nanocomposite. The adsorption results exhibited a gradual increase in the adsorption capacity from 48 to 64 mg/g of methylene blue (MB) with increasing the pH of the initial dye solution from 3 to 7 respectively. These results showed that a neutral or basic solution is preferred for improvement the adsorption capacity of the carboxymethylcellulose/Fe₃O₄nanocomposite. The pH study results showed that the adsorption capacity equilibrated after pH 7. As a result, the next adsorption experiments were carried out at pH 7, which taken as optimum pH value. Increasing the adsorption capacity of MB with increasing pH values has been reported in other different studies (Zhao et al. 2015).

Figure 3.14: shows the effect of time onadsorption capacity of nanocomposite. MB concentration changes as a function of time were calculated, keeping the solution pH and the adsorbent weight at 7 and 0.05 g, respectively. The adsorption of MB on carboxymethyl cellulose/Fe₃O₄ nanocompositewas found to be rapid (~40 min) and then became slower (~40 to ~60 min). It finally reached a plateau after 60 min. In general, the adsorption rate of the dye is initially fast which may be attributed to the presence of high numbers of vacant adsorption sites. The adsorption process then progressively decreases with time until it reaches the equilibrium due to the difficulty to accessible the remaining vacant adsorption sites. The highly hydrophilic nature of the nanocomposite is responsible for the fast adsorption due to surface mass transport.

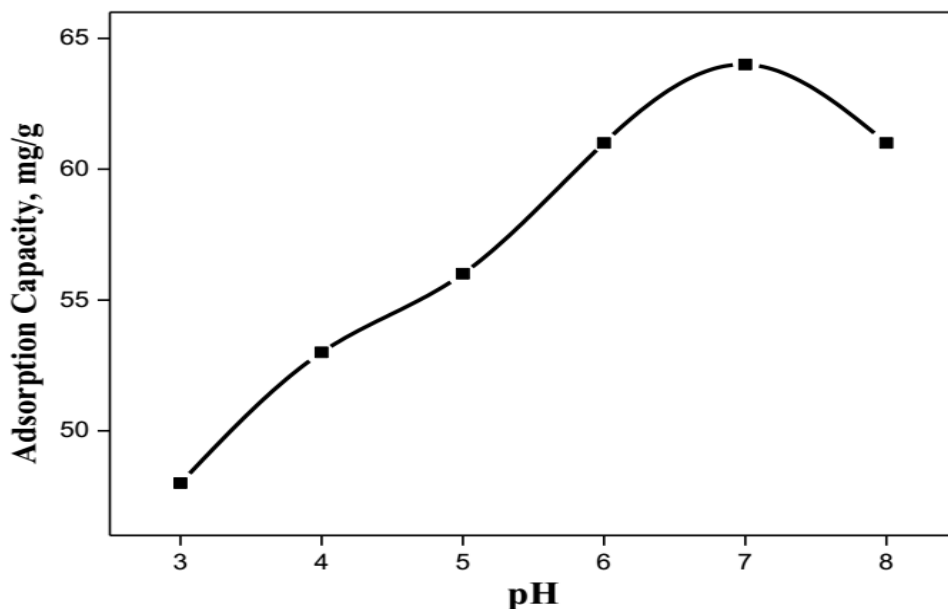


Figure 3.13: Effect of PH on adsorption capacity of nanocomposite.

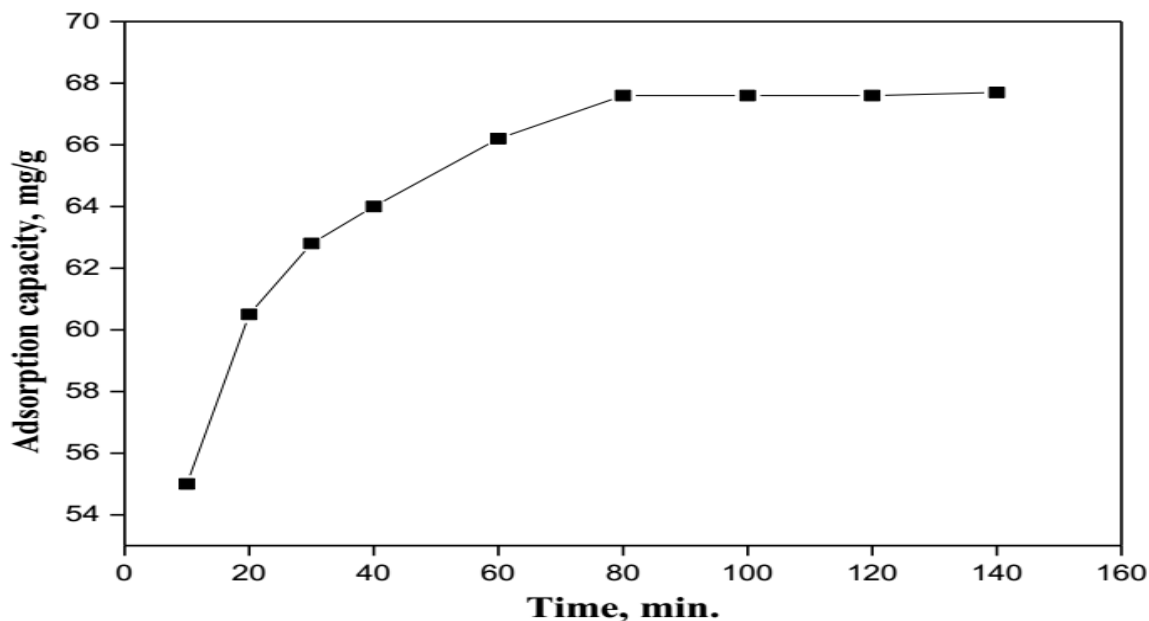


Figure 3.14 effect of time on adsorption capacity of nanocomposite

Figure 3.15 demonstrates the effect of the concentration of MB on the adsorption% using CMC/Fe₂O₃ nanocomposites as adsorbent phase. It is obvious that the dye removal increases from 47 to 1225 mg/g with an increase in MB concentration from 50 to 1500 ppm then tend to levels off with higher concentrations. This trend may be explained by the fact that the initial dye concentration provides the

sufficient force for mass transfer from the aqueous phase to the solid phase (Zhang et al. 2012). As a result, the increasing of initial MB concentration was accompanied by the increasing of driving force for transferring MB from aqueous phase to solid phase, enhancing the interaction between MB and nanocomposite. However, the leveling off of the adsorption process has been monitored after 1500 ppm due to the saturation of the active adsorption sites within microhybrids.

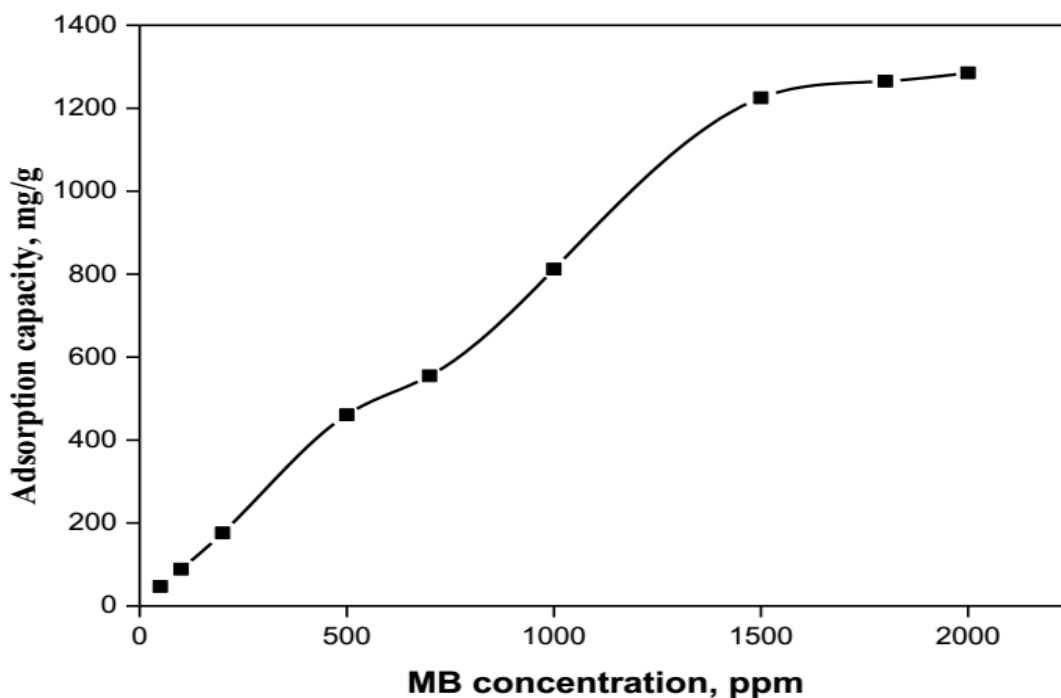


Figure 3.15: Effect MB concentration on adsorption capacity nanocomposite

Table 3.4 shows the kinetic parameters for MB adsorption by carboxymethyl cellulose/Fe₃O₄ nanocomposite. MB adsorption on the carboxymethyl-cellulose/Fe₃O₄ nanocomposite possesses a higher R² value, compared to the pseudo-first-order. Moreover, the calculated value ($q_{e,cal}$) for the pseudo-second-order model deviates less from the experimental data ($q_{e,exp}$). This compatibility with the second-order kinetics model refers to the probability of chemical interactions including valence forces through sharing or exchange of electrons between the dye molecules and the nanocomposite.

Table 3.4 Kinetic parameters for MB adsorption by carboxymethyl cellulose/Fe₃O₄ nanocomposite.

Pseudo first order-model				Pseudo second- order model		
$q_e, \text{exp (mg/g)}$	$q_e, \text{cal (mg/g)}$	$K_1(\text{min}^{-1})$	R^2	$q_e, \text{cal(mg/g)}$	$K_2(\text{g mg}^{-1}\text{min}^{-1})$	R^2
67.7	34	1.89	0.63	69.4	2.1×10^{-3}	0.999

3.1 Conclusions

- 92% alpha cellulose could be extracted from mesquite tree wood by anthraquinone Kraft pulping method.
- Carboxymethylcellulose (CMC), hydroxypropylcellulose (HPC), methylcellulose (MC) ether derivatives could be synthesized at the optimized conditions successfully and their degree of substitution were found to be 1.3, 1.72, 1.68 and yield of 190%, 160.61%, and 115.55% respectively.
- Carboxymethylcellulose (CMC), hydroxypropylcellulose (HPC), methylcellulose (MC) showed a good solubility in water and suitable viscosity and classified as high viscosity. .
- Carboxymethylcellulose (CMC), hydroxypropylcellulose (HPC), methylcellulose (MC) could be used successfully as stabilizer to prepare magnetite nanocomposite. Carboxymethylcellulose/ magnetite nanocomposite was the best.
- Carboxymethylcellulose/ magnetite nanocomposite showed a high dye adsorption capacity in aqueous solution.

3.2 Recommendations:

- To investigate the potential of synthesis of other commercial cellulosic derivatives from mesquite cellulose.
- To find novel applications of the products.
- To find other uses of mesquite hemicellulose and lignin such ethanol production and biofuel.
- To examine the prepared magnetite nanocomposite in other field such as removal of organic pollutants in aqueous solution, and magnetic resonance imaging (MRI).

References

- Aaltonen O., Johnson A., Ylinen P., (1987). Organosolv pulping methods and pulp properties. *,biomass*,**13**(5) 45-65.
- Abdel-Halim, E.S., (2014). Chemical modification of cellulose extracted from sugarcane bagasse: Preparation of hydroxyethyl cellulose. *Arabian Journal of Chemistry*, **7**(3), 362–371.
- Abreu V., Latorraca P., Pereira M., MONTEIRO O.,(2009). A supramolecular proposal of lignin structure and its relation with the wood properties. *,Annals of the Brazilian Academy of Sciences*,**81**(1) ,137–142.
- Akgul, M. and Kirci, H., (2009). An environmentally friendly organosolv (ethanol-water) pulping of poplar wood. *Journal of Environmental Biology*, **30**(9), 735–740.
- Ashrafi M., Chamjangali M., Bagherian, G., Goudarzi N., (2017). Application of linear and non-linear methods for modeling removal efficiency of textile dyes from aqueous solutions using magnetic Fe₃O₄ impregnated onto walnut shell. *Spectrochimica Acta - Part A: Molecular and Biomolecular Spectroscopy*, **171**, 268–279.
- Bajpai, P., (2012). Ozone Bleaching. *Environmentally Benign Approaches for Pulp Bleaching*.**5**(2),59-95.
- Barai, B.K., Singhal, R.S. and Kulkarni, P.R., (1997). Optimization of a process for preparing carboxymethyl cellulose from water hyacinth (*Eichornia crassipes*). *Carbohydrate Polymers*, **32**(3), 229–231.

- Barnett, J.R. and Bonham, V.A., (2004). Cellulose microfibril angle in the cell wall of wood fibres. *Biological Reviews*, **79**(2), 461–472. .
- Barrows S., Dulles F., Cramer C., French A., Truhlar D., (1995). Relative stability of alternative chair forms and hydroxymethyl conformations of β -d-glucopyranose. *Carbohydrate Research*, **276**(2), 219–251.
- Batalha R., Larisse A., Colodette J., Gomide J., Barbosa L., Maltha C., Broges F., (2012). Dissolving pulp production from bamboo. *BioResources*, **7**(1), 640–651.
- Bhatt, N., Gupta, P.K. and Naithani, S., (2011). Hydroxypropyl cellulose from α -cellulose isolated from Lantana camara with respect to DS and rheological behavior. *Carbohydrate Polymers*, **86**(4), 1519–1524.
- Biswal, D.R. and Singh, R.P., (2004). Characterisation of carboxymethyl cellulose and polyacrylamide graft copolymer. , **57**, 379–387.
- Brown, R.M., (1999). Cellulose structure and biosynthesis. *Pure and Applied Chemistry*, **71**(5), 1-12.
- Budtova, T. and Navard, P., (2016). Cellulose in NaOH–water based solvents: a review. *Cellulose*, **23**(1), 5–55.
- Cash, M.J. and Caputo, S.J., (2010). *Cellulose Derivatives*, *Advances in Polymer Science*, **107**, 199-265.
- Cerqueira, D.A., Filho, G.R. and Meireles, C., (2007). Optimization of sugarcane bagasse cellulose acetylation. *Carbohydrate Polymers*, **69**(3), 579–582.
- Chen, C.L., Capanema, E.A. and Gracz, H.S., (2003). Reaction mechanisms in delignification of pine Kraft-AQ pulp with hydrogen peroxide using Mn(IV)-

- Me4DTNE as catalyst. *Journal of Agricultural and Food Chemistry*, **51**(7), 1932–1941.
- Chen C., Huang Y., Zhu C., Nie Y., Yang J., Sun D., (2014). Synthesis and characterization of hydroxypropyl cellulose from bacterial cellulose. *Chinese Journal of Polymer Science (English Edition)*, **32**(4), 439–448.
- Cheng H., and Neiss T., (2012). Solution NMR Spectroscopy of Food Polysaccharides. *polymer reviews*, **52**, 81–114.
- Crestini C. Annibale A., Serrmani G., Saladino R., (2000). The reactivity of phenolic and non-phenolic residual kraft lignin model compounds with Mn(II)-peroxidase from *Lentinula edodes*. *Bioorganic and Medicinal Chemistry*, **8**(2), 433–438.
- Davis, K., (1985). structure and function of plant cell wall polysaccharides, *J. Cell Sci. Suppl*, **2**, 203–217.
- Dourado, F. Cardoso S., Silva A., Gama F., Coimbra M., (2006). NMR structural elucidation of the arabinan from *Prunus dulcis* immunobiological active pectic polysaccharides. *Carbohydrate Polymers*, **66**(1), 27–33.
- Feddersen, R.L. and Thorp, S.N., (2012). Sodium Carboxymethylcellulose. In *Industrial Gums: Polysaccharides and Their Derivatives*: **3**, 537–578.
- Filho, G., Messadeg Y., (2007). Characterization of methylcellulose produced from sugar cane bagasse cellulose: Crystallinity and thermal properties. *Polymer Degradation and Stability*, **92**(2), 205–210.
- Fišerová, M. and Opálená, E., (2014). Influence of Green Liquor and Hot Water Pre- Extraction of Hardwoods on Kraft Pulping. *Wood Research*, **59**(4), 557–

570.

Fox, S., Li B., Xu D., and Edgar K.,(2011). Regioselective esterification and etherification of cellulose: A review. *Biomacromolecules*, **12**(6),1956–1972.

Gamelas, J., Tavares A.,Evtuguin D., Xavier A., (2005). Oxygen bleaching of kraft pulp with polyoxometalates and laccase applying a novel multi-stage process. *Journal of Molecular Catalysis B: Enzymatic*, **33**(3–6), 57–64.

Gardner, K.H. and Blackwell, J., (1974). The hydrogen bonding in native cellulose. *BBA - General Subjects*, **343**(1), 232–237.

Garza-navarro, M.A. and Gonz, V.,(2011). Preparation of chitosan / magnetite polymeric-magnetic films. , **57**(2), 51–56.

Gellerstedt, G., (2010). Chemistry of Pulp Bleaching. *Lignin and Lignans: Advances in Chemistry*. 415-450.

Gellerstedt, G., Ek, M. and Henriksson, G., (2009). *Wood Chemistry and Wood Biotechnology*,355-400.

Gellerstedt, G., Majtnerova, A. and Zhang, L., (2004). Towards a new concept of lignin condensation in kraft pulping. Initial results. *Comptes Rendus - Biologies*, **327**(9–10), 817–826.

Germgård, U. and Larsson, S., (1983). Oxygen bleaching in the modern softwood kraft pulp mill. *Paperi Ja Puu*, **65**(4), 287–290.

Gierer, J., (1980). Chemical aspects of kraft pulping. *Wood Science and Technology*, **14**(4), 241–266.

Gierer, J., (1985). Chemistry of delignification - Part 1: General concept and reactions during pulping. *Wood Science and Technology*, **19**(4), 289–312.

- Goel, V. and Behl, H., (2001). Genetic selection and improvement of hard wood tree species for fuelwood production on sodic soil with particular reference to *Prosopis juliflora*. *Biomass and Bioenergy*, **20**(1), 9–15.
- Granström, M. and Kilpeläinen, P.I., (2009). *Cellulose Derivatives: Synthesis, Properties and Applications*. delet
- Gratzl, J.S. and Chen, C.-L., (1999). Chemistry of Pulping: Lignin Reactions. *Lignin: Historical, Biological, and Materials Perspectives*, **742**, 392–421.
- Grover, J.A., (2012). Methylcellulose and Its Derivatives. *Industrial Gums: Polysaccharides and Their Derivatives: Third Edition*, Academic press, pp 475–490.
- Gurd, F., (1967). Carboxymethylation. *Methods in enzymology*, **11**, 532–541.
- Gustafson, R., Sleicher C., Mckean W., Finlayson B., (1983). Theoretical model of the kraft pulping process. *Ind. Eng Chem. Process Des. Dev.* **22**(1), 87–96.
- Haleem, N., Arshad M., Shahid M., Ashraf M., (2014). Synthesis of carboxymethyl cellulose from waste of cotton ginning industry. *Carbohydrate Polymers*, **113**, 249–255.
- Hamza, N.A.E., (2013). Adsorption of Metals (Fe(II) , Cr(III) and Co(II)) from Aqueous Solution by Using Activated Carbon Prepared from Mesquite Tree. *Science Journal of Analytical Chemistry*, **1**(2),12.
- Hanhikoski, S., Warsta E., Antero V., Klaus N., Tapani H., (2016). Sodium sulphite pulping of Scots pine under neutral and mildly alkaline conditions. *Holzforschung*, **70**(7), 603–609.
- Hashem, A., Abou-okeil A., El-shafie A., El-sakhawi M., (2006). Grafting of High

- α -Cellulose Pulp Extracted from Sunflower Stalks for Removal of Hg (II) from Aqueous Solution. *Polymer-Plastics Technology and Engineering*, **45**(1), 135–141.
- Hedjazi, S., Tschirner U.,(2009). Alkaline sulfite-anthraquinone (AS/AQ) pulping of wheat straw and totally chlorine free (TCF) bleaching of pulps. *Industrial Crops and Products*, **29**(1), 27–36.
- Heinze T., and Pfeiffer K., (1999). Studies on the synthesis and characterization of carboxymethylcellulose. *Die Angewandte Makromolekulare Chemie*, 266, 37–45
- Heinze, T. and Koschella, A., (2005). Carboxymethyl ethers of cellulose and starch - A review. *Macromolecular Symposia*, **223**, 13–39.
- Hickman, W.S., (2002). Peracetic acid and its use in fibre bleaching. *Review of Progress in Coloration and Related Topics*, **32**(3),13–27.
- Hivechi, A.,Bahrami S., Arami M.,Karimi A.,(2015). Ultrasonic mediated production of carboxymethyl cellulose: Optimization of conditions using response surface methodology. *Carbohydrate Polymers*, **134**,278–284.
- Hoffmann, G.C. and Timell, T.E., (1970). Isolation of a β -1,3-glucan (laricinan) from compression wood of *Larix laricina*. *Wood Science and Technology*, **4**(2), 159–162.
- Hu, J., Lo, I., and Chen, G., (2004). Removal of Cr(VI) by magnetite nanoparticle. *Water Science and Technology*, **50**(12), 139–146.
- Hutomo, G.S., Marseno, D.W. and Anggrahini, S., (2012). Synthesis and characterization of sodium carboxymethylcellulose from pod husk of Cacao

- (Theobroma cacao L.). *African Journal of Food Science*, **6**(6),180–185.
- Ibbett, R.N. Philip K., Price M.,(1992). ^{13}C NMR , studies of the thermal behaviour of aqueous solutions of cellulose ethers, *polymer*,**33**(19), 4087–4094.
- J. W. S. Hearle, (1958). A fringed fibril theory of structure in crystalline polymers. *journal of polymer chemistry*, **28**(117), 432–435.
- Jiménez, L., Ferrer J.,(2008). Bleaching of soda pulp of fibres of *Musa textilis* nee (abaca) with peracetic acid. *Bioresource Technology*, **99**(5), 1474–1480.
- Kamitakahara, H., Enomoto Y., Hasegawa C.,Nakatssubo F.,(2005). Synthesis of diblock copolymers with cellulose derivatives: Characterization and thermal properties of cellulose triacetate-block-oligoamide. *Cellulose*, **12**(5), 527–541.
- Kennedy, J.F. and Pons, R.J.S., (1995). Cellulose: Structure, accessibility and reactivity. *Carbohydrate Polymers*, **26**(4), 313–314.
- Khattak, T.M. and Mahmood, A., (1986). Estimation of lignin, holocellulose and alpha cellulose content of earlywood and latewood among innerwood and outerwood of blue pine, *Pak. J. Bot.*, **18**(2), 235–241.
- Klemm, D., Philipp, B., Heinze, T., Heinze, U., Wagenknecht W.,(1998).Chemical analysis of cellulose and cellulose derivatives , *Comprehensive cellulose chemistry: Volume I*, Wiley-VCH, Weinheim, Germany, p., 173-181.
- Klemm, D., Philipp, B., Heinze, T., Heinze, U.,WagenknechtW.,(1998). Etherification of cellulose.*Comprehensive Cellulose Chemistry*, Volume 2, Wiley-VCH, Weinheim, Germany, p., 207-210..
- Kolar, J.J., Lindgren, B.O. and Pettersson, B., (1983). Chemical Reactions in

- Chlorine Dioxide Stages of Pulp Bleaching. *Wood Science and Technology*, **17**(2), 117–128.
- Kumar, A., Negi Y., Bhardwaj N., Choudhary V., (2012). Synthesis and characterization of methylcellulose/PVA based porous composite. *Carbohydrate Polymers*, **88**(4), 1364–1372.
- Kumar, S. and Walia, Y.K., (2014). Harnessing economic potential of methylcellulose from Wheat Straw : A Review. *Asian J. of Adv. Basic Sci.*, **2**(3), 12–22.
- Latif, A., Anwar, T. and Farrukh, M.A., (2006). Two step synthesis and characterization of carboxymethylcellulose from rayon grade wood pulp and cotton linter. *Journal of Saudi Chemical Society*, **10**(1), 95–102.
- Lindgren, B.O., (1979). Reactions of lignins with chlorine and chlorine dioxide during bleaching. *Svensk Papperstidning*, **82**(5), 126–30.
- Liu, C.-F. and Sun, R.-C., (2010). Cellulose. *Cereal Straw as a Resource for Sustainable Biomaterials and Biofuels*. 131–167.
- Liu, R., Yu, H. and Huang, Y., (2005). Structure and morphology of cellulose in wheat straw. *Cellulose*, **12**(1), 25–34.
- Lundquist, K., Parkas J., Paulson M., Heinter C., (2007). Reactions of lignin chromophores of the enal and enone types with sulfite. *BioResources*, **2**(3), 334–350.
- Maes, C. and Delcour, J.A., (2001). Alkaline Hydrogen Peroxide Extraction of Wheat Bran Non-starch Polysaccharides. *Journal of Cereal Science*, **34**, 29–35.

- Majewicz, T.G. and Podlas, T.J., (2000). Cellulose ethers. *Kirk-Othmer Encyclopedia of Chemical Technology*, **5**, 445–466.
- Majewski, P. and Thierry, B., (2007). Functionalized Magnetite Nanoparticles - Synthesis, Properties, and Bio-Applications. *Critical Reviews in Solid State and Materials Sciences*, **32**(3),203–215.
- Mansour, O.Y., Nagaty, A. and El-Zawawy, W.K., (1994). Variables affecting the methylation reactions of cellulose. *Journal of Applied Polymer Science*, **54**(5), 519–524.
- Marchessault, R.H. and Liang, C.Y., (1960). Infrared spectra of crystalline polysaccharides. III. Mercerized cellulose. *Journal of Polymer Science*, **43**(141), 71–84.
- Marseno, D.W., Haryanti, P. and Adiseno, B., (2014). Synthesis and Characterization of Hydroxypropylcellulose from Oil Palm Empty Fruit Bunches. *Indonesian Food and Nutrition Progress*, **13**(1), 24–30.
- Mascolo, M.C., Pei, Y. and Ring, T.A., (2013). Nanoparticles in a Large pH Window with Different Bases. *Materials*, **6**, 5549–5567.
- McDonald, D., Miles, K. and Amiri, R., (2004). The nature of the mechanical pulping process. *Pulp and Paper Canada*, **105**(8), 27–32.
- McDonough, T.J.,(1992). The chemistry of organosolv delignification. *IPST Technical paper series*, **455**, 1–17.
- Mohta, D., Roy, D.N. and Whiting, P.,(2000). Refiner mechanical pulping of kenaf bark fibre. *Pulp and Paper Canada*, **101**(8), pp.27–31.
- Mondal, M.I.H., Yeasmin, M.S. and Rahman, M.S.,(2015). Preparation of food

- grade carboxymethyl cellulose from corn husk agrowaste. *International Journal of Biological Macromolecules*, **79**, 144–150.
- Monica E., Larson P., Ibarra D., Copke V., (2010). Optimization of treatment sequences for the production of dissolving pulp from birch kraft pulp. *Nordic Pulp and Paper Research Journal*, **25**(1), 031–038.
- Morel, M., Martínez, F. and Mosquera, E.,(2013). Synthesis and characterization of magnetite nanoparticles from mineral magnetite. *Journal of Magnetism and Magnetic Materials*, **343**, 76–81.
- Morris, G., Ralet M., Bonnin E., Thibault J., Harding S.,(2010). Physical characterisation of the rhamnogalacturonan and homogalacturonan fractions of sugar beet (*Beta vulgaris*) pectin. *Carbohydrate Polymers*, **82**(4), 1161–1167.
- Murray, J.P. and Fletcher, E.A., (1994). Reaction of steam with cellulose in a fluidized bed using concentrated sunlight. *Energy*, **19**(10),1083–1098.
- Nasatto, P., Pignon F., Silveira J., Duarte M.,Nosedá M., and RinaudoM.,(2015). Methylcellulose, a cellulose derivative with original physical properties and extended applications. *Polymers*, **7**(5),777–803.
- Nasser, R.A., (2008).Specific gravity, fiber length and chemical components of *Conocarpus erectus* as affected by spacing. *J.Agric.&Env.Sci.Alex.Univ.*, **7**(3), 49–68.
- Ngeneleme F., Eko N., Mbom ., Tantohv N.,Rui K., (2013). A One Pot Green Synthesis and Characterisation of Iron Oxide-Pectin Hybrid Nanocomposite. *Open Journal of Composite Materials*, **3**(2), 30–37.

- Nishimura, H. and Sarko, A., (1987). Mercerization of cellulose. IV. Mechanism of mercerization and crystallite sizes. *Journal of Applied Polymer Science*, **33**(3), 867–874.
- Olaru, N., Olaru L., Stoleriu A., Timpu D., (1998). Carboxymethylcellulose Synthesis in Organic Media Containing Ethanol and / or Acetone. *Journal of Applied Polymer Science*, **67**, 481–486.
- Oliet F.; Santos, A.; Gilarranz, M.A.; García-Ochoa, F.; Tijero, J., M.. R., (2000). Organosolv delignification of Eucalyptus globulus: kinetic study of autocatalyzed ethanol pulping. *Industrial & Engineering Chemistry Research*, **39**(10), 34–39.
- Oliveira, R.Vieira J., Barud H., Rosana Assunção M., Filho G ., Ribeiro S., and Messadeqq Y., (2015). Synthesis and characterization of methylcellulose produced from bacterial cellulose under heterogeneous condition. *Journal of the Brazilian Chemical Society*, **26**(9), 1861–1870.
- Onigbinde, M. and Vivian, A., (2015). Synthesis of industrial raw material from cellulosic agricultural wastes : Focus on Carboxymethyl Cellulose. , **4**(1), 1–6.
- Oshino, B. Karamalla A., Abd Elbasit M., Yoda K., Suliman M., Elgamari M., Nawata H., Yasoda H., (2012). Evaluating the Invasion Strategic of Mesquite (*Prosopis juliflora*) in Eastern Sudan Using Remotely Sensed Technique. *Journal of Arid Land Studies*, **22**(1), 1–4.
- Perez, S. and Mazeau, K., (2005). Conformations, Structures, and Morphologies of Celluloses. *Polysaccharides: Structural Diversity and Functional Versatility*, 341–68.
- Pham, X., Nguyen T., Pham T., Tran T., Tran V., (2016). Synthesis and

characterization of chitosan-coated magnetite nanoparticles and their application in curcumin drug delivery. *Advances in Natural Sciences: Nanoscience and Nanotechnology*, **7**(4), 1-10

Pierre, G. Dilattre C., Laroche C., Mechaud P., (2014). Galactans and Its Applications. *Polysaccharides*, **4**, 1-38.

Poletto M.attera A., Forte M., Santana R., (2012). Bioresource Technology Thermal decomposition of wood: Influence of wood components and cellulose crystallite size. *Bioresource Technology*, **109**, 148–153.

Polle A., (2009). Mannans in primary and secondary plant cell walls. *New Zealand Journal of Forestry Science*, **39**, 225–231.

Prabha, D.S., Dahms, H.-U. and Malliga, P., (2014). Pharmacological potentials of phenolic compounds from *Prosopis* spp.-a review. *Journal of Coastal Life Medicine*, **11**, 918–924.

Qi, H., Liebert T., Meister F., Heinze T.,(2009). Homogenous carboxymethylation of cellulose in the NaOH/urea aqueous solution. *Reactive and Functional Polymers*, **69**(10), 779–784.

Rangelova N.,Feranandes M., Herzog M., (2011). Methylcellulose/SiO₂ hybrids: sol-gel preparation and characterization by XRD, FTIR and AFM. *Central European Journal of Chemistry*, **9**(1), 112–118.

Reddy, K.,Prabhakar M., Rao K., Suhasini D.,Reddy V., Babu P., Sudhakar K.,Babu A., Subha M., Rao C., (2013). Development and Characterization of Hydroxy Propyl Cellulose / Poly (vinyl alcohol) Blends and Their Physico-Chemical Studies.*Indian Journal of Advances in Chemical Science* , **2**(1), 38–45.

- Reddy, K.,Prabhakar M., Babu P., Venkatesulu G., Rao U., Rao K., Suha M., (2012). Miscibility Studies of Hydroxypropyl Cellulose / Poly (Ethylene Glycol) in Dilute Solutions and Solid State.*International Journal of Carbohydrate Chemistry* , **2012**(8), 1-9.
- Roger, A., Albersheim P., and Darvill A., (1989). Purification and Characterization of a Xyloglucan Oligosaccharide- specific Xylosidase from Pea Seedlings .*The journal biological chemistry*, **264**(5), 20430–20437.
- Runge, T.M., Ragauskas, A.J. and McDonough, T.J., (1998). Lignin structural changes by oxidative alkaline extraction. *Pulping Conference, Proceedings of the Technical Association of the Pulp and Paper Industry*.**3**, 120-130.
- Silva P., Moraes C., and Samios D., (2016). Iron Oxide Nanoparticles Coated with Polymer Derived from Epoxidized Oleic Acid and Cis-1 , 2- Cyclohexanedicarboxylic Anhydride : Synthesis and. *Journal of Material Science & Engineering*, **5**(3),1–7.
- Sarkanen, K.V.,(2010). hypochlorite bleach mechanism.The chemistry of delignification in pulp bleaching. Cellulose Researches Institute , N.Y USA 55-70.
- Schlufte, K. and Heinze, T., (2010). Carboxymethylation of bacterial cellulose.*Macromolecular Symposia*. pp. 117–124.
- Schuerch, C., (1968). Methods of wood chemistry.*Journal of Polymer Science Part A-2: Polymer Physics*, **6**(11),1943–1944.
- Silva C., Stamford T., Andrade S., Souza E., Araujo J., (2011). Production of ethanol from mesquite [Prosopis juliflora (SW) D.C.] pods mash by *Zymomonas mobilis* in submerged fermentation. *Scientia Agricola*, **68**(1),

124–127.

Sixta, H., (2006). pulping chemistry. Handbook of Pulp first addition. Weinheim: Wiley-VCH. 20-30.

Sjostrom, E.,(1993). The Structure of Wood. Wood Chemistry, Academic Press, 1–20.

Solomon, K.R., (1996). Chlorine in the bleaching of pulp and paper. *Pure and Appl. Chem*, **68**(9), 1721–1730.

Stimers, D.P. and Greminger Jr., G., (1983). Methylcellulose. *Ceramics monthly*, **31**(3), 8388.

Suliman, M., Nawata H.,Hoshino B., andFangama I., , (2015). Understating dilemma and sophism of *Prosopis juliflora* eradication in Sudan. *International Journal of Current Microbiology and Applied Sciences*, **4**(8), 10–16.

T.J. McDonough, (1991). Bleaching Agents - Pulp and Paper Industry. *The Kirk-Othmer Encyclopedia of Chemical Technology*.

Tai, D., Chen, C.L. and Gratzl, J.S., (1990). Chemistry of Delignification During Kraft Pulping of Bamboos. *Journal of Wood, Chemistry and Technology*, **10**(1), 75–99.

Talaat A., , El SiddigE., Salam A.,andAhmed M., (2016). Mesquite in Sudan : A Boon or Bane for Dry lands, Its Socioeconomic and Management Aspects in Kasala state. *journal forest products and industries* . **3**(4), 182-190.

Tasaso, P., (2015). Optimization of Reaction conditions for Sythesis of carboxymethylcellulose from iol Palm Fronds. *International Journal of Chemical Engineering and Applications*, **6**(2), 3–6.

- Teleman, A., and Dahlman O., (2002). Characterization of O-acetyl-(4-O-methylglucurono)xylan isolated from birch and beech. *Carbohydrate Research*, **337**(4),373–377.
- Teleman A., Larson P., Iversen T., (2001). On the accessibility and structure of xylan in birch kraft pulp. *Cellulose*, **8**(3), 209–215.
- Theiliander, H., (2009). chemistry of chemical pulping. In *pulping chemistry and technology*. Stockholm Sweden: *the KTH Royal Institute of Technology*, 103.
- Vani T., Rao K., Reddy N., rao S., (2013). Synthesis and Characterization of Sodium Carboxy Methyl Cellulose / Poly (Acrylamide) Magnetic Nano Composite Semi Ipn ' s for Removal of Heavy Metal Ions. *World Journal of Nano Science and Technology*, **2**(1), 33–41.
- Verbbeek J.,(2012). Xylan , a Promising Hemicellulose for Pharmaceutical Use. *Products and Applications of Biopolymers*, In tech, pp.61–84.
- Vieira, J., and Motta L., (2009). Production, characterization and evaluation of methylcellulose from sugarcane bagasse for applications as viscosity enhancing admixture for cement based material. *Carbohydrate Polymers*, **78**(4),779–783.
- Vieira, J., Filho G., Meireles C., Faria F., Gomide D., Pasquini D., Cruze S., Assuncao R., Motta L.,(2012). Synthesis and characterization of methylcellulose from cellulose extracted from mango seeds for use as a mortar additive. *Polímeros*, **22**(1), 80–87.
- Viera, R., Rodrigues F., Assuncao G., Meireles R., (2007). Synthesis and characterization of methylcellulose from sugar cane bagasse cellulose. *Carbohydrate Polymers*, **67**(2),182–189.

- Vila, C., Santos, V. and Paraj, J.C., (2004). Dissolving pulp from TCF bleached Acetosolv beech pulp. *Journal of Chemical Technology and Biotechnology*, **79**(10),1098–1104.
- Whettena, R. and Sederoff R., (1995). Lignin Biosynthesis. *The Plant Cell*7(7),1001–1013.
- Willför, S., Sjöholm R., Laine C., Holmbom B., (2002). Structural features of water-soluble arabinogalactans from Norway spruce and Scots pine heartwood. *Wood Science and Technology*, **36**(2),101–110.
- Wong, A. and Chiu, C., (2001). Alkaline sulphite pulping of abaca (*musa textilis* née) from the philippines and ecuador. In *Pulping Conference, Proceedings of the Technical Association of the Pulp and Paper Industry*. 49–59.
- Wong, Y., Szeto Y., Cheung W., McKay G., (2004). Pseudo-first-order kinetic studies of the sorption of acid dyes onto chitosan. *Journal of Applied Polymer Science*, **92**(3),1633–1645.
- Yan, F., Krishniah D., Rajin M., Bono A., (2009). Cellulose extraction from palm kernel cake using liquid phase oxidation. *Journal of Engineering Science and Technology*, **4**(1), 57–68.
- Yeasmin, M.S. and Mondal, I.H., (2015). International Journal of Biological Macromolecules Synthesis of highly substituted carboxymethyl cellulose depending on cellulose particle size. *International Journal of Biological Macromolecules*, **80**, 725–731.
- Yoji Kato and Seiko Ito, (2008). Studies on the Chemical Structure of a Plant Cell-Wall Polysaccharide , Xyloglucan. *Foods Food Ingredients J. Jpn.*, 213(5), 8560.

Zhang, J., Zhou, Q. and Ou, L., (2012). Kinetic, isotherm, and thermodynamic studies of the adsorption of methyl orange from aqueous solution by chitosan/alumina composite. *Journal of Chemical and Engineering Data*, **57**(2), 412–419.

Zhao R., Wang Y., Li X., Sun B., and Wang C., (2015). Synthesis of β -cyclodextrin-based electrospun nanofiber membranes for highly efficient adsorption and separation of methylene blue. *ACS Applied Materials and Interfaces*, **7**(48), 26649–26657.

